PivotBuoy

An Advanced System for Cost-effective and Reliable Mooring, Connection, Installation & Operation of Floating Wind

Call identifier: H2020-LC-SC3-RES-11-2018

D5.4 Benchmark of PivotBuoy Compared to Other Floating Systems

Due Date of Deliverable: 28/02/2021
Completion Date of Deliverable: 31/05/2021

Start date of project: 1 April 2019 Duration: 36 months

Lead partner for deliverable: WavEC – Offshore Renewables

Dissemination Level		
PU	Public	X
PP	Restricted to other programme participants (including the Commission Services)	
RE	Restricted to a group specified by the consortium (including Commission Services)	
CO	Confidential, only for members of the consortium (including Commission Services)	

This project has received funding from the European Union's Horizon H2020 research and innovation programme under grant agreement No 815159

Authors:

Name	Organization	Role
António Maximiano	WavEC	Lead Author

Reviewers:

Name	Organization	Role
Guilherme Vaz	WavEC	Internal reviewer
Rocío Torres	X1Wind	Reviewer
Laura Voltá	DTU	Reviewer
Tiago Lourenço	EDP CNET	Reviewer

Document History

Issue Date	Version	Changes Made / Reason for this Issue
18/03/2021	0.0	First draft, to circulate within WP5 partners for feedback
14/04/2021	1.0	Included feedback from partners
22/04/2021	1.1	Included new round of feedback from X1Wind

This document only reflects the author's view. The programme authorities are not liable for any use that may be made of the information contained therein.

This project has received funding from the European Union's Horizon H2020 research and innovation programme under grant agreement No 815159

INDEX

This project has received funding from the European Union's Horizon H2020 research and innovation programme under grant agreement No 815159

This project has received funding from the European Union's Horizon H2020 research and innovation programme under grant agreement No 815159

ACKNOWLEDGMENTS

The authors are grateful to João Graça Gomes from the Sino-Portuguese Centre for New Energy Technologies (Shanghai) Co., Ltd (SCNET) for his contribution to section 2.1 *Historic Perspective of Floating Offshore Wind* and the floating offshore wind projects located in the Asian region.

This project has received funding from the European Union's Horizon H2020 research and innovation programme under grant agreement No 815159

ACRONYMS

CAPEX	Capital Expenditure
FOW	Floating Offshore Wind
LCoE	Levelized Cost of Energy
NTM	Normal Turbulence Model
O&G	Oil and Gas
OPEX	Operational Expenditure
TLP	Tension Leg Platform
TRL	Technology Readiness Level

This project has received funding from the European Union's Horizon H2020 research and innovation programme under grant agreement No 815159

EXECUTIVE SUMMARY

The present deliverable aims to benchmark the full scale PivotBuoy X140 system against other large scale floating offshore wind systems, as an outlook for the future commercial floating offshore wind systems in the 15MW range. This benchmark is carried out in two fronts: a design benchmark, positioning the PivotBuoy concept and design approach amongst the current floating offshore wind systems; and a simulation benchmark, by comparing the simulation approach and estimated response of the full scale PivotBuoy X140 system against other 15MW floating offshore wind designs.

The design benchmark begins by introducing the need for optimizing offshore floating wind systems using a different perspective than commonly used in oil and gas. Floating offshore wind, as a novel industry, has adopted the best practices of the oil and gas industry, which have higher redundancy and safety margins than are arguably necessary for floating offshore wind. If a competitive LCoE is to be reached, these safety margins need to be shaved by optimizing for the offshore wind risk profile and design drivers. As the floating offshore industry is taking its first steps, many different concepts at different TRL stages are currently being developed. A review of concepts above TRL 3 is presented and then categorized according to their main underlying static stability principle.

The PivotBuoy design falls in the hybrid category due to its innovative blend of single point TLP mooring, weathervane capacity, downwind turbine, and semi-submersible type floater. Due to its innovative and risky approach, the hybrid category is lagging in TRL when compared to the more established mooring stabilized category (spars) or buoyancy stabilized category (semi-submersibles). However, the PivotBuoy concept is well placed within its class in terms of TRL and development plan.

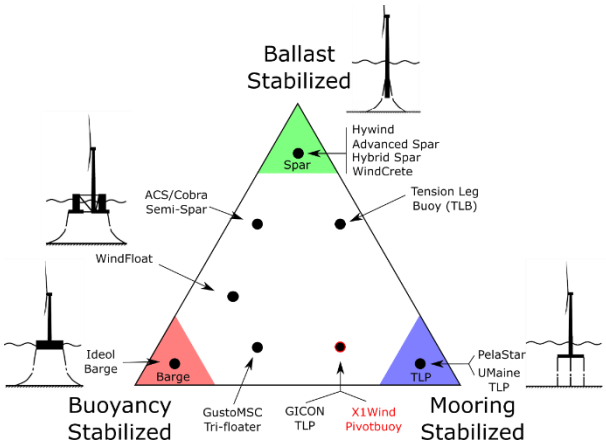

The second approach starts by introducing a review of the main challenges related to the numerical modelling of floating offshore wind systems, which adds a new layer to the common offshore wind approach: to model the floating foundation hydrodynamic response and resulting coupled interaction between hydrodynamics and aerodynamic performance. While these excitations have been studied individually in the past, floating offshore wind systems are unique in that the aerodynamic and wave loading are not only of similar importance, but also heavily coupled. The current state of the art regarding simulation of floating offshore wind systems is then summarized, presenting different modelling approaches, at different fidelity levels, commonly used for floating offshore wind systems.

Following the review of the numerical modelling approaches, the simulation work carried out so far within WP5 of the PivotBuoy project is summarized, with the relevant results presented, including a comparison of two different numerical codes, one more suited to aeroelastic modelling, HAWC2, and the other to hydrodynamic modelling, OrcaFlex. The simulation results for the full-scale PivotBuoy X140 design is then discussed in more detail for the three sites considered. Yaw misalignment is found in extreme (unlikely) cross-directional cases for the PivotBuoy design, which leads to

This project has received funding from the European Union's Horizon H2020 research and innovation programme under grant agreement No 815159

suboptimal turbine performance under these conditions. Despite having a conservative prediction of the yaw misalignment, this suggests that the weathervane capacity can be improved. An individual pitch controller (IPC) strategy is found to remove yaw misalignment at the expense of higher blade loading. This work has been published elsewhere [1]. Additional research is proposed to further investigate this approach.

Finally, open literature results for floating offshore wind foundations equipped with the novel 15MW offshore reference turbine are compiled. The relevant cases found are the WindCrete spar and ActiveFloat semi-submersible, both developed within the EU H2020 COREWIND project, and the VolturnUS-S semi-submersible platform developed within the IEA Wind Task 37. The COREWIND concepts are particularly relevant since their site selection coincides with one of the sites used for the PivotBuoy X140 analysis (Canary Islands).

The system main characteristics are compared, and despite having the largest steel consumption, the PivotBuoy design enables a weight reduction factor of 3.5 to 7.5 when compared to the other designs. The hydrodynamic and aeroelastic models used are discussed, and the lack of second order wave forces on the PivotBuoy is identified as a limitation of the current numerical model.

The maximum nacelle accelerations, a key performance indicator of floating foundations, are then compared between the different projects, showing that PivotBuoy X140 performs similar to other concepts, and under the limits identified in the COREWIND project.

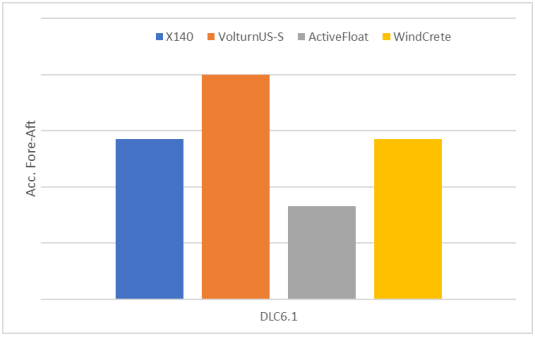

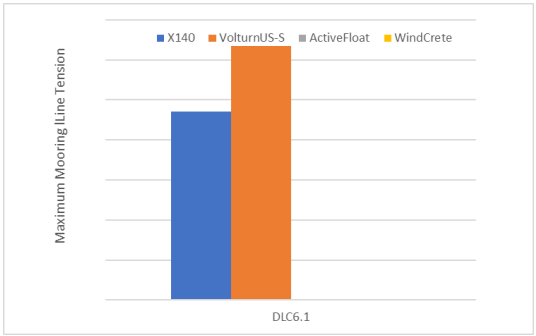

The maximum mooring line tension is then compared with the VolturnUS-S design, which is moored with a catenary system, while the Pivotbuoy is moored by small TLP system. The COREWIND mooring line tensions were not publicly available. The maximum loads on the tendons of the Pivotbuoy X140 design are comparable to those found in the catenary mooring of the VolturnUS-S, despite the different mooring system.

This review has found the large scale PivotBuoy X140, designed for the 15 MW offshore reference turbine, to be on par with other hybrid concepts in terms of TRL and development plan, and comparable in terms of predicted performance when compared to other floating designs for the same turbine.

Furthermore, future areas of research and development are identified, such as investigating the IPC strategy to improve the yaw alignment, or augmenting the numerical model of the PivotBuoy X140 design with second order wave excitation in order to capture the expected low frequency response of the floater.

This project has received funding from the European Union's Horizon H2020 research and innovation programme under grant agreement No 815159

1 INTRODUCTION

Floating offshore wind (FOW) is a nascent industry that has been fast developing, partly because it has benefited from the existing offshore oil and gas (O&G) industry to leverage its own growth, as seen by the common substructure designs in Figure 1, which are directly adapted from the O&G industry. While these are good starting designs, there are differences between both industries that justify further optimization to lower the levelized cost of energy (LCoE), thus increasing the competitiveness of FOW.

Traditional O&G industry designs need to address the high environmental risks and possible human loss in the event of serious failure. To mitigate these risks, a healthy dose of conservatism and design redundancy is embedded in the O&G standard practices. While these are proven well-known designs, they can be overly conservative for the FOW industry, where not only the environmental risks are much smaller, but the platforms are unmanned, limiting the human loss risk [2]. Other design drivers become relevant for FOW systems, which are less important or negligible for O&G designs. For example, FOW systems have a significant mass located at ever increasing hub heights, leading to a higher center of gravity, and larger overturning moments while in operation, which need to be supported by the substructure.

In order to achieve a competitive LCoE, the FOW industry needs to optimize these classic O&G designs with an economic-driven perspective, or embrace innovative and disrupting concepts, such as PivotBuoy, that better suit these new constraints. A sign of this optimization process is the significant number of floating offshore wind concepts under development, with at least 34 different FOW concepts above TRL 3, as seen in Figure 2. An overview of these designs, their categorization, and how they address this optimization will be presented in section 2, together with the PivotBuoy design and its positioning within the FOW concepts.

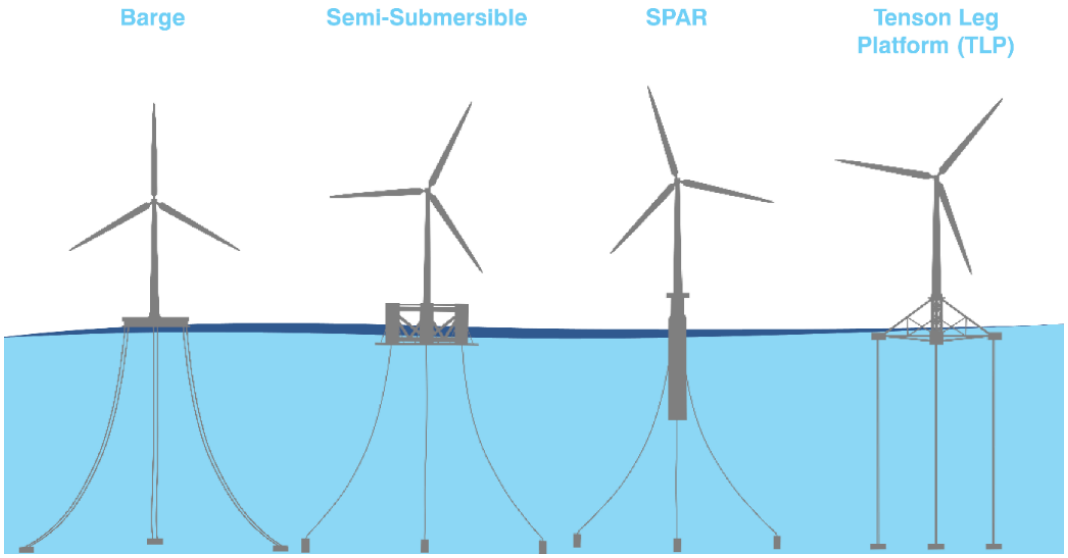

Figure 1 Main types of classic offshore industry designs adapted for floating offshore wind systems. Reproduced from [3].

This project has received funding from the European Union's Horizon H2020 research and innovation programme under grant agreement No 815159

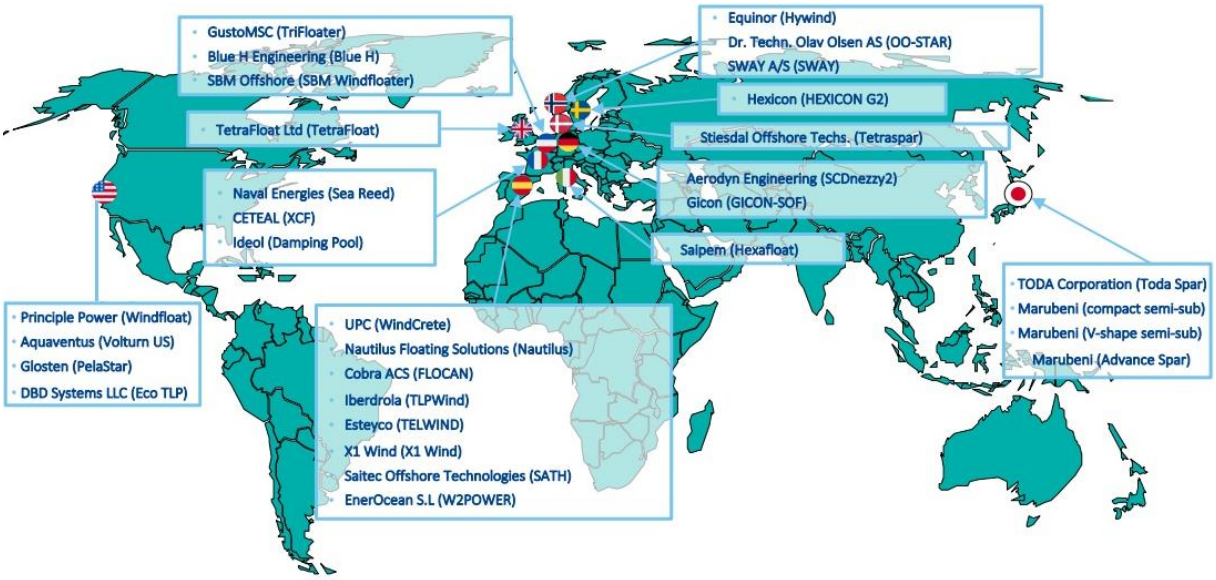

Figure 2 Geographic distribution of the main floating offshore wind projects above TRL 3 (total of 34). Adapted from [4]

This optimization process to achieve competitive FOW systems is not trivial, and ultimately it will be determined by site-specific (e.g. met-ocean data) and project specific (e.g. turbine capacity, local infrastructure) conditions. A key tool for this optimization process is the numerical modelling of FOW systems. Numerical simulations enable the exploration of different design variations in a cost-effective manner when compared to model scale testing in laboratories, or prototype testing in the ocean.

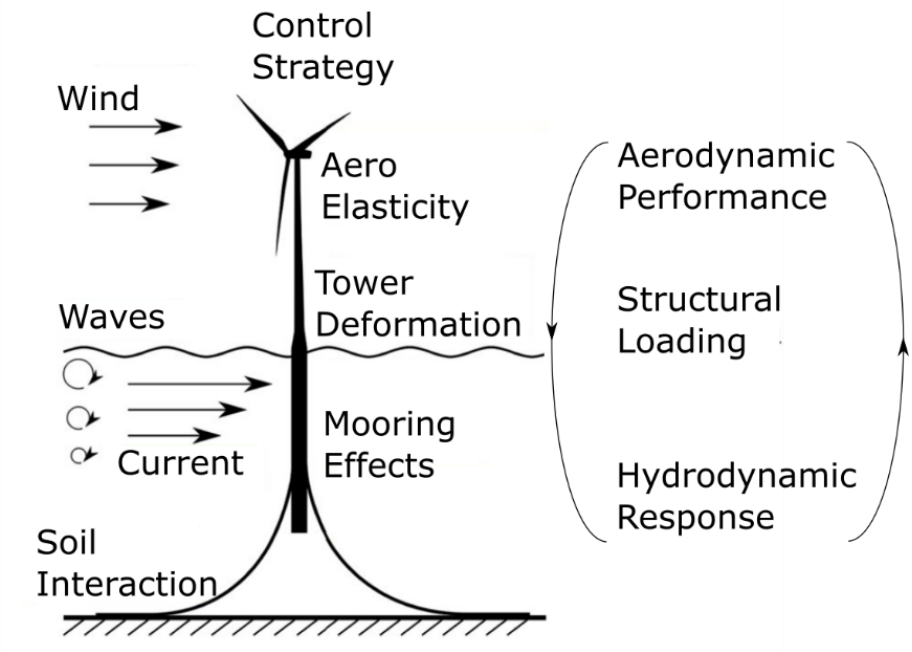

Figure 3 Complexity of a floating offshore wind system. Adapted from [5].

This project has received funding from the European Union's Horizon H2020 research and innovation programme under grant agreement No 815159

However, as illustrated in Figure 3, a FOW structure is a complex dynamic non-linear system, with different physics involved, which is not trivial to model. This becomes a challenging exercise in order achieve accurate results within reasonable computational costs, given the large design space involved. Furthermore, the need for optimization and reducing conservative safety margins, places higher demands on the numerical modelling accuracy, if such objectives are to be accomplished safely. As a result, significant effort is currently being placed in developing, testing, and validating simulation tools for FOW systems, such as the landmark IEA Task 30 Offshore Code Comparison Collaboration OC3-OC6 project series led by NREL. The numerical modelling of floating offshore wind systems is briefly reviewed in section 3, focusing on the state of the art, main challenges, and open literature results.

The simulation work carried out for PivotBuoy is summarized in section 3, followed by the comparison with other reference projects from the literature and the resulting discussion, which is presented in section 4. Finally, the main conclusions and future work are given in section 5

1.1 Objectives

The work developed on this deliverable focuses on positioning the PivotBuoy and assessing its merits when compared to other floating offshore wind systems. Namely, the objectives are to:

1. Compare the PivotBuoy design approach to other floating offshore wind systems.

2. Benchmark the performance of the large-scale 15 MW PivotBuoy X140 design, estimated from numerical simulations, against other similar floating offshore wind systems using publicly available simulation data.

1.2 Approach

The objectives stated above are achieved with the following approach:

1. Design Benchmark
    a. Literature review of the main FOW systems
    b. Categorization of these systems in groups with defining characteristics
    c. Description and position of the PivotBuoy concept
    d. Comparison of the different FOW categories and the positioning of the PivotBuoy within the context presented.

2. Simulation Benchmark
    a. Literature review of the numerical modelling of FOW systems
    b. Survey of publicly available data for other FOW systems
    c. Summary of the simulations carried out for the PivotBuoy concept
    d. Benchmark of PivotBuoy performance compared to other FOW systems.

This project has received funding from the European Union's Horizon H2020 research and innovation programme under grant agreement No 815159

2 REVIEW OF CURRENT FLOATING OFFSHORE WIND CONCEPTS

A review of FOW concepts is presented in this section. A brief historical perspective of FOW development if given in section 2.1. A common categorization used to classify these systems is introduced in section 2.2, followed by a brief discussion of each category main characteristics and leading designs. A few hybrid concepts that overlap these categories are also discussed. The PivotBuoy design is presented in section 2.3, and its categorization discussed. Finally, a general comparison of these systems is presented in section 2.4, with the PivotBuoy positioning within the reviewed concepts discussed in section 2.5.

2.1 Historic Perspective of Floating Offshore Wind

The historical evolution of the installed capacity of Floating Offshore Wind (FOW) projects is shown in Figure 9, where the most relevant projects are highlighted, including a prediction of the installed capacity in 2021 and 2022. It is clear that the research and development of FOW is still very recent. The first floating offshore wind project started only in 2008, installing an 80kW turbine in Brindisi, Italy. Since 2008 the increase in the number of projects, the number of turbines installed per project, and the increase in the turbine's total power capacity is a noticeable trend.

In the following years, the installed capacity rose markedly due to the WindFloat demonstration unit (2 MW) and the 2.3 MW Hywind installation in Norway. From 2013 to 2015, three turbines for a total of 16 MW were commissioned in Fukushima, Japan. After Fukushima's project, dramatic growth in installed capacity occurred in 2017 due to the Equinor project. Equinor consists of five 6MW turbines, totaling 30 MW, located 25 km off the East Coast of Scotland. Another relevant project is located in the UK. Kincardine B has 47.5 MW and is developed by Principle Power, one of WindFloat consortium partners. In 2021, another sharp increase in the cumulative installed capacity is expected due to 4 French floating projects totaling 97 MW. In 2021, CTG is also expecting to install its 5.5 MW floating offshore wind prototype. In 2022, Equinor, Korea National Oil Corporation and the Korean power company Korea East-West Power plant started constructing a 200 MW project called Donghae 1. Donghae 1 is located in Ulsan, South Korea. The installation is, however, dependent on feasibility studies [6, 7].

By 2030, industry experts estimate that around 5 GW to 30 GW of floating offshore capacity could be installed worldwide and that, based on the pace of developments across various regions, floating wind farms could cover around 5% to 15% of the global offshore wind installed capacity, which is estimated at almost 1 000 GW by 2050.

This project has received funding from the European Union's Horizon H2020 research and innovation programme under grant agreement No 815159

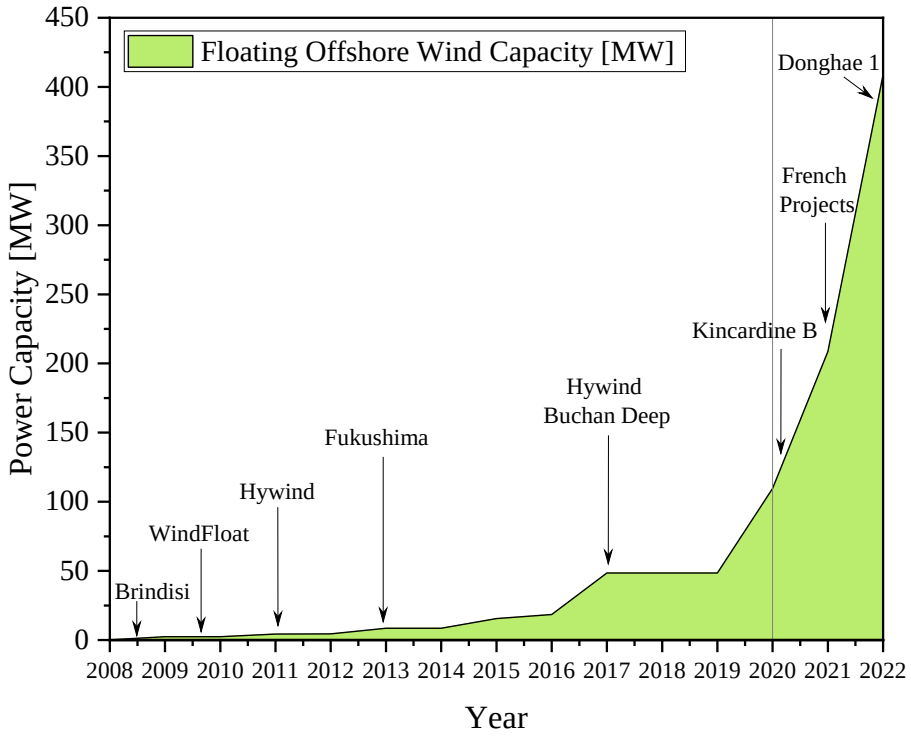

Figure 4 Historical cumulative installed capacity of floating offshore wind projects. Adapted from [6].

Regarding the distribution of floating offshore wind projects per country, Figure 5 identifies Japan's predominance, which accounts for 41.7 % of the total already developed projects. The following country is the UK, mainly due to Kincardine B and Hywind projects. Portugal, Sweden, Norway, the USA and France all rank in third place with a project developed per country. The review of projects, including decommissioned, planned, and in-place projects, identifies a worldwide total of 61 projects. As Figure 5 exemplifies, most floating offshore projects are in the concept/planning stage, while only 19.7 % (12 projects) are operational. According to the current status of the projects, the expectation of installed capacity growth is reinforced.

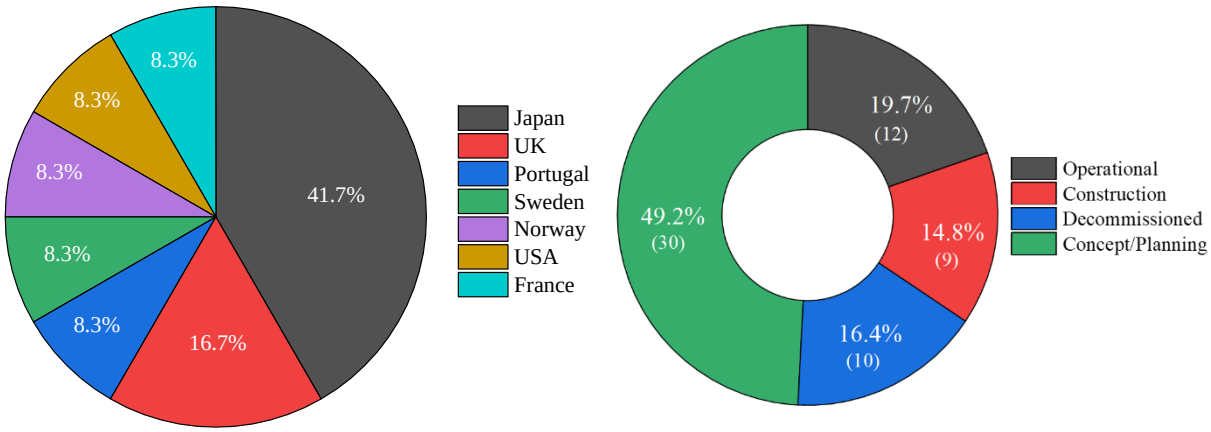

Figure 5 Share of developed floating wind projects by country (left) and status of the worldwide floating wind projects (right) as of 2019. Adapted from [6].

This project has received funding from the European Union's Horizon H2020 research and innovation programme under grant agreement No 815159

2.2 Categorization of Floating Offshore Wind Systems

A common categorization proposed by [8] is to distinguish the different floating wind systems based on their underlying static stability mechanisms. The three main categories are as follows:

- **mooring line stabilized**, where tensioned mooring lines provide the main restoring moment, e.g., tension leg platform (TLP);
- **ballast stabilized**, where a deep ballast lowers the center of gravity bellow the center of buoyancy providing the main restoring moment, e.g., spar;
- **buoyancy stabilized**, where the water plane area induces a large second moment of area, either by a large area (barge) or large are moment arm (semi-submersible), providing the necessary righting moment.

These categories are typically shown in a ternary plot, as seen in Figure 6, with the idealized cases on the vertices. In practice, the floating wind concepts rely on a combination of different mechanisms and fall somewhere between the vertices. This is particularly noticeable for hybrid concepts, which present innovative designs that rely on different features and cannot be completely described by a single category.

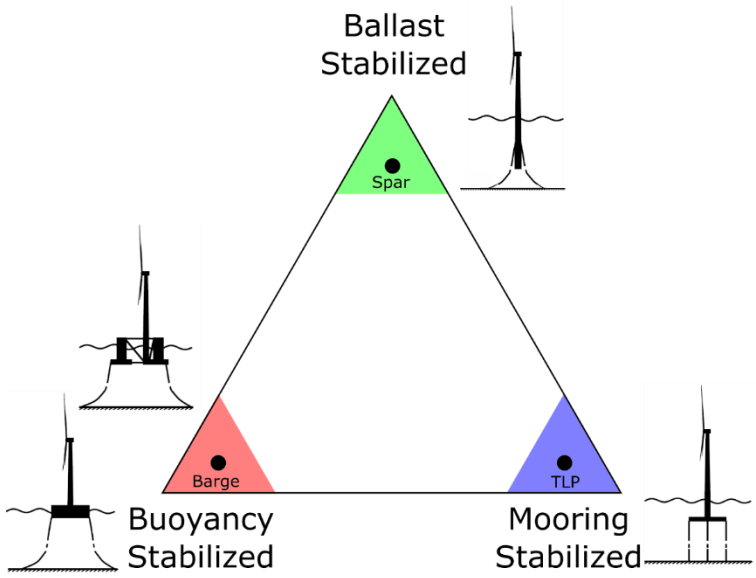

Figure 6 Representation of floating wind concepts as a function of their main stability drivers. Adapted from [8, 9, 10].

2.2.1 Mooring stabilized floaters

These concepts rely mostly on the mooring system to provide the necessary righting moment. The prime example of a mooring stabilized floater is the tension leg platform (TLP). The mooring system is comprised by several vertical tendons which are kept under tension in all conditions, due to the high net positive buoyancy, provided by the high-displacement, low-density floater. The anchors of the structure are typically gravity-based, suction or pile driven. Since the stability is provided by the mooring lines, the transit to site can be challenging, especially if the turbine is already integrated, and can require additional buoyancy elements or special support barges [11].

This project has received funding from the European Union's Horizon H2020 research and innovation programme under grant agreement No 815159

This approach enables a smaller lightweight design of the substructure, which is easier to fabricate and assemble, lowering costs and restrictions on port facilities. However, it requires special moorings (tendons) and anchoring system to withstand the high vertical loading, resulting not only in a more expensive mooring and anchoring system, but also in a more complex installation as well. Therefore, there is a shift in the CAPEX from the floater towards mooring/anchors costs and installation costs. This should result in a net reduction of the CAPEX for the TLP to be a competitive option [4, 12].

A significant benefit is the limited response in heave, roll and pitch due to the stiff tendons which typically shift the natural resonance to higher frequencies outside of the wave excitation. This reduces the turbine fatigue and dynamic cabling fatigue. However, it faces specific challenges, such as the 'pull-down' effect, which increases the draft as the platform is offset from its equilibrium position, or the ‘ringing’ phenomenon, where structural deformation response can be excited by higher order wave loads. A summary of the main benefits and challenges are presented in Table 1.

Table 1 Generic advantages and disadvantages of TLP type concepts.

TLP Advantages	TLP Disadvantages
Enables a lightweight floater design which lowers construction costs and provides good scalability for larger turbines.	Requires some form auxiliar stability during tow, such as temporary buoyancy elements or support barges [11].
Limited hydrodynamic response, with significant reduction of heave, roll and pitch.	The mooring/anchoring system is costly and requires complex offshore operations to install.
Small mooring footprint facilitates underwater management of umbilical cables and farm layout	Complex installation procedure requiring special vessels.

Several concepts have been presented that fall within this category. Examples of conventional TLP type structures include the TLP by MIT/NREL [13], the UMaine TLP [14], or the PelaStar TLP developed by Glosten Associates [15].

The PelaStar TLP, shown in Figure 7, is an example of classic TLP solution adapted for floating offshore wind. It consists of a single column with a five-arm foundation, each being moored by fiber rope tendons to high vertical-load anchors in the seabed [15]. This structure is sufficiently underwater to reduce its exposure to wave action and provides minimal response in heave, roll and pitch. There are publicly available estimations for the CAPEX and LCoE using this technology, with a median forecast of $LCoE_{2020}$ of 110 £/MWh in 2013 currency presented for exploitable UK waters [12]. The PelaStar TLP is currently at a “demonstrator-ready” stage for a 6MW turbine in the Celtic Sea off Cornwall, UK, although no developments seem to be made in the past years [16]. A recent partnership between GE and Glosten is developing a 12 MW turbine using the PelaStar foundation [17].

This project has received funding from the European Union’s Horizon H2020 research and innovation programme under grant agreement No 815159

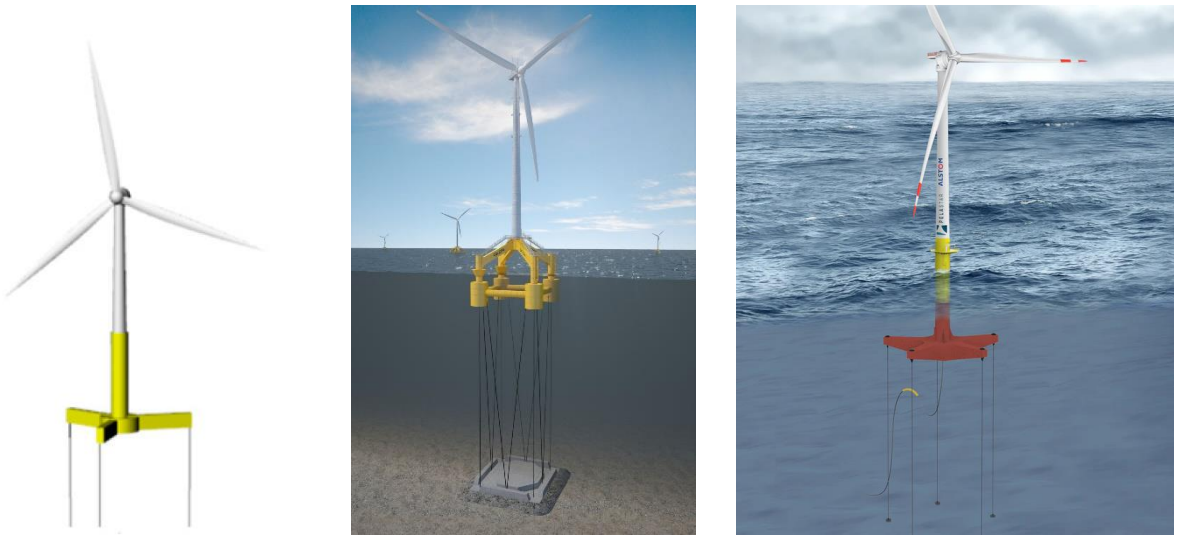

Figure 7 Several TLP concepts for floating offshore wind: the UMaine TLP (left) [14]., the GICON-SOF hybrid TLP [18], and the PelaStar TLP (right) [16].

There are other concepts in different stages of development that are not conventional TLPs. A notable example is the innovative GICON-SOF project which combines the advantages of a semi-submersible with those of a TLP. This project has iterated through a number of different designs [19], with the current iteration shown in Figure 7. This concept couples the TLP design with a lowerable gravity anchor base, which works as barge during transit to provide stability, and simplifies installation by ballasting the anchor to the seabed with the tendons already pre attached, as shown in Figure 8. This design adopts a buoyancy stabilized approach for assembly and transit, reverting to a mooring stabilized structure for operation. This approach retains the favorable motion response of the TLP and simplifies its installation process [20].

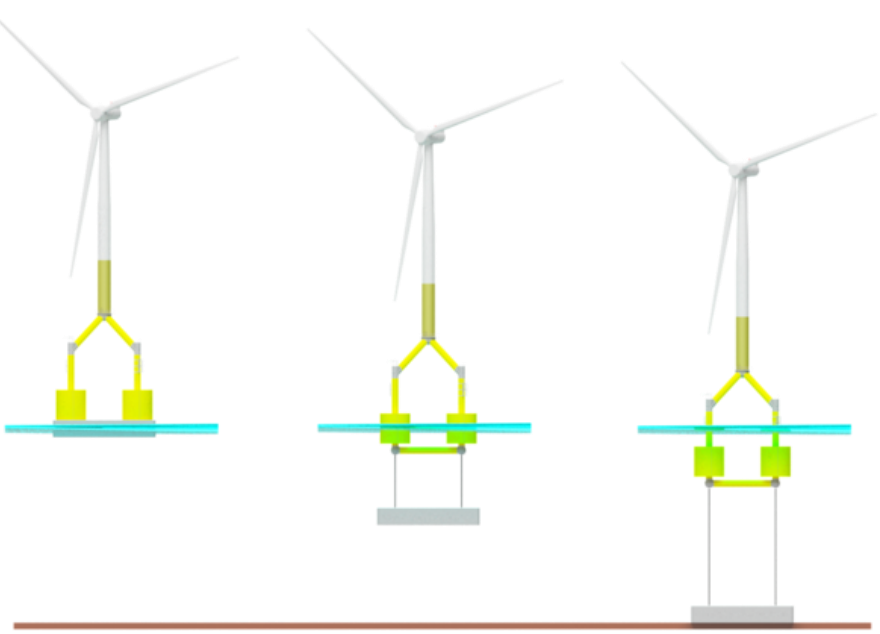

Figure 8 Transit and installation process of the GICON-SOF design. From left to right: transit to site with the gravity anchor base providing stability; at site ballasting the anchor to lower it to the seafloor; tension the tendons to achieve the operational draft. Source: Daniel Walia, Chair for Windenergy Technology, University of Rostock. [20]

This project has received funding from the European Union's Horizon H2020 research and innovation programme under grant agreement No 815159

In order to lower the CAPEX, two construction approaches are taken. The first is to use prefabricated components that are then transported to port, which allows for cheaper construction and puts less demands on the port facilities. However, transport needs to be considered. The second is to keep the design as light as possible using prestressed ultra-high-performance concrete (UHPC), which is 5 to 6 times cheaper than welded steel structures. A LCoE between 50-80€/MWh is expected for an 80x6MW farm in 2030, which is estimated to be up to 10% lower than a similar farm with a conventional TLP design [21].

2.2.2 Ballast stabilized floaters

Ballast stabilized concepts often rely on long cylindrical floaters which are ballasted at the bottom to lower the center of gravity below the center of buoyancy, thus providing the needed restoring moment. These foundations are simple shapes with a narrow profile, which is easy to fabricate and assemble, but are quite large and heavy structures. Only a small part of the foundation is exposed to wave action, limiting the wave forces [22].

A main feature of this design is the high stability achieved through high drafts, at the expense of some logistic challenges for the installation, namely the turbine integration and transit to site, and large water depths, especially for larger turbines. Turbine integration at port is unfeasible due to water depth requirements. The foundation is towed to sheltered waters where it is upended, and turbine integration is carried out using heavy lifting vessels. The water depth requirement also limits the tow-to-port maintenance strategy, which is only viable if sheltered waters at a sufficient depth are available close by. Therefore, heavy lifting at sea is expected for major repairs using this substructure, which will increase operational costs [12].

The standard mooring option for spars is a catenary mooring system, which is a simple low-cost mooring using drag embedment anchors and applicable to a wide range of water depths. However, relatively higher excursions are allowed, and the wide mooring footprints require effective subsea space management [22, 23]. Due to the low water plane area, cylindric shape, and catenary mooring, the heave and yaw response have low stiffness and damping, which can lead to unfavorable motion response, impacting turbine performance. A summary of advantages and disadvantages of spars is given in Table 2.

Table 2 Generic advantages and disadvantages of Spar type concepts.

Spar Advantages	Spar Disadvantages
Simple structural design facilitates fabrication and assembly	Requires a large and heavy structure, increasing costs.
Inherently stable once it is ballasted	Long draft poses logistic challenges, with turbine integration done in sheltered waters.
Simple mooring design	Can have large motions, with implications for the turbine accelerations and fatigue.

This project has received funding from the European Union's Horizon H2020 research and innovation programme under grant agreement No 815159

Figure 9 Spar buoy concepts: the OC3-Hywind (left) taken from [24]; 5MW downwind advanced spar (center) [25], and Hywind Scotland (right).

The most notable example of a classic spar for floating offshore wind is the Hywind spar project, which started with the 2.3MW Hywind Demo installed in 2009 and still in operation. Based on the lessons learned in the Hywind Demon, the Hywind Scotland project was developed in 2017, consisting of five 6MW turbines installed off Aberdeenshire, Scotland. The project Hywind Tampen is scheduled to start late 2022, installing 11 spars equipped with 8MW turbines to power five offshore platforms in the North Sea [26].

Within the phase IV of the OC3 project [24], a Hywind spar buoy concept was adapted to support the NREL 5MW turbined, which was named the OC3-Hywind (Figure 9). An extensive simulation campaign with different codes was carried out for this concept, from static equilibrium checks and eigenmode analysis, up to aero-hydro-servo-elastic response in irregular waves. Therefore, the OC3-Hywind spar is one the most simulated FOW spar concepts.

The Japanese Kabashima Goto Island project installed a 2MW downwind turbine on a hybrid spar in 2013. The design is optimized for lower construction costs by using two independently manufactured sections: a top section made of ring-stiffened steel; and a lower section made of precast prestressed concrete, including horizontal fins to mitigate yaw response. The downwind turbine has the capacity to passively weathervane [27]., which removes the need for an active yaw system, reducing mass at hub height at a small turbine efficiency penalty. A smaller 100kW prototype installed in 2012 was operational for one year, where it was exposed to a severe typhoon event [28]. This event led to a series of simulations of the typhoon event with satisfactory results [29, 30, 31].

The Fukushima FORWARD Project includes Fukushima Hamakaze, a 5MW downwind turbine with an “advanced spar” foundation [32] shown in Figure 10. This design aims to provide a more compact design by reducing the draft at the expense of diameter, while improving its motion characteristics by adding stabilizing fins and heave plates [23]. This project has since been scheduled for decommissioning due to low profitability.

This project has received funding from the European Union’s Horizon H2020 research and innovation programme under grant agreement No 815159

Figure 10 Advanced spar design of the fukushima Hamkaze showing underwater section (left) and floating substation (Fukushima Kizuna) with the advanced spar design being towed to site (right). [25]

Another approach is taken by WindCrete, which minimizes the CAPEX by reducing construction costs through a single continuous spar and tower concrete structure. This single continuous structure does not require any joints between the foundation and the tower, which is often a weak point susceptible to fatigue. The concrete substructure is expected to have more than 50 years lifetime, contributing to a lower LCoE. A 2015 analysis estimates a LCoE of 120€/MWh for a 500MW farm using 4MW turbines [33], with a more recent analysis estimating from 70-120€/MWh for a 500MW using 10MW turbines, depending on site selection [34].This concept is currently being adapted for a 15MW turbine within the COREWIND project [35].

2.2.3 Buoyancy stabilized floaters

These concepts rely on a large second moment of area to provide the necessary the righting moment. This can be achieved with a large waterplane area (barge type) or by increasing the moment arm of the water plane area using column stabilized floaters (semi-submersible type). While there are several developers using semi-submersibles, only a few currently pursue the barge type solution. These concepts often adopt a catenary mooring system and some type of motion improving device, such as the damping pool for the barge type Floatgen by Ideol, or water entrapment plates in the semi-submersible WindFloat.

The semi-submersibles rely on column buoyancy to provide the restoring moment, which can lead to larger designs as the turbines increase in size. The hull is often comprised of three to four steel columns, connected by steel bracers, which requires significant welding at port increasing costs. These larger dimensions can pose some logistic challenges, but the overall low draft and stability facilitate turbine integration at port and installation without specializes vessels, lowering installation costs [12]. The lower draft enables operation at shallower waters, making this design feasible for a wide range of water depths and ports. Furthermore, the low draft and transit stability also enable a tow-to-port maintenance strategy for major repairs, which can significantly lower operational costs [12]. Once at site, the semi-submersible is ballasted to its operational draft. Semi-submersibles typically have a large area exposed to wave action, which can lead to significant wave loading on the

This project has received funding from the European Union's Horizon H2020 research and innovation programme under grant agreement No 815159

structure, including higher order wave loading effects which cannot be neglected [18, 19].

The dimensions of the semi-submersible can be optimized such that its response is outside the wave excitation frequency. However, heave and pitch modes can be challenging, which is often mitigated by adding heave plates or water-entrapment plates to mitigate its response. The mooring system is usually a simple catenary mooring using low cost drag embedment anchors, which simplifies installation and lowers mooring costs. However, relatively higher excursions are allowed, and the wide mooring footprints require effective subsea space management [22, 23]. A summary of advantages and disadvantages is given in Table 3.

Table 3 Generic advantages and disadvantages of semi-submersible type concepts.

Semi-submersible Advantages	Semi-submersible Disadvantages
Low draft enables turbine integration at port	Larger dimensions and complex structure increase costs of the foundation
Simple installation due to stability at a low draft	More exposed to wave action, increasing the loading on the structure.
Simple mooring design	Can have large motions, with implications for the turbine accelerations and fatigue.

The barge design relies on a large continuous waterplane area to provide its static stability, as opposed to the discontinuous columns stabilized approach of the semi-submersibles. One of the drawbacks of this structure is its susceptibility to the roll and pitch motions. Thus, the barge structure is better suited for calm seas. The barge-type structure's advantages are easy installation, no need for specialized vessels, and high adaptability to a wide range of seabed geologies, implying a low site dependency

A barge floater developed by Ideol is comprised by a ring-shaped floater featuring a damping pool inside the ring, which counters the wave excitation to improve performance and stability. This concept is unique among other floating wind foundations due to its compact design and damping pool feature, which makes non-linear effects important [36, 37]. A 2MW demonstrator called Floatgen was installed in the French Atlantic coast in 2018. A second demonstrator named Hibiki-Nada with 3 MW is operating in Kitakyushu, Japan, where it survived three typhoons since its installation in 2018 [38]. The fist pre-commercial project with three units with a total of 30MW is scheduled to start operating 2022-2023 in the French Mediterranean Sea [39].

A significant number of developers have adopted a semi-submersible design with a catenary mooring system, of which only a few will be mentioned here. For a broader review see [4, 23].

This project has received funding from the European Union's Horizon H2020 research and innovation programme under grant agreement No 815159

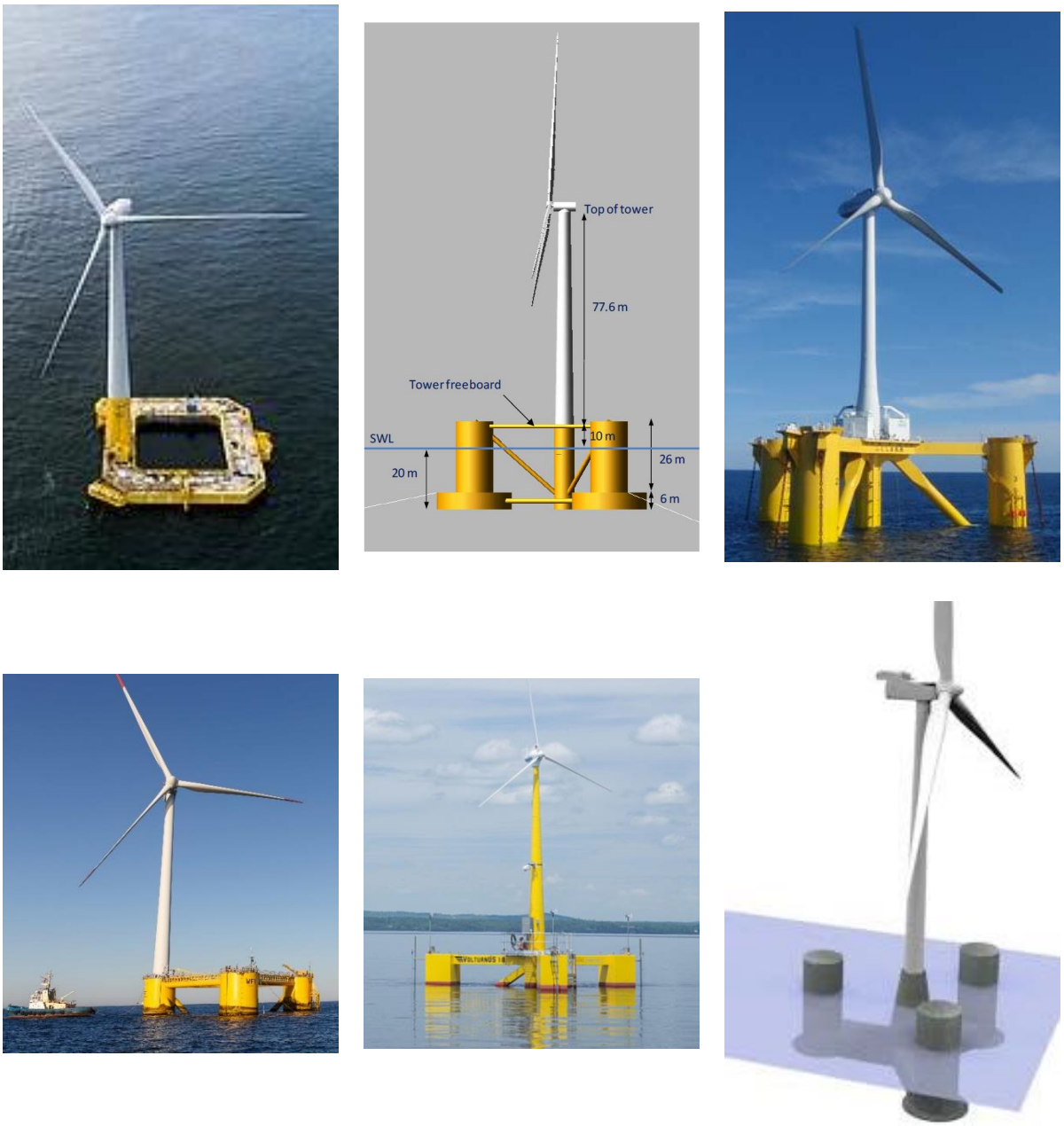

Figure 11 Examples of buoyancy stabilized floaters for wind turbines, top row, from left to right: Floatgen barge [39]; the OC4-DeepCwind floater [40]; Fukushima Mirai [41]. Bottom row, from left to right: one of the three floaters of the Windfloat Atlantic [42]; VolturnUS prototype [43]; and ActiveFloat concept [44].

A notable example is the Windfloat semi-submersible by Principle Power [45], which features a three column semi-submersible with heave plates, an active ballasting system, and is supported by a catenary mooring system. A full scale 2MW prototype (WF1) operated for 5 years in Portugal under the North Atlantic conditions, after which it was successfully decommissioned. In 2020 the Windfloat Atlantic (WFA) project (Figure 11) completed its first pre-commercial offshore floating wind farm with 25MW (3x8.3MW) installed offshore Portugal. Other projects currently being developed with the Windfloat technology include the Eoliennes Flottantes du Golfe du Lion (EFGL) in the Mediterranean Sea, Kincardine Offshore Windfarm (KOWL) in the North Sea, where the first WF1 is now currently installed, and the Windfloat Japan [46].

This project has received funding from the European Union's Horizon H2020 research and innovation programme under grant agreement No 815159

The Fukushima Offshore Wind Consortium has developed an installed a “compact semi-submersible” with a 2MW downwind turbine in 2013 which is still in operation, commonly referred as Fukushima Mirai (Figure 11). This is a catenary moored four-column semi-submersible, with three outer columns and a smaller center column where the turbine is mounted [41]. In 2015, during the second phase of the Fukushima FORWARD project, a “V-shaped” floater designed by Mitsubishi Heavy Industries (MHI) was deployed. This semi-submersible has three columns connected by two long pontoons, which provide enough buoyancy for a low draft float-out from port with the 7MW turbine installed. This semi-submersible has since been decommissioned due to low profitability [47].

The OC4-DeepCwind semi-submersible [40] with the NREL 5MW reference turbine [48] was used as a benchmark to test, improve, and compare several codes [49]. The subsequent OC5 project carried out model test of the same floater to validate the ultimate and fatigue loads predicted by the numerical models [50]. The numerical simulations showed a consistent trend to underpredict the ultimate and fatigue loads when compared to the experimental results, as reproduced in Figure 12. It was proposed that the differences stem from the hydrodynamic modelling, in particular the low frequency response outside of the wave excitation range that excite surge and pitch response [50]. These areas are currently under investigation in the new OC6 project phase I [51], which focuses on the validation and uncertainty quantification of the nonlinear hydrodynamic loading, while also adding higher fidelity tools (CFD) to the simulation approaches considered [52]. In fact, higher fidelity simulations tools (CFD) have been applied to the OC4-DeepCwind semi-submersible to assess damping [53, 54] or response in waves [55], including recommendations on how to apply CFD to floating offshore wind turbines [5]. This large scope of work carried out for the OC4-DeepCwind semi-submersible makes it an ideal candidate for benchmarking simulations tools or methods.

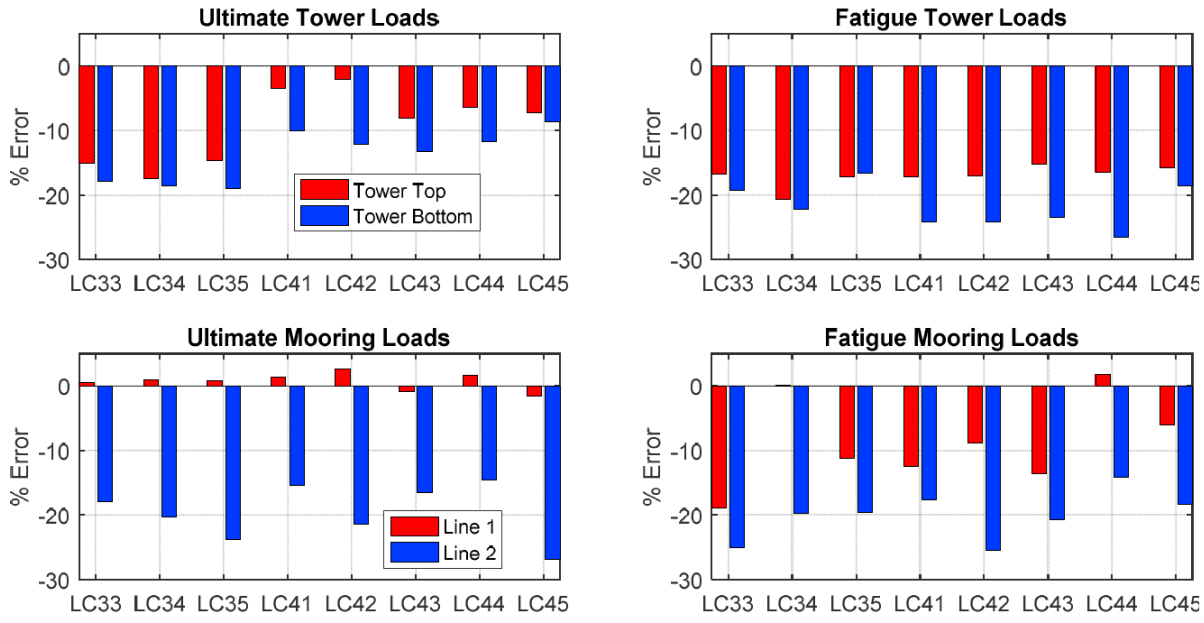

Figure 12 Underprediction trend of the numerical models’ estimation for ultimate and fatigue loads when compared to the experimental results for the OC4-DeepCwind semi-submersible. Reproduced from [50].

This project has received funding from the European Union’s Horizon H2020 research and innovation programme under grant agreement No 815159

The VolturnUS, which has been developed by the DeepCwind consortium [56] led by the University of Maine (UMaine), is currently the only floating offshore wind project implemented in the US. The 20 kW 1:8 prototype is located in Maine and started operation in 2013. Some of the VolturnUS project developers plan to install a 12 MW demonstration project in 2022. The new project, entitled Maine Aqua Ventus, is the only recently approved floating project in the US. It will feature two 6 MW turbines using the same floating structure of VolturnUS. Recently, a steel-based variation named VolturnUS-S has been developed within the IEA Wind Task 37 [57] to be ablet to support the new 15MW offshore reference turbine. A recent report estimated an LCoE under $60/MWh for the VolturnUS technology at commercial scale [58, 43]. If these LCoE forecasts are verified during the Maine Aqua Ventus project, this will be the lowest LCoE for a floating offshore wind solution to date.

The ActiveFloat is a concrete semi-submersible concept developed by Esteyco. The choice of concrete potentially leads to a durable and cheaper design when compared to steel. This floater is comprised of three external columns, each with a heave damping plate, connected by three prismatic pontoons to a central conical column, where the turbine tower is installed. The pontoons are permantely ballasted with sea water, while the external columns are partially filled with water, using an active ballast system. A catenary mooring system is employed for stationkeeping [44].

2.2.4 Hybrid concepts

Hybrid concepts refer to designs that rely on a combination of the previous stability principles, often taking an innovative approach that does not lend itself to the typical TLP, semi-submersible, or spar classification. These concepts can combine in a single floater benefits associated with different structures, however there is higher risk and uncertainty due to the higher degree of innovation involved. A few concepts (see Figure 13) will be discussed here, with more extensive lists available elsewhere (e.g. [23]).

The **Tension Leg Buoy (TLB)**, shown in Figure 13, is a spar type floater with excess buoyancy to keep six inclined mooring lines under tension, which provide the necessary stability. This approach allows for a lightweight spar design with lower drafts. The taut moorings provide high stiffness, resulting in smaller wave excitation response, at the expense of the more complex and costly mooring system [23, 59]. This concept first iteration was in 2005 and is known as the MIT Double Taut Leg [8]. A key concern for this concept is the high mooring and anchor loads, increasing costs and limiting site selection due to the seabed and depth restrictions. Newer iterations have been proposed, such as the TLB B with the 5MW reference turbine, which addresses these concerns and is a step forward in its development. [2].

The **Swinging Around Twin Hull (SATH)** developed by Saitec Offshore is an innovative concept that consists of an upwind turbine, installed on a floating platform built in concrete, with a semi-submerged twin hull to improve stability, and a single point mooring turret (SPM) based system which connects to all mooring lines as well as the power cable. The turret system of the SATH platform is moored to the seabed through drag anchors and six catenary lines in three groups of two lines oriented at 120 degrees to each other [60]. In August 2020, a SATH demonstrator (BLUESATH) at a 1:6 scale of the 10 MW concept was deployed for a 12-month period of testing in open sea

This project has received funding from the European Union's Horizon H2020 research and innovation programme under grant agreement No 815159

waters, offshore of Santander, Spain. Unfortunately, this testing period was cut short in November, when an historic swell capsized the structure. The prototype was exposed to 10-meter waves when it capsized, which corresponds to a 60 meter wave at full scale. Prior to that it had survived storms with 8-meter waves, which corresponds to 48 meter wave full-scale. Considering the prototype was designed for a 30 meter wave, this was considered a successful demonstrator despite its short operation time [61].

Figure 13 Examples of hybrid concepts, top row from left to right: TLB conceptual design, source: [2]; BlueSATH demonstrator; and Eolink demonstrator, source: [62]. Bottom row, from left to right: W2Power demonstrator, source: [63]; and Hexicon concept TwinWind, source: [64].

The **EOLINK** concept, patented by the French company Eolink, consists of a semi-submersible floater with 4 columns, and an external single point mooring system which is connected to the floater by two hawsers. The typical wind turbine tower is replaced by four inclined masts, two upwind and two downwind, which reduce the mass and improves structural resistance. This allows for the installation of larger rotors in a more compact floater, reducing the costs. Model test results were used to

This project has received funding from the European Union's Horizon H2020 research and innovation programme under grant agreement No 815159

calibrate numerical models [65, 66], however there is limited public information on the simulation work carried out for this concept. A 1:10 demonstrator was anchored and connected to the grid in April 2018, undergoing a series of tests for over a year. In March 2020, Ocean DEMO, a EUR 13 million Interreg-funded project has greenlighted the deployment of Eolink's 5 MW project, scheduled to be installed in 2022 [67].

The **TwinWind,** developed by Hexicon, is a semi-submersible with three columns, two of which carry upwind turbines, while the third is moored with a turret type system that handles station keeping and electrical cable connection. This mooring approach allows the system to passively weathervane and orient itself with the wind. The double turbine per floater increases power density at the expense of added complexity and loading on the system [68]. A 10 MW demonstrator was expected to be deployed in 2020 in Scotland, however the project is currently on-hold.

The **W2Power** is a mixed energy concept promoted by EnerOcean which combines wind and wave energy in the same floater in order to increase power density and lower the LCOE. However, this increases the overall complexity of the system, which remains a challenge for mixed energy concepts [23, 69]. The W2Power concept features a twin-turbine (upwind) floating offshore wind power concept, with a triangular-shaped semi-submersible platform built in steel that weathervanes into the wind. The platform is connected to the seabed through a single point turret-based mooring system, integrated in the leading column of the semi-submersible. The W2Power concept is currently at TRL 6, with a 1:6th scale demonstrator that has been under sea trials since June 2019 at the PLOCAN testing site with two 100kW turbines, however the ongoing sea trials do not include the wave energy converters [70].

2.3 PivotBuoy Concept

2.3.1 PivotBuoy subsystem

The PivotBuoy (PB) is a novel subsystem that integrates the mooring system and the electric cable into a single point mooring (SPM). This combines the advantages of single point mooring systems with the stability and low weight of TLP designs, reducing construction costs.

Its modular design is comprised of two bodies, the lower body and upper body, as seen in Figure 14. The lower body is simple three-legged body with excess buoyancy that is permanently moored to a gravity-based anchor through a tension leg system, where the umbilical cable is also connected, as shown in Figure 14. The upper body of the PB is integrated into the floating foundation and can be quickly connected or disconnected from the lower body in case of need.

One advantage of this system is the possibility to disconnect the floating foundation quickly and simultaneously from its mooring system and electrical cable, tow the foundation to a nearby port or sheltered waters, either to perform complex maintenance operations or to avoid extreme weather, and tow it back to site to resume operation. Therefore, the PivotBuoy system enables a so-called

This project has received funding from the European Union's Horizon H2020 research and innovation programme under grant agreement No 815159

Tow-to-Port (TTP) maintenance approach, where the large repairs can be carried out at port, which can be an advantage and a significant driver to reduce the O&M costs, and ultimately the LCOE [12].

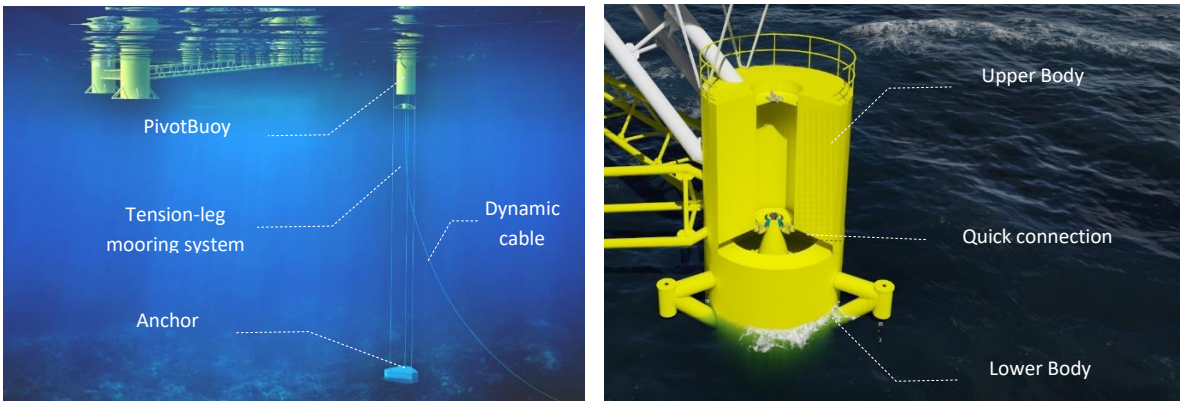

Figure 14 Schematic representation of the PivotBuoy subsystem, showing the mooring system and electrical cable (left) and the connection system to the floating foundation (right).

2.3.2 X1Wind X140 Floating Offshore Wind Design

The X1Wind X140 is the full-scale PivotBuoy platform system developed by X1Wind to accommodate a downwind version of the 15MW offshore reference turbine developed within the IEA Wind Task 37 [71]. A view of the whole assembly is presented in Figure 15.

Figure 15 X1Wind X140 concept design, including the PivotBuoy subsystem and the reference offshore 15MW turbine (left). Artist impression of the X30 prototype in the Canary Islands (right).

This project has received funding from the European Union's Horizon H2020 research and innovation programme under grant agreement No 815159

Similarly to the part-scale prototype X30 to be installed at PLOCAN, the platform structure itself is split in a small tension leg platform (TLP), which is installed independently and provides the station keeping and electrical connection, and the rest of the structure, resembling a low weight semi-submersible. This semi-submersible is comprised of two main columns and the PivotBuoy top column. The columns are connected by a twin pontoon with a jacket style bracing system. Heaving plates installed in the two aft columns and in between the pontoons, to mitigate the heave and pitch motion response. The turbine nacelle is supported by three upper masts that connect to each column, instead of the typical single tower support, reducing tower bending moments. A downwind turbine is installed, allowing the concept to weathervane freely around the mooring point and passively orient itself with the incoming wind. This removes the need for an active yaw system, reducing the mass located at hub height. Furthermore, there is no need for preconing and blade pre-bending, since the turbine blades will deflect away from the support masts while under load.

This concept merges a TLP mooring system, with the ease of installation of a semi-submersible, and the weather vanning capacity of single point mooring systems with a downwind turbine. The TLP mooring solution enables a low weight design of the platform, lowering construction costs. The stability during transit is provided by the three columns, which enables turbine integration at port and facilitates the installation process, reducing the costs. The ability to quickly disconnect the platform is designed for a tow-to-port strategy, which reduces operational costs.

2.4 Comparison Between Foundations

A general overview of the discussed benefits and challenges of each category is given in Table 4, with a more detailed analysis of these systems found for example in [23]. The hybrid designs attempt to merge some of these concepts to combine desirable features and mitigate possible weaknesses. A general overview of current concepts above TRL 3 is given in Figure 16, showing the distribution of designs according to their category, with the indicative TRL of the different concepts given in Figure 17.

Regarding the classic oil and gas designs, there are more floating offshore wind designs adopting a semi-submersible approach than spars or TLPs. The more advanced designs are the Hywind Spar and the Windfloat semi-submersible, both with active pre-commercial arrays, as seen in Figure 17. The TLP design is still lagging behind in terms of TRL when compared to the other categories. A significant number of innovative hybrid designs are emerging, typically associated with lower TRLs, with the front runners of this class reaching TRL 5-6.

This project has received funding from the European Union's Horizon H2020 research and innovation programme under grant agreement No 815159

Table 4 Summary of the strengths and weaknesses for the classic oil and gas foundations applied to floating offshore wind systems. See e.g., [23] for a more detailed assessment.

	Strengths	Weaknesses
Spar	• Inherently stable • Simple structural design facilitates fabrication and assembly • Cheap and simple moorings • Limited wave action exposure	• Large and heavy structure • Large excursions • Complex turbine integration offshore requires special vessels • Large mooring footprint • Unsuitable for shallow waters
Semi-submersible	• Low draft reduces port restrictions • Allows turbine assembly at port and simple installation process • Cheap and simple moorings • Applicable to a wide range of water depths	• Larger complex structure • Exposed to wave action • Large excursions • Hydrodynamic response (can be mitigated by heaving plates • Large mooring footprint
TLP	• Simple, small, and lightweight • Limited motion response • Limited wave action exposure • Small mooring footprint • Allows turbine integration at port if supported with buoyancy elements.	• Only stable when moored • Complex mooring and anchoring system, requiring pre-installation work. • Complex installation procedure using special vessels • Unsuitable for shallow waters • Seabed restrictions due to special anchoring system

This project has received funding from the European Union's Horizon H2020 research and innovation programme under grant agreement No 815159

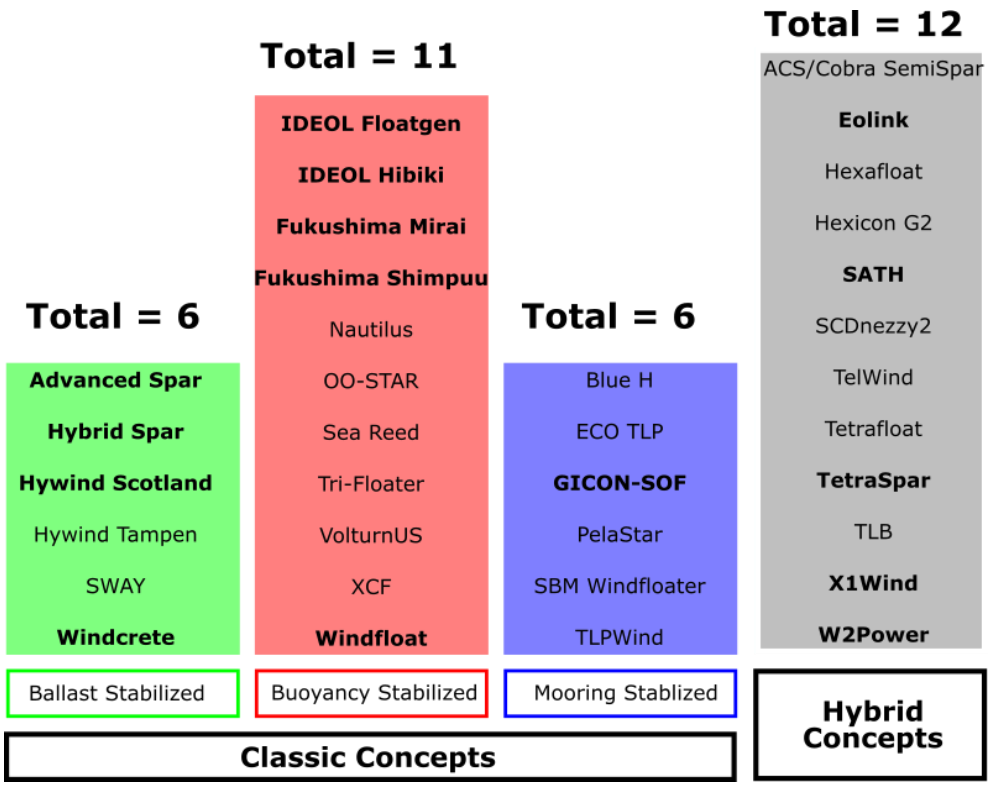

Figure 16 Number of different concepts per category, above TRL 3. Projects that are on active demonstration or pre commercial phase are highlighted in bold. Adapted from [4, 72].

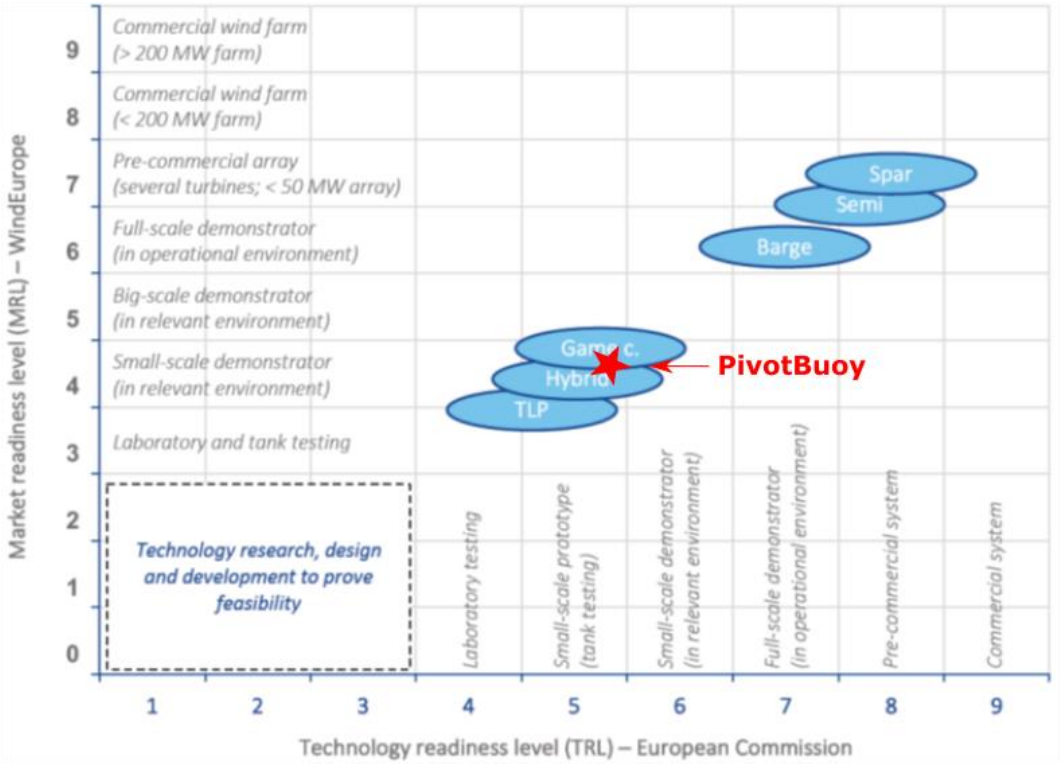

Figure 17 Indicative TRL and MRL levels for floating offshore wind systems for different foundations, including the X1Wind floating wind system using PivotBuoy. Adapted from [4].

This project has received funding from the European Union's Horizon H2020 research and innovation programme under grant agreement No 815159

There is no commercial floating offshore wind farm operating, even the most advanced designs are just entering their pre-commercial phase. Therefore, LCoE estimations have a high uncertainty and need to be interpreted with caution. A comparison of the estimated LCoE for a 100x5MW floating offshore wind farm is shown in Figure 18. However, the main take way is the need to reduce the overall LCoE floating wind systems in order to be competitive with renewable energy systems. The necessary LCoE reduction can be achieved by targeting three main areas [72]:

- CAPEX reduction, where manufacturing costs and installation costs have potential for reduction using new materials or by simplifying the installation, avoiding the use of dedicated vessels with high charter rates.
- OPEX reduction, such as reducing the fatigue damage to the system so that higher reliabilities can be achieved, or simplifying O&M operations.
- Increase energy production, through continued development of turbine technology such as blade manufacturing, control strategies, or simply scaling up the turbine rated power.

The PivotBuoy system tackles all these factors. CAPEX reduction through a significant platform weight reduction in the foundation construction, and simplification of the assembly and installation process when compared to the classical TLP concepts. OPEX reduction by its quick (dis)connection system that allows a tow-to-port maintenance strategy. The scalability of the PivotBuoy system favors larger wind turbines, promoting the power produced per weight ratio.

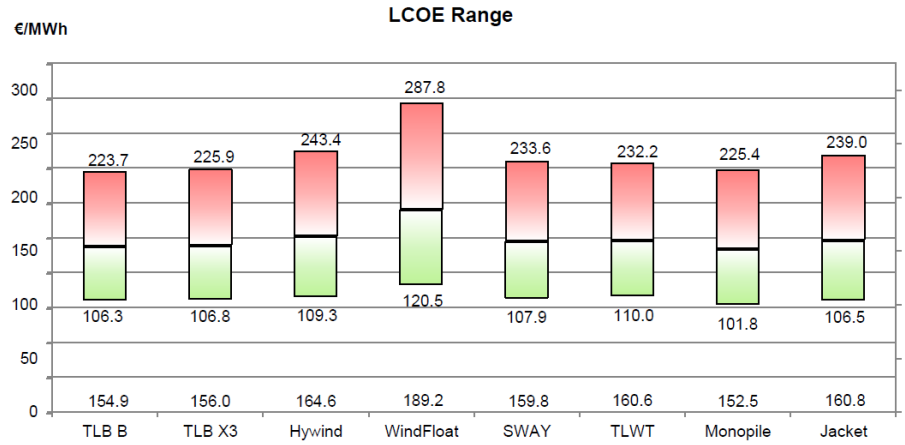

Figure 18 Estimated LCoE range for a 100x5MW farm using different floating offshore wind systems. Reproduced from [2]

This project has received funding from the European Union's Horizon H2020 research and innovation programme under grant agreement No 815159

2.5 Benchmarking PivotBuoy Against Other Floating Offshore Wind Systems

The X1wind floater is clearly positioned within the hybrid concepts with its innovative and disruptive design. A significant number of innovative hybrid concepts are emerging and installing small scaler prototypes as they progress to the demonstrator stage. The PivotBuoy system is well placed within its class as a hybrid TLP concept, with the X1Wind X30 the first PivotBuoy prototype in real operational environment, reaching TRL levels of 5-6 by the end of the PivotBuoy project.

Due to the integration of the PivotBuoy system, the floater can achieve the TLP simple lightweight platforms with limited hydrodynamic response while keeping the semi-submersible low draft and some tow stability. This is a similar approach to the TLP GICON-SOF, that also bridges TLP and semi-submersible characteristics.

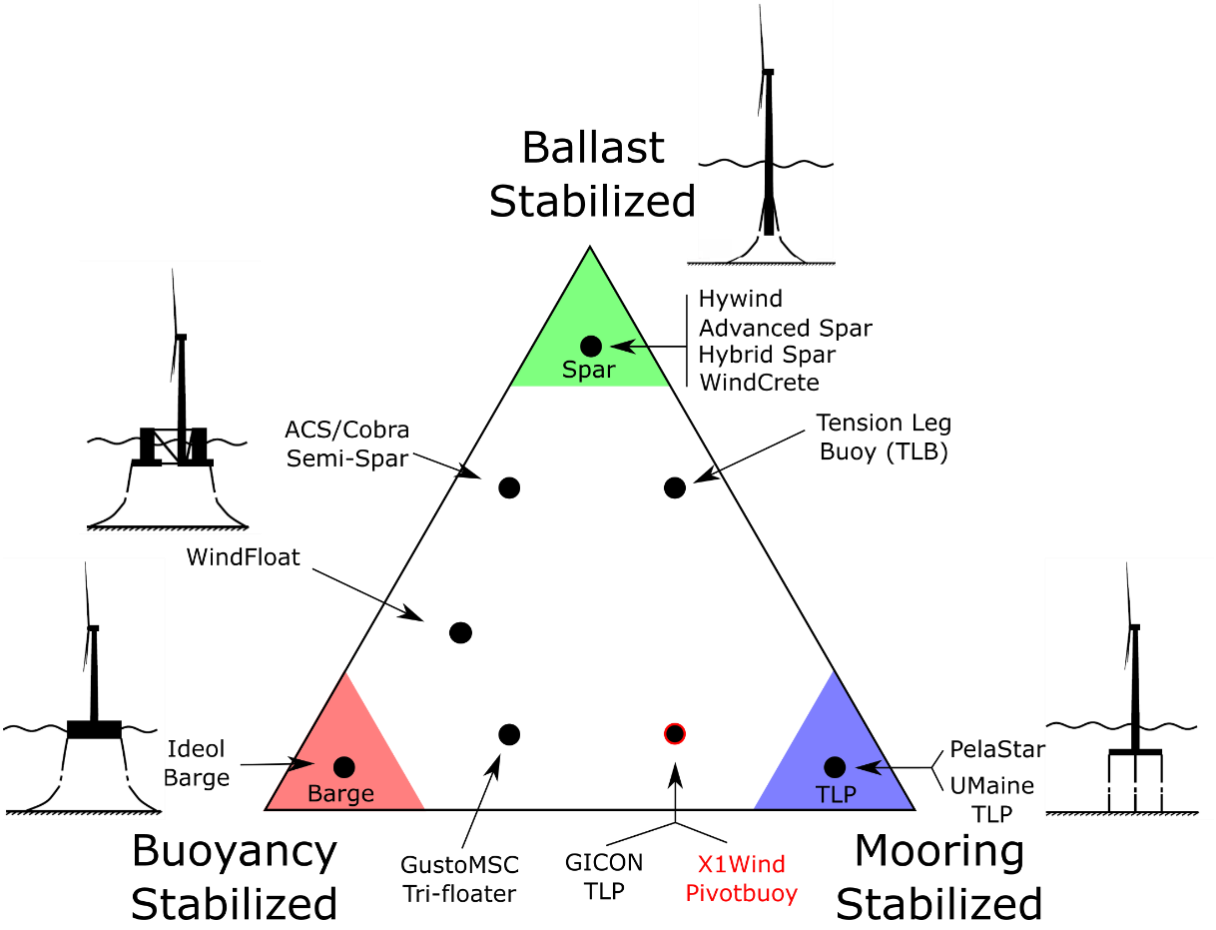

Figure 19 Positioning of X1Wind PivotBuoy amongst other floating wind concepts as a function of their main stability drivers. Adapted from [8, 9, 10].

This project has received funding from the European Union's Horizon H2020 research and innovation programme under grant agreement No 815159

Another characteristic of the PivotBuoy system is its single point mooring system approach that allows the connected platform to weathervane. The weathervanning single point mooring approach is present in other concepts as shown in Figure 20. It can be found integrated into the foundations, as seen in the single upwind turbine SATH concept developed by Saitec, or the multiple upwind turbine concepts such as W2Power or Hexicon-G2. Eolink also utilizes a single point mooring buoy that is then connected to the foundation by a hawser system, instead of integrating the single point mooring system into the foundation itself. However, the PivotBuoy system allows a quick connection/disconnection of the foundation to the seabed, which enables a tow to port strategy. The possible integration of PivotBuoy into these systems has been investigated within the PivotBuoy project based on the following metrics: technology TRL; levelized cost of energy (LCOE); benefits due to PivotBuoy; retrofitting effort; expected PivotBuoy design adjustments [73].

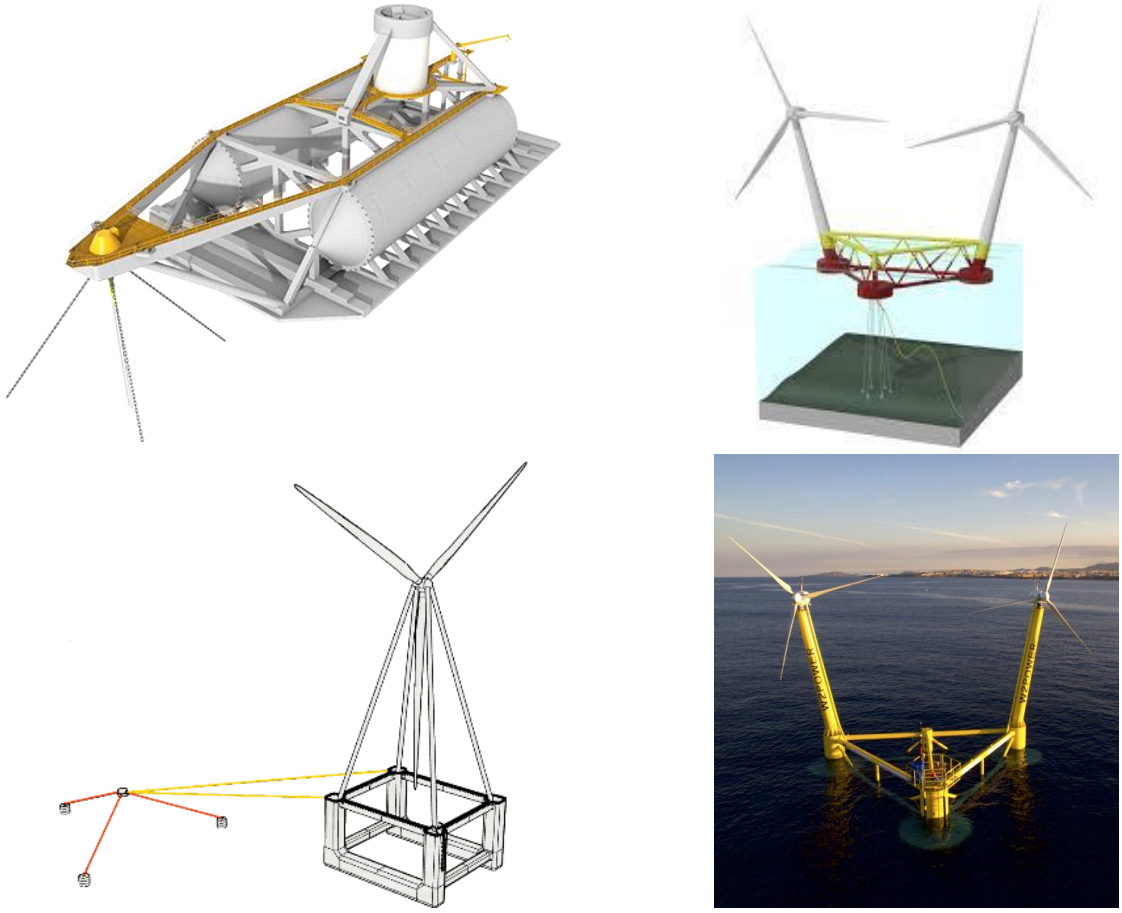

Figure 20 Hybrid floating offshore wind concepts that use a single point mooring system (SPM). From the top right, in a clockwise direction: SATH concept with the SPM with taut mooring lines; Hexicon-G2 with a TLP type SPM; W2Power with the mooring connected to the column without a turbine; and Eolink, with a catenary SPM connected by two hawsers to the foundation.

This project has received funding from the European Union's Horizon H2020 research and innovation programme under grant agreement No 815159

3 REVIEW OF MODELLING FLOATING OFFSHORE WIND SIMULATIONS

A brief review of floating offshore wind numerical modelling is presented in section 3.1, focusing on the different areas of interest that need to be modeled to accurately represent a floating offshore wind turbine. A summary of the simulations carried out for the full scale X1Wind X140 foundation, equipped with a downwind version of the IEA 15MW offshore reference turbine [71], is provided in section 3.2.

3.1 Numerical Modelling of Floating Offshore Systems

Numerical models have been instrumental to the development of wind energy, leading wind turbines to become one of the largest flexible rotating man-made structures in the world [74]. However, new challenges arise as the wind turbines become larger, in particular for floating offshore wind, due to the motions of the floating foundations [62]. The dynamic interaction between wave response and turbine performance is one of these challenges. The floater is constantly moving in response to the wave loading, with this motion transmitted through the tower to the rotor, where the large, flexible turbine blades are constantly rotating due to wind action. These motions are imparted to the flexible blades, changing the aerodynamic loading and performance. On the other hand, the aerodynamic loading is also transmitted through the tower to the floater, influencing the hydrodynamic response, resulting in a coupling between aerodynamic and hydrodynamic loading. While these excitations have been studied in the past, e.g., wind excitation for onshore wind turbines or wave excitation of oil and gas platforms, floating offshore wind systems are unique in that the aerodynamic loading and wave loading are not only of similar importance, but also heavily coupled. This dynamic coupling is critical, and thus needs to be captured by the numerical models in order to accurately predict the behaviour of the system [62].

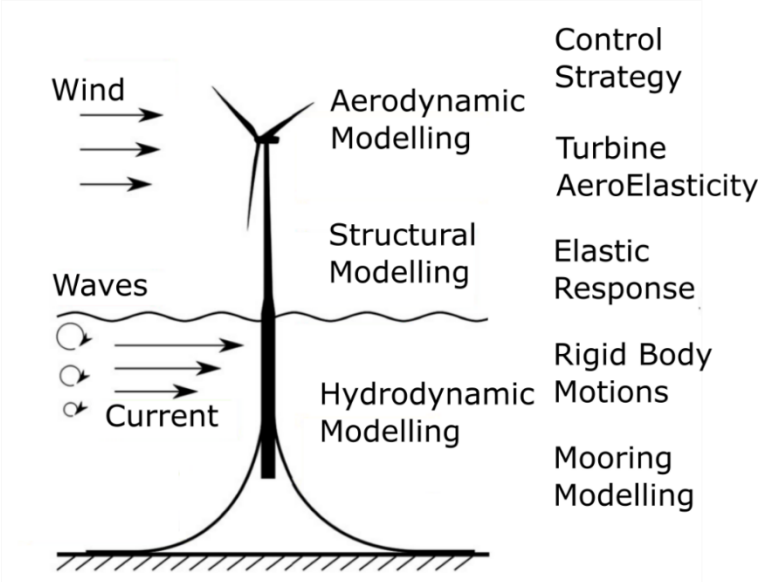

Figure 21 Complexity of a floating offshore wind system. Adapted from [5]

This project has received funding from the European Union's Horizon H2020 research and innovation programme under grant agreement No 815159

Another point of difference when compared to land based, or offshore bottom-fixed systems, is that the control system can interact with this coupling between aerodynamic loading and motion response, even leading to instabilities or “negative damping” effects. This requires adaptation of the control system from the fixed system to the floating systems [75, 76, 77]. However, this adaptation of the control system can also be used to improve the overall floater motion response, not only the aerodynamic response, leading to an overall better optimized system [78, 77].

Developing numerical models to model floating offshore wind systems is not a trivial task. A floating offshore wind turbine is a complex nonlinear system, involving different physics, and therefore requires a multidisciplinary approach to accurately model its behaviour. Typically, this has been accomplished by coupling aeroelastic codes, originally developed for the onshore wind industry, with hydrodynamic and mooring codes, originally developed within the oil and gas industry. However, to address the needs of the nascent offshore wind industry, hydrodynamic codes such as OrcaFlex have been extending their internal capabilities to allow for aeroelastic modelling, and vice-versa (e.g. HAWC2).

There are different modelling approaches for different computational cost/accuracy set points, which are often distinguished by their different fidelity levels, from low fidelity to high fidelity, as shown in Figure 22. Low fidelity models are often the simplest models available, sacrificing accuracy for fast simulation times, which allow to efficiently explore a wide design space and pre-select potential designs. Medium fidelity models, or engineering models, capture the main physics involved while making compromises for simulation speed, thus enabling to run many simulations to optimize potential concept designs. Higher fidelity models use few simplifications, effectively modelling all the relevant physics, providing accurate simulations but at a higher computational cost, which limits their application to a limited number of cases.

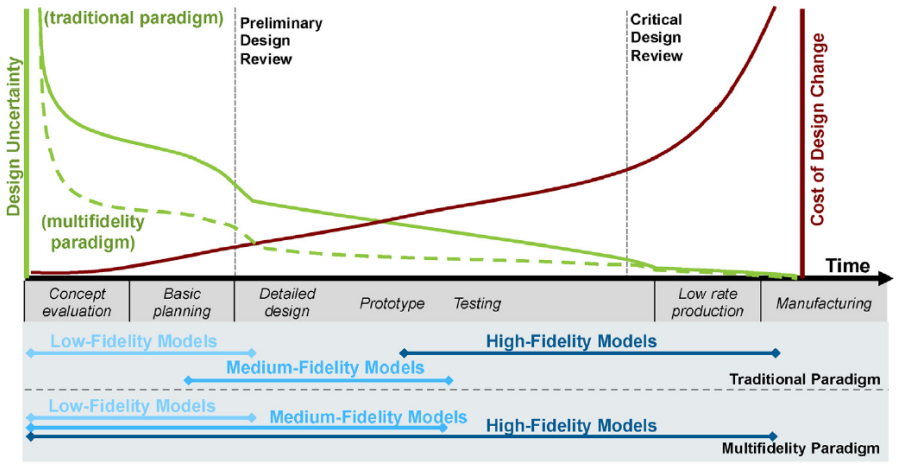

Figure 22 Application of different fidelity models using a traditional approach, or multi-fidelity approach. Reproduced from [63].

Traditionally, these tools are used sequentially, with the simulation models transitioning to higher fidelity levels as the design matures. Floating offshore wind systems have not been an exception to

This project has received funding from the European Union’s Horizon H2020 research and innovation programme under grant agreement No 815159

this approach. Recently, a more integrated multi-fidelity approach has been proposed for floating offshore wind systems due to the highly coupled physics involved [67]. This approach requires a more integrated use of different fidelity models, allowing for cross-validation between models, and minimizing the risk of lower order models converging to local optima, resulting in a suboptimal design [79].

A brief overview of the common modelling approaches for different aspects of a floating offshore wind turbine is given below.

3.1.1 Aerodynamic Modelling

Currently there is no dedicated offshore wind turbines designed specifically for floating offshore foundations, as the turbine manufacturers seem reluctant to take that step until a sizeable market develops [80]. Therefore, the same modelling techniques used for fixed foundations can be applied for floating foundations. Nevertheless, the floating wind turbines tend to be larger than those installed in fixed foundations, which brings additional simulations challenges due to more prominent aeroelastic effects and higher Reynolds flow regimes. Aeroelastic instabilities such as edgewise instability or flutter can have detrimental effects on turbine longevity, with possibly new instabilities appearing as the turbine size increases [81]. In addition, in floating offshore wind higher excursions are expected due to floater response, raising other issues such as the interaction between the turbine and its own wake, which is not typically considered by numerical models [74, 81].

Another point of difference with implications for the aerodynamic simulation is that a few floating concepts, including the X1Wind PivotBuoy X140, use downwind turbines in foundations that can weathervane to align themselves with the wind, as described in section 2. This configuration places the turbine in the immediate wake of the support structure, which results in a non-symmetric unsteady wind flow through the rotor disk, resulting in an unbalanced rotor loading. Furthermore, the weathervane, or passive yaw, design can result in higher yaw misalignments, with higher skewed wind inflow conditions than normally experienced in upwind turbines. The downwind design leads to simpler and lighter turbines with a 6% to 10% mass reduction in high energy sites [82, 83], and up to 25% mass reduction in low energy sites [83, 84]. This mass reduction at the hub height is more critical for floating foundation designs than for bottom-fixed designs. When compared to upwind configuration, the downwind turbines experience higher wind shadowing due to the support tower wake, and produces a smaller swept area under loading, thus reducing the annual energy production (AEP) from 1% to 2% [82, 83, 84]. Nevertheless, due to the lower mass and blade costs (up to 27%), the overall LCOE variation is between -1.3% and +0.9% [84].

In order to capture aeroelasticity effects, the determination of the aerodynamic loads on the blade needs to be coupled with a structural model to calculate the resulting deformations. There are different choices for both aerodynamic and structural modelling, with different degrees of fidelity, as shown in Figure 23. A brief discussion of some of these models follows, with a more complete discussion given in [81].

This project has received funding from the European Union's Horizon H2020 research and innovation programme under grant agreement No 815159

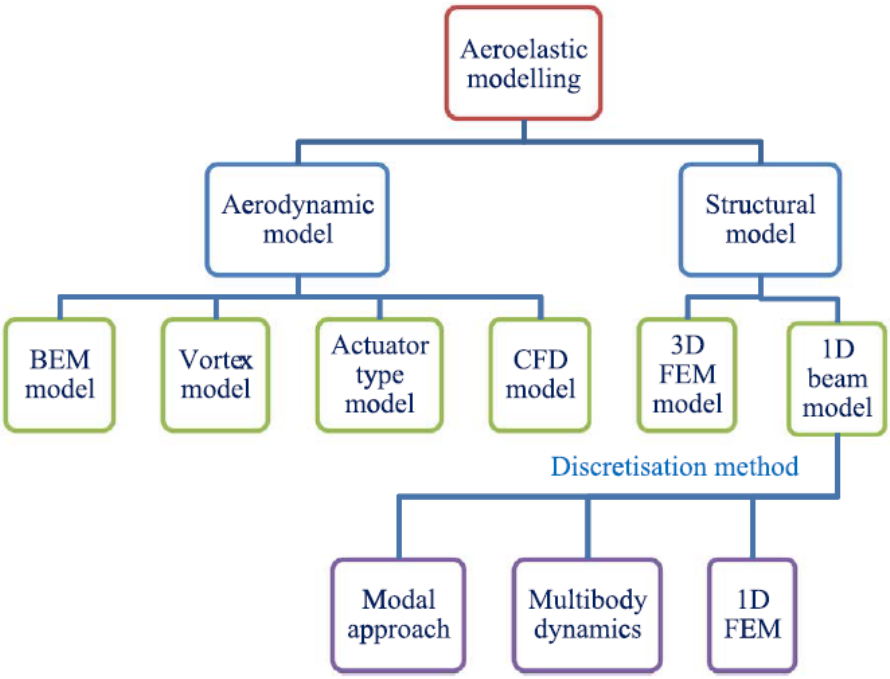

Figure 23 Aeroelastic modelling of wind turbines, adapted from [81].

Two main structural approaches to describe the blades are commonly found, an equivalent 1D beam model or a full 3D finite element method (FEM) [85, 81]. The latter is the more accurate approach and lends itself to be coupled with CFD for a high fidelity computationally expensive aeroelastic simulation. The 1D beam model is a simpler and less computational demanding approach, where the blade is reduced to a sequence of 1D beam elements, with equivalent structural properties to the real blade section. This structural response of this 1D beam is then analyzed with a modal approach, MBD (multi-body dynamics), or a 1D FEM analysis. The 1D equivalent beam is reasonable accurate for most cases, which coupled with its computational efficiency, makes it the standard approach [81].

The aerodynamic modelling of wind turbines concerns itself with the aerodynamic loading on the blades due to the relative air flow between the blades and the environment. The most common aerodynamic models used for this purpose, arranged from lower to higher fidelity, are the blade element momentum (BEM) model, the vortex method, actuator type model, and CFD model [81, 85, 86]. A brief description of the BEM and CFD is given below.

The blade element momentum (BEM) model is currently the industry standard due to its simplicity, low computational cost, and maturity. The blade loads are obtained using blade element theory, where the blade is discretized into small, independent, 2D airfoil sections, whose aerodynamic loads are calculated based on the airfoil properties (tabulated lift and drag coefficients) and wind conditions (wind speed and angle of attack). However, the presence of the rotor has an impact in the local air flow. This impact is quantified through a momentum balance applied in a stream tube across the turbine, producing new local velocities at the blade. These new velocities in turn impact the aerodynamic loading on the 2D airfoil sections, requiring an iterative process between the blade element theory and the momentum theory. Once converged, the loads are then integrated along the complete blade to obtain the total aerodynamic loading [81, 87].

This project has received funding from the European Union's Horizon H2020 research and innovation programme under grant agreement No 815159

This model has a handful of assumptions that limit its accuracy, such as the 2D steady flow across the blade sections, neglecting non-axial flow, or the blade being always in the rotor plane, which breaks when blade deformation occurs. Other limitations of this model are the inability to address tip and hub vortices, inability to account for turbulent wakes present with high tip speed rations, dynamic inflow conditions, yaw misalignment, flow separation and dynamic stall. These limitations have been addressed using some form of correction coefficients or models, with different degrees of success [81, 87]. Nevertheless, the BEM model remains the standard method to address wind turbine blade performance due to its low computational costs and accuracy level sufficient for blade design optimization. Its accuracy is highly dependent on the input airfoil properties (drag, lift, and even pitch coefficients as a function of the different Reynolds number and angle of attack) which are typically obtained from experimental work or higher fidelity simulations [81].

On the other end of the fidelity spectrum, CFD models solves the complete flow field around the turbine, directly calculating the loads on the blades and wake field without the need for airfoil properties. This model overcomes the limitations of the BEM model by directly calculating all the instances where correction factors are necessary, such as tip losses or dynamic stall conditions, however this comes at significant increase in computational cost, duration, and complexity. An overview of the grid, turbulence model, discretization schemes, or how to accommodate the rotor motion can impact the accuracy and computational costs is provided in [88, 89], and the adoption of verification and validation methods become relevant for uncertainty quantification as shown in [90]. A common and time efficient use of CFD is to couple it with BEM models by obtaining highly accurate airfoil properties to feed the BEM models, improving the accuracy of the BEM models, as carried out in [91]. However, CFD is becoming less expensive as the availability of computational resources increases. This enables some cross-validation of the aeroelasticity of lower order models, which show good agreement except if platform surge motions are considered, where a 10%-20% overprediction of the thrust and power was found [92]. A review of recent CFD studies can be found in e.g., [93].

An overview of the most common models is given in Table1, where the wide use of BEM models for the aerodynamic model coupled with an equivalent 1D beam for the structural response is adopted by 6 of the 7 codes listed. Furthermore, all these codes use linear beam models for the structural analysis which assumes small deformations. This assumption is violated with the increasingly large and flexible turbine blades, especially for floating offshore wind systems where higher motions occur due to the floater hydrodynamic response in waves.

Table 5 Overview of aeroelastic modelling choices used in the most common implementations. Reproduced from [81].

Name	Structural part		Aerodynamic part	Requires blade cross-sectional properties as input?
	Blade representation	Discretisation method		
ADAMS/WT	1D beam	MBD	BEM	Yes
FAST	1D beam	Modal approach	BEM	Yes
FLEX5	1D beam	Modal approach	BEM	Yes
GAST	1D beam	1D FEM	Free-wake vortex	Yes
GH-Bladed	1D beam	Modal approach	BEM	Yes
HAWC2	1D beam	MBD	BEM	Yes
PHATAS	1D beam	1D FEM	BEM	Yes

This project has received funding from the European Union's Horizon H2020 research and innovation programme under grant agreement No 815159

3.1.2 Hydrodynamic Modelling

The hydrodynamic modelling of floating offshore wind systems is based on the well documented body of knowledge developed within the naval and offshore industry. However, the interaction between aerodynamic and hydrodynamic forces in floating offshore wind systems requires a coupled analysis that is not often relevant in those fields. Another difference is the reduced size of floating offshore wind systems when compared to the classic offshore structures, which is expected to become more apparent for optimized designs. This sizing makes floating offshore wind foundations fall between small body and large body approximations, requiring more sophisticated hydrodynamic models to provide enough accuracy for detailed design optimization [74, 94]. In addition, this optimization process leads to a weight reduction and increased flexibility, which might justify addressing hydroelasticity effects, while most common hydrodynamic models assume rigid body motions [85].

The hydrodynamic models concern themselves with determining the wave loads acting on the floater when it is subjected to incoming waves. The most common hydrodynamic models applied to floating offshore wind systems are, from low fidelity to high fidelity, Morison's equations, potential flow theory with different degrees of nonlinearities included, or CFD models [85]. These models are well documented in the literature, e.g. [95, 96], and will only be briefly mentioned here.

The Morison equation is a well-known empirical model developed for monopiles which is considered applicable to structures whose characteristic dimension does not exceed 1/5 of the wavelength, often described as slender cylinders or members. The assumption is that the structure is small enough that the incoming wave is not affected, and therefore diffraction effects are negligible. This model is often applied to obtain the wave loads in bottom fixed offshore wind foundations [97]. The wave loading is divided into an inertia and viscous drag component, proportional to the local acceleration and velocity, respectively. Added mass and drag coefficients are used to obtain the loads, which depend on the Reynolds number, Keulegan-Carpenter number, among other factors. These components can be applied with a strip theory approach to the structure, and then integrated up to the mean water surface to obtain the total wave loads. This model can be augmented by integrating the loads up to the instantaneous water level using a wave stretching approach, or by applying the forces at the instantaneous body position, resulting in higher order loading such as a mean drift force [49]. The hydrodynamic restoring force and dynamic pressure variations on the bottom surface of the underwater floater can be added to the model formulation, with the latter being especially relevant for semi-submersibles with heave damping plates [49]. Even though the slender assumption is arguably inappropriate for most floating foundations, which limits the accuracy of the Morison model [86, 97], it was shown to perform similarly to potential flow theory for the OC4-DeepCwind semi-submersible [49], with an overestimation of pitch excitation at higher wave frequencies where the slender body assumption is most tested [50].

If the structure size is such that its characteristic dimension is larger than 1/6 of the wavelength then potential flow theory is applicable. In its simplest form, it assumes linearity to solve the radiation, diffraction, and hydrostatic problems independently and then uses superposition of these effects to obtain the total wave excitation forces in the frequency domain. The equations of motion are then solved in the time domain, e.g. through a Cummins formulation, which allows to included possible nonlinear effects as external loads, for example using a Morison drag formulation to include viscous

This project has received funding from the European Union's Horizon H2020 research and innovation programme under grant agreement No 815159

effects. The first order wave excitation forces (Froude-Krylov, radiation, and diffraction force) are included through linear response amplitude operators (RAOs), which are obtained assuming a fixed structure in linear waves by solving the corresponding frequency domain problem. These first order excitation forces are then superimposed to obtain the loading in irregular sea state conditions. Second order wave excitation forces occur at lower frequencies than the first order wave excitation range, and despite being smaller in magnitude, they can excite the floater natural responses. These loads can be included with more sophisticated models. Second order wave forces can result from the multiplication of first order terms (e.g. mean drift loads) which are relatively cheap to compute, and second order terms (sum-frequency and difference-frequency forces) which are computationally demanding to calculate. These second order wave excitation forces can be important to accurately predict the response of floating offshore wind systems, in particular the sum-frequency and difference-frequency forces which can be represented by quadratic transfer functions (QTFs) [97, 98, 86, 99, 94]. The hydrostatic force is originally linearized by assuming constant waterplane, which is valid only for small displacements. However, a nonlinear correction that accounts for the instantaneous waterplane and body position can be included if significant motions or waterplane area variations are expected [97]. External forces to simulate viscous damping can be included in this formulation, from an element wise Morison drag approach [100] to higher order damping models, which are often calibrated using model test data or higher fidelity CFD simulations [5, 101].

CFD models solve the complete flow field around the floater, directly calculating the total wave loads, including viscosity effects and other nonlinearities. This method requires significant computational resources and is time consuming, and while it is mostly used to cross validate lower order methods [5, 102, 53, 55], some effort has been placed into developing a fully coupled CFD model [103, 104].

The hydrodynamic response of the floater is also dependent on the mooring system. The mooring system can be modelled in a simple quasi-static approach. In its simplest form, the mooring system is linearized around the equilibrium position, providing a restoring force in the horizontal plane. More advanced quasi-static models can solve the catenary equations and include multiple elements, such as the open-source library MAP++ coupled with OpenFAST [105]. A more complex dynamic model can be used to model the hydrodynamic effects of the mooring lines being dragged through the water along with the structure. A common approach is to discretize the mooring lines as a lumped-mass system, where the mooring line is modeled by mass points connected by spring dampers. Different forces can be applied to the mass points, such as weight, buoyancy, line axial stiffness, structural and hydrodynamic drag, or seabed contact forces. The mooring line tensions are then calculated at each segment, following a linear or nonlinear stress-strain relationship, depending on the mooring line properties. An example of a dynamic mooring model is the open-source mooring line modelling tool MoorDyn which is coupled to OpenFAST for floating offshore wind simulations [106]. The experience from the offshore industry is that dynamic effects should be accounted for structures with significant displacements, water depths above 150m, or for mooring lines with large drag elements such as chain moorings [86]. For a semi-submersible floating offshore wind system, it was found that a quasi-static mooring model underpredicts the mooring line fatigue and tensions, especially the extreme loads in higher sea states [107, 108], but has less impact in the overall system dynamics [50, 49].

This project has received funding from the European Union's Horizon H2020 research and innovation programme under grant agreement No 815159

The most common approach across the submissions within the OC4 and OC5 project for the modelling of the DeepCwind semi-submersible was a potential flow approach complemented by a Morison formulation, with a dynamic line mooring model [50, 49]. In general, it was found that viscous damping effects are better captured by a Morison drag formulation than a global damping matrix to predict the viscous damping [109, 40]. Furthermore, and regardless of the hydrodynamic model, nonlinear hydrodynamic loads are important to model since they can excite surge, pitch and tower natural frequencies which often lie outside the wave excitation range [50]. These areas are currently under investigation in the new OC6 project phase I [51], which focuses on the validation and uncertainty quantification of the nonlinear hydrodynamic loading, while also adding higher fidelity tools (CFD) to the simulation approaches considered [52].

Table 6 Most commonly used time domain solvers to model hydrodynamic response of floating offshore wind systems.

Name	Developer	Type	Hydrodynamic Theory		Mooring solver
			Morison Formulation	Potential Flow	
OrcaFlex	Orcina	Commercial	Yes	Yes	Included
AQWA	ANSYS	Commercial	Yes	Yes	Included
aNySIM	MARIN	Commercial	Yes	Yes	Included
HydroDyn	NREL	Open-Source	Yes	Yes	Requires coupling
3DFloat	IFE	Commercial	Yes	Yes	Included
Proteus DS	DSA Ocean	Commercial	Yes	Yes	Included
SIMO	SINTEF	Commercial	Yes	Yes	Requires coupling

3.2 Numerical Modelling of the PivotBuoy System

The work package 5 of the PivotBuoy project has been focusing on the numerical simulation of the PivotBuoy system. The simulations were carried out using two different numerical codes: OrcaFlex, an offshore industry standard for hydrodynamic and mooring assessment that recently introduced aeroelastic capabilities; and HAWC2, a well-established aeroelastic code within the fixed wind industry, complemented with hydrodynamic capabilities. This approach enables cross-validation between the codes and better insight into the modelling of the system. A brief description of these codes is given in section 3.2.1.

The objectives of this work are: (1) develop and calibrate the numerical models using previous model test data; (2) optimize the design of the PivotBuoy prototype X30, to be installed in the PLOCAN site located in the Canary Islands in 2021, and (3) later compare the numerical models with the measure real data; (4) model a PivotBuoy system in a large scale 15MW design for different metocean conditions; and (5) finally to improve the numerical modelling capabilities of floating offshore wind systems through cross-validation of numerical models, model test data, and real sea data.

The first two objectives were accomplished and are detailed in the respective confidential

This project has received funding from the European Union's Horizon H2020 research and innovation programme under grant agreement No 815159

deliverables [110, 111], although a brief summary is provided in section 3.2.2 for context. The fourth objective was accomplished by modelling the performance of a full scale X140 platform designed for a downwind version of the 15MW offshore reference turbine, which represents a near-future commercial wind turbine size (see in section 2.3). Following the practice in the previous studies mentioned above, isolated aerodynamic-aeroelastic simulations and hydrodynamic simulations were carried out prior to the coupled analysis. This approach provides valuable insight when comparing both numerical models, which enables the improvement of the numerical modelling carried out. The main outcomes of this analysis will be presented in section 3.2.3, with the complete (confidential) study presented [112]. The validation with real sea measured data is expected to be carried out in the first quarter of 2022, when a significant amount of data has been measured.

It should be noted that the numerical models used are constantly under review and improvement, and the results discussed here are the latest ones at the time of either this report, or the specific deliverables within the PivotBuoy project.

3.2.1 Numerical Codes

Two well-known commercial simulation codes were used, OrcaFlex and HAWC2. OrcaFlex is more suited to model the hydrodynamic and structural response of the PivotBuoy TLP subsystem, while HAWC2 is expected to provide better aeroelastic modelling of the turbine, which is critical for the loading on the PivotBuoy system. Using these two codes, with strengths in different modelling aspects, allows a better insight into their modelling capabilities and overall improvement of their estimations. A brief description of these codes is given below.

3.2.1.1 HAWC2

HAWC2 is an aeroelastic nonlinear multibody code developed at DTU Wind Energy for simulation of wind turbines including their support structure. HAWC2 performs time domain simulations of the system, where the dynamics are described by differential equations and solved using the Newmark numerical integration scheme. It is divided into modules which can be combined depending on the user requirements. The structural, the aerodynamics, the wind, the hydrodynamics and the soil modules are prebuilt in the main code. Additionally, there are many external modules (systems) that can be connected whenever are needed, including but not limited to the WT controller, the mooring lines, far wakes and any other special future that can be implemented creating DLLs and link them with the main code. More information on HAWC2, from user manual to a list of publications, can be found online [113].

Structural module: A multibody formulation is used which couples different independent bodies together. These bodies can be either rigid or flexible. Different bodies are joint together using algebraic constraints. The joints define a fully fixed relative position among bodies, or allow for free degrees of freedom in order to represent a bearing. To account for flexibility, each body is divided in a set of Timoshenko beam elements with 6 degrees of freedom. The user defines the beam element mass, stiffness, and inertia properties.

This project has received funding from the European Union's Horizon H2020 research and innovation programme under grant agreement No 815159

Hydrodynamics: Hydrodynamic load interaction is applied inside HAWC2 using the Morison equation. The implemented water kinematics include a variety of different wave types such as regular airy waves, irregular airy waves, stream function waves, deterministic waves, and white noise waves. Wheeler stretching and non-linear wave kinematics are also available as second order effects. It is possible to account for the flexibility of the floating members, and the MacCamy Fuchs correction for water particle acceleration can also be applied for larger diameter structures and/or shorter wave lengths. Alternatively, a HAWC2-WAMIT coupling is available for a complete diffraction analysis.

Aerodynamics: The aerodynamic model in HAWC2 is based on the Blade Element Momentum (BEM) theory. The accuracy of the solution is improved by applying well known corrections such as the Prandtl tip-loss factor to account for a finite number of blades, the Glauert correction for heavily loaded rotors, the Glauert and Colemann correction to account for induction variations due to non-uniform inflow, and the dynamic inflow model to capture the dynamics of the near wake which in turn change the loads on the rotor. The aerodynamic forces that act on the blades are computed using the airfoil lift, drag, and moment coefficients. Finally, a Beddoes-Leishmam dynamic stall model is implemented to account for changes in the airfoil coefficients due to dynamic variations of the angle of attack.

Wind module: Both deterministic and stochastic wind fields can be generated in HAWC2. The wind conditions are defined in a general way including various wind shear profiles such as constant, logarithmic, power law or user defined. Furthermore, extreme coherent and extreme operating gusts according to IEC 61400-1 ed.3 international standard can be generated and used in the simulations.

Wires: A dynamic wires model has been developed as an external DLL and can be used in the case of floating substructures to represent the mooring line system for offshore wind turbines. The wires are implemented as non-linear beam elements with longitudinal flexibility and no bending stiffness. Drag and buoyancy forces can be included too.

Examples of floating platforms modelled in HAWC2: Benchmark studies and validation of offshore turbines using HAWC2 has been performed under various projects. Among them the IEA task 30-OC5 project where a wind turbine scaled model atop a floater has been studied. HAWC2 code was used to replicate the experimental conditions and compare the WT tower and blade loads as well as the loads acting on the semi-submersible structure. The overall performance of HAWC2 simulation tool was found to be above average in comparison with other numerical tools [50]. Another project where HAWC2 was used as the main simulation tool was the DeepWind project. A vertical axis turbine was placed on a floating cylinder which was anchored to the seabed using mooring lines. HAWC2 results have been compared with real measurements from a scaled model and reasonable agreement was found [114].

3.2.1.2 OrcaFlex

OrcaFlex is a Multibody, time-domain Simulation (MBS) commercial software developed by Orcina, that is widely used in the offshore industry. Through a non-modular structure, it integrates a wide range of objects (lines, buoys, vessels, links, constraints, etc.), each very powerful, which easily allow

This project has received funding from the European Union's Horizon H2020 research and innovation programme under grant agreement No 815159

for simple or complex models to be built. It supports fully flexible non-linear mooring system definition, as well as flexible beams, and can either use Morison formulation to define hydrodynamic interactions or import diffraction model data. Additionally, it includes most of the usual linear and non-linear wave models. It can also model active winches and has libraries to add new functionality through External Functions, which can be written in C++, Matlab, or Python. In its latest version (10.3) the long-established hydrodynamic capabilities of OrcaFlex can be coupled with a built-in aerodynamic turbine feature, providing a fully coupled dynamic analysis tool suitable for both fixed and floating platform offshore wind turbines. Details on the OrcaFlex theory and usage can be found online [115].

Structural and hydrodynamic modelling: different independent objects or bodies are coupled together. The most important available objects used to model offshore wind structures are summarised below.

6D Buoys are rigid bodies with all six degrees of freedom. OrcaFlex calculates their translational and rotational motion. Buoys have both mass and moments of inertia, forces and moments from many different effects can be modelled, including weight and inertial loads, buoyancy, added mass, damping and drag calculated based on the instantaneous wetted surface (i.e. as a function of submergence), water entry / exit slam loads (per DNV H103, RP-C205), compressibility specified by bulk modulus, applied and contact loads such as friction with sea bed and elastic solids. Several different types of 6D buoy are available, for modelling different sorts of marine object, including Lumped option with overall properties and a Spar option for co-axial cylinders, each with its own properties. Hydrodynamic loads on spar buoys are calculated from Morison's equation (though they do have some limited diffraction capability).

Lines are flexible linear elements used to model pipes, beams, cables, mooring lines, etc. Lines are represented in OrcaFlex by a lumped mass model. The lumps of mass are called nodes and the springs joining them are called segments. Each segment represents a short piece of the line, whose properties (mass, buoyancy, drag, etc.) have been lumped at the end nodes for modelling purposes. Line properties may vary along the length, assigning different line types, which are essentially a collection of properties (for example diameter, mass per unit length, bend stiffness), to user defined sections. Bending stiffness, drag and added mass can be non-isotropic. Axial, bending, and torsional stiffness can be non-linear. Once more, added mass is treated as a function of submergence or height above seabed and slam loads and compressibility effects are considered. Finally, it is possible to choose between finite element or analytic catenary representation.

Constraints are massless objects intended to provide general-purpose connections between objects. Constraint objects comprise two frames of reference that can translate and rotate independently. One frame may be connected to a master object, and the other frame can have one or more slave objects connected to it. Constraint objects allow degrees of freedom to be introduced, to be fixed, or to have imposed motions.

Aerodynamics: for floating wind turbines, there is a need for coupled dynamic analysis of the entire system –including the mooring system, platform, tower, and the turbine. With this purpose OrcaFlex has developed a dedicated wind turbine object.

This project has received funding from the European Union's Horizon H2020 research and innovation programme under grant agreement No 815159

The OrcaFlex wind turbine uses a Blade Element Momentum (BEM) model for aerodynamic loading. Turbine blades are represented by beam elements, closely related to OrcaFlex line objects. The feature includes Prandtl tip and hub loss correction models, Pitt and Peters skewed wake model, and Øye dynamic inflow model. Currently neither tower shadow effect, nor dynamic stall effects are modelled. Blade pitch can be controlled by an external function. The generator can be controlled by either rate of rotation or applied torque, each of which may take a constant value or be calculated by an external function.

Environmental description: OrcaFlex presents many options to apply environmental loads.

The user can define the water density (including horizontal and vertical variation), temperature (constant or varying with depth) and kinematic viscosity. Different wave trains can be defined; the overall sea conditions are the superposition of all the wave trains. In most cases a single wave train is sufficient, but multiple wave trains can be used for more complex cases, such as a crossing sea with locally generated waves in one direction and distant storm-generated swell in a different direction. A wave train can be one of the following: a regular wave (with a choice of wave theory: Airy, Stokes' 5th, Dean Stream Function, Cnoidal), a random wave (with a choice of spectrum), given by time history or given explicitly by a list of wave components. Irregular waves have directional wave spreading option. Seabed can be chosen flat or profiled and different models exist to define its properties (elastic, nonlinear soil model). Currents may be defined (3D, non-linear) both in magnitude and direction and can be time varying. Finally, both constant and spectrum-based winds can be defined (API or DNV spectra). Wind can also be a time history file of speed and direction. Furthermore, a full field wind model can be imported via TurbSim, software developed by NREL. Air density can be user defined and vertical shear can be specified as a profile.

3.2.2 PivotBuoy Prototype X30 System

The first goal was to set-up and calibrate the numerical models with tank test results and provide a first basis of the aerodynamic comparison between HAWC2 and the recently included aerodynamic modelling in OrcaFlex. The calibration data included two model test data shown in Figure 24. The first set originates from the proof-of-concept model tests carried out in January 2018 for a wind floating platform with the NREL 5MW reference turbine [48] at 1:64 scale at the CIEMLAB wave flume (UPC). The second and more extensive model test campaign was carried out in February 2019 at ECN Hydrodynamic and Ocean Engineering Tank, within the MaRINET2 programme, using a low Reynolds turbine adapted from the NREL 5MW reference turbine. The main objective was to conduct tests on a 1:50 physical model of X1 design to allow high fidelity system characterization and further numerical model adjustment and validation, supporting design optimization activities for the 2020 PLOCAN deployment.

It was found that the damping plates dominated the hydrodynamic response, and its proper modelling is critical for accurate hydrodynamic representation. After calibration of the hydrodynamic coefficients used in the Morison formulation, a reasonable match was found between both codes and the experimental data. A similar agreement was found for the aerodynamic performance of both codes using a generic V27 FAST turbine, which was developed within the IEA Wind Task 31

This project has received funding from the European Union's Horizon H2020 research and innovation programme under grant agreement No 815159

(WakeBench). The step-by-step approach taken allowed to gain better insight into the strengths and weaknesses of both numerical codes used, with OrcaFlex showing better hydrodynamic capabilities and HAWC2 better aeroelastic capabilities, as expected. [110].

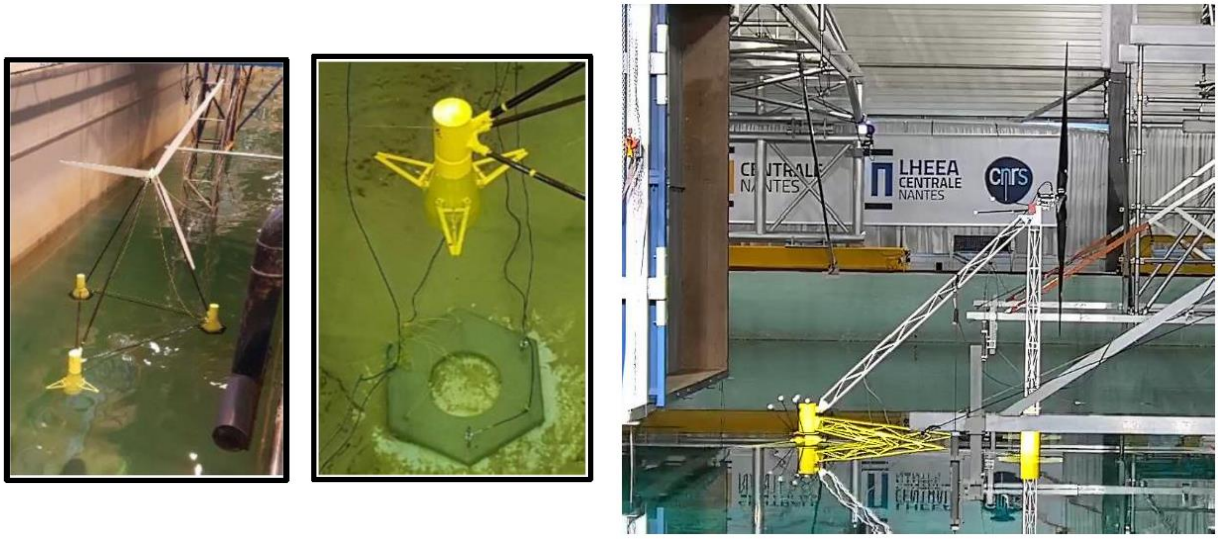

Figure 24 Model test data used for the calibration of numerical models: at 1:64 scale in the CIEMLAB wave flume in January 2018 (left); and at 1:50 scale in ECN Hydrodynamic and Ocean Engineering Tank within the MaRINET2 programme in February 2019 (right).

In a second phase, the numerical models were used to assess the dynamic behaviour of the X30 prototype to be installed at PLOCAN test site. The local metocean data was used to establish a comprehensive design load matrix, including operational conditions, extreme conditions and some failure cases. Aero-servo-hydro-elastic simulations were carried out with both codes and a reasonable agreement was found, despite the different controllers used in OrcaFlex and HAWC2. Comparing both codes aeroelastic performance, it was found that the first five natural frequencies agreed within 3%, the thrust within 2.3%, with the biggest difference occurring in the blade flapwise root moment.

The hydrodynamic performance shows a variation of the natural periods under 4%, with the RAOs showing reasonable agreement in surge, but some differences in heave and yaw misalignment due to the different hydrodynamic modelling approaches used in both codes. The coupled simulations show a better agreement between models, both in operation and extreme conditions. The power production, rotor speed, and pitch angle vary less than 1% of their mean value, while the mean tension in the mooring lines differs less than 3.5%. Based on the results, it is possible to conclude that the aerodynamic modelling and the controller performance for the normal operation case is similar between models [111].

This project has received funding from the European Union's Horizon H2020 research and innovation programme under grant agreement No 815159

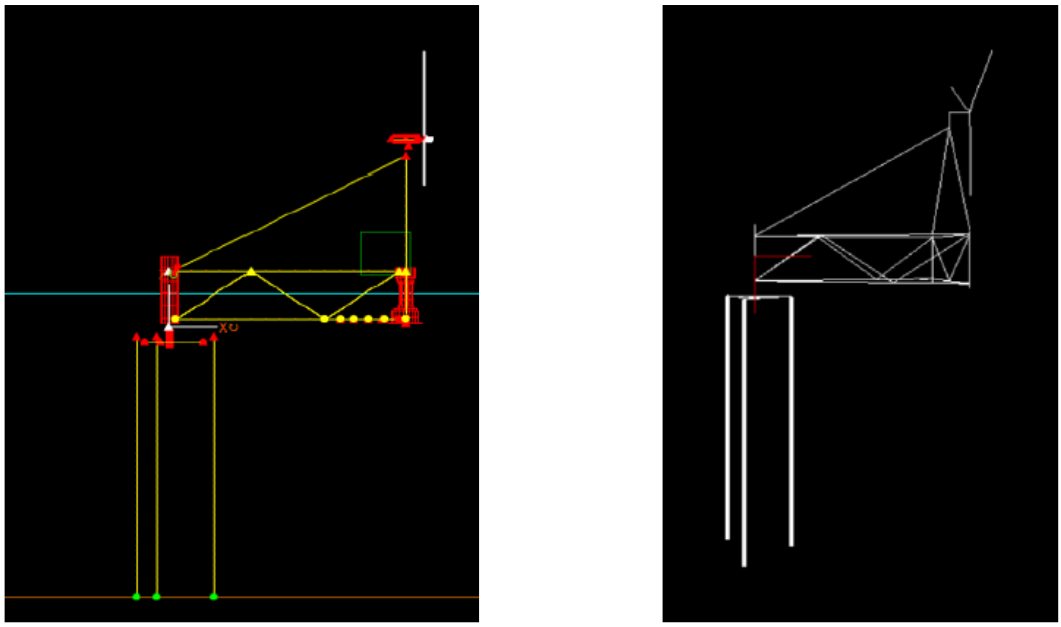

Figure 25 Numerical representation of the prototype X30 floating offshore wind platform, including the PivotBuoy system, in OrcaFlex (left) and HAWC2 (right). [111]

3.2.3 PivotBuoy Full-Scale X140 System

The analysis of the X140 PivotBuoy full-scale design for a downwind version of the 15MW offshore reference turbine was carried out for three different sites, which are briefly described in section 3.2.3.1. The aeroelastic and hydrodynamic modelling approach and code comparison is presented in section 3.2.3.2, and section 3.2.3.3, respectively. The controller tuning is described in section 3.2.3.4. Finally, a subset of the results obtained is summarized in sections 3.2.3.5, 3.2.3.6, and 3.2.3.7. It should be noted that the complete analysis carried out is described in a confidential PivotBuoy project deliverable [73], and this section presents a selection of those results and conclusions.

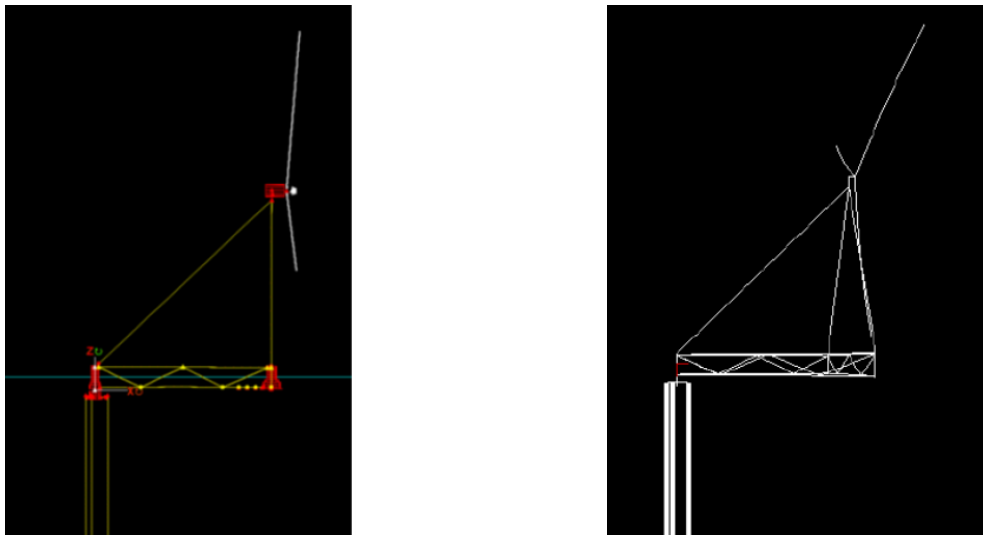

Figure 26 Numerical representation of the prototype X140 floating offshore wind platform, including the PivotBuoy system, in OrcaFlex (left) and HAWC2 (right). [112]

This project has received funding from the European Union's Horizon H2020 research and innovation programme under grant agreement No 815159

3.2.3.1 Site Selection and Design Load Conditions

The full-scale X140 PivotBuoy floating offshore wind system was designed for the Canary Islands site. However, the performance of the X140 design has been evaluated for two other potentially commercial sites as well. For all sites a metocean analysis was carried out and a DLC matrix defined. These three sites, shown in Figure 27, from the least energetic: Canary Islands, in the Atlantic Sea; Begur, in the Mediterranean Sea; and Silleiro, in the North-Atlantic Sea. A summary of the wave and wind climate is shown in Table 8. A water depth of 150m was assumed for all sites.

The metocean data was then processed to populate a DLC matrix for each site according to the IEC 61400-3 standards [116], which was later used to simulate the full-scale PivotBuoy X140 response. The DLC considered for the analysis is summarized in Table 7.

Figure 27 The three locations considered for the analysis of the PivotBuoy X140 15MW floating offshore wind system. From left to right, Canary Islands, Silleiro, and Begur.

Table 7 Total number of simulations for each site, per design load condition (DLC).

	Number of Simulations		
	Canary	**Begur**	**Silleiro**
DLC 1.1 – Power Production in Normal Turbulence	2052	1350	3240
DLC 1.3 – Power Production in Extreme Turbulence	2052	1350	3240
DLC 1.4 – Power Production with Extreme Coherent Gust	54	54	216
DLC 1.6 – Power Production in Severe Sea States	720	720	2880
DLC 3.2 – Start-up during extreme operating gust	81	81	324
DLC 3.3 –Start-up during extreme direction change	81	81	324
DLC 6.1 – Parked, standstill or idling	648	648	2529
DLC 7.1 – Parked with rotor locked	648	648	2529
Total number of simulations	**6336**	**4932**	**15282**

This project has received funding from the European Union's Horizon H2020 research and innovation programme under grant agreement No 815159

The wave and wind conditions were associated and discretized in up to 10 Hs-Tp bins per wind speed, achieving a coverage of 25% of the total number of combinations corresponding to each wind speed bin, which was found to be a good compromise between simulation effort and representation. In order to be conservative for the loads, the wind shear coefficient for all sites is defined to be 0.14, as defined in the 61400-3 standards [116]. This implies a possible overestimation of the mean hub height wind speed, which results in conservative loads but also an overestimation of AEP.

The turbulence intensity for the Normal Turbulence Model (NTM) was calculated for the three sites based on the standard deviation, as defined in the 61400-3 standards [116]. The standard deviation was computed from the surface roughness expression derived from Charnock. Begur and Silleiro were considered open sea distance and the Canary Islands as near costal, for the Charnock's constant dependency on distance from shore. The reference turbulence intensity for the NTM was defined to be 12% for the three sites, which can be considered a conservative value. For the also needed Extreme Turbulence Model, the equations in the 61400-3 standards were used, and the reference turbulence intensity for the ETM was computed from the standard deviation at 15 m/s of the NTM.

Codirectional and cross-direction wave-wind cases were considered for the operational DLC, with the latter being particularly relevant to assess the weathervanning capabilities of the full-scale PivotBuoy X140 platform. A Von-Misses probability was used to correlate wind and wave direction. In general, higher winds are more correlated with wave direction, however the spread differs for each site: Silleiro finds the distribution with higher spread while the lowest spread is found for the Canary Islands, as shown in Figure 28. A similar analysis was used to define cross-directional wind-current conditions.

Table 8 Comparison of the wave storm (significant wave height, Hs, and peak period Tp) and windstorm (wind speed Wsp) for 1-year, 20-years, and 50-years return periods

			Canary Islands	Begur	Silleiro
1 year	**Hs**	**[m]**	4.00	6.23	9.59
	Tp	**[s]**	10.00	9.00	14.00
	Wsp	**[m/s]**	24.83	35.85	40.00
20 years	**Hs**	**[m]**	5.13	7.92	12.71
	Tp	**[s]**	11.82	9.80	16.11
	Wsp	**[m/s]**	27.52	42.58	41.03
50 years	**Hs**	**[m]**	5.50	8.42	13.71
	Tp	**[s]**	12.24	10.00	16.49
	Wsp	**[m/s]**	28.02	43.96	45.00

This project has received funding from the European Union's Horizon H2020 research and innovation programme under grant agreement No 815159

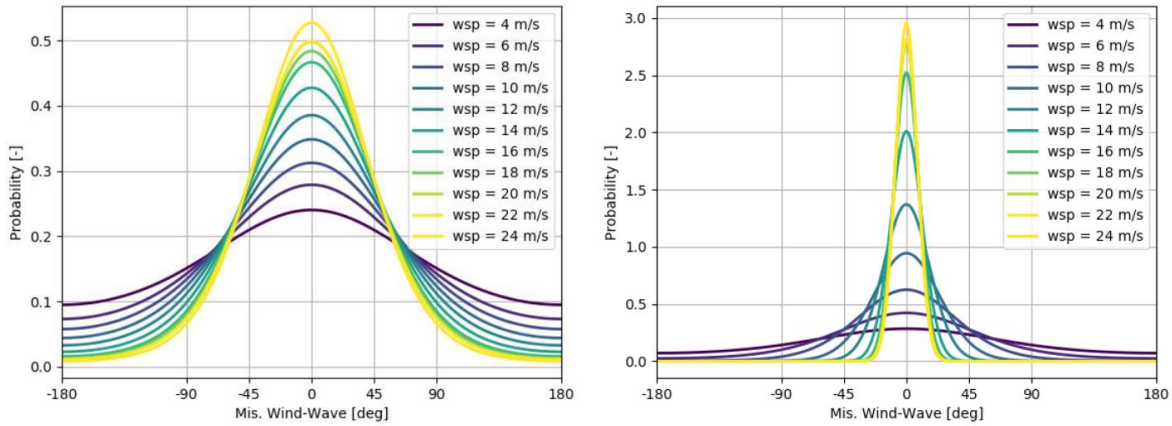

Figure 28 Wind-wave misalignment as a function of wind speed for the Silleiro (left) and Canaray Islands (right) site. The Begur site (not shown) is in between these profiles.

3.2.3.2 Aerodynamic Modelling

The turbine selected for this analysis was the offshore 15 MW offshore reference turbine [71] was adapted for downwind configuration. Due to its novelty, the community is frequently updating the model, freely available in the GitHub repository[1]. The main characteristics of this turbine are given in Table 9.

Table 9 IEA 15MW reference turbine overall characteristics [59].

Rated Power	15	MW
Rotor Diameter	240	m
Nominal Thrust	2750	kN
Cut-in Wind Speed	3.0	m/s
Rated Wind Speed	10.59	m/s
Cut-out Wind Speed	25.0	m/s
Minimum-rated rotor speed	5 – 7.56	rpm
Gearbox Ratio	None - Drivetrain	
Configuration	Upwind, Variable Speed, Collective Pitch	
Nacelle Mass	630.8	t
Rotor Assembly (hub incl.)	385.7	t

Due to the limited aeroelastic capabilities of OrcaFlex when compared with the dedicated aeroelastic code HAWC2, a series of simple verification tests were carried out to better understand the aeroelastic performance of both codes, improving the overall modelling of the X140 system.

[1] *The model used was the latest update available on 31/03/2020 (GIT commit 6742a58) https://github.com/IEAWindTask37/IEA-15-240-RWT*

This project has received funding from the European Union's Horizon H2020 research and innovation programme under grant agreement No 815159

The first step was to compare both numerical models for a rigid, fixed turbine under constant wind speed, without induction. Since OrcaFlex cannot model blade prebend, HAWC2 was used with and without prebend to allow a better comparison. A very good match between the no prebend models was found. When including prebend, lower perpendicular loading for the outer radial sections was found, impacting the outcome of the model.

When adding induction effects, a good match of the tangential and axial induction coefficients is found between OrcaFlex and the HAWC2, nevertheless a mismatch in the aerodynamic coefficients is found for the outermost blade positions, likely due to the different tip loss corrections used in both codes.

When blade flexibility is included in the simulations, differences in the axial induction coefficient are found between OrcaFlex and HAWC2, which might indicate that cross-sectional effects such as bend-twist coupling are modeled differently.

Nevertheless, a reasonable match is found between both simulation models, as seen in Figure 29, where OrcaFlex predicts up to 13% higher normal loading on the outer sections of the blade. These results are in agreement with the findings of previous simulation work carried out within the PivotBuoy project for the V27 Vestas turbine [110, 111], where similar differences due to hub/tip loss corrections and axial induction coefficient were found.

Furthermore, the RNA clamped natural frequencies are predicted with good agreement between both codes. OrcaFlex predicts larger natural frequencies for higher order flap modes and edge modes, however the differences in the natural frequencies between OrcaFlex and HAWC2 never exceed 5%. These results are in agreement with the findings of previous simulation work carried out within the PivotBuoy project for the V27 Vestas turbine, where differences between 3% and 5% were found [110, 111].

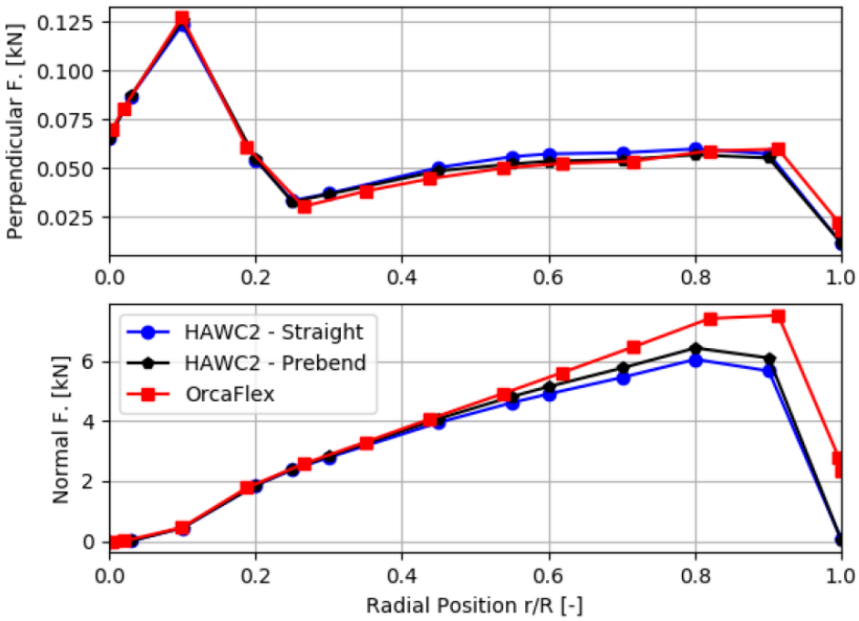

Figure 29 Loading comparison of the IEA 15MW turbine, including induction effects and flexible blade. [112]

This project has received funding from the European Union's Horizon H2020 research and innovation programme under grant agreement No 815159

The normal steady-state operation of the turbine is then evaluated form cut-in to cut-out wind speeds, with a uniform wind field and without transient controller effects. Figure 30 presents four of the main control-related channels, rotor speed, pitch, torque and power, and two important design loads, the thrust loading for the X140 connector and the blade flapwise moment for the IEA 15MW blade integrity. The controller related channels find good agreement in the partial-load region and full load region, from 6 to 10 m/s and from 12 to 24 m/s, where rotor speed, pitch, torque and power match. On the other hand, the start-up region, for wind speeds below 5 m/s and the transition region, between 10 and 12 m/s are modeled differently. OrcaFlex uses a simpler controller than the HAWC2 model, which results in some modelling simplifications which can be observed specially in the start-up region. However, given the complexity and novelty of the IEA 15MW model, the results are satisfactory.

The thrust and blade root flapwise moment present higher differences between models. Regarding the blade root flapwise moment, the results reflect the discussion above, showing a higher distributed load in the OrcaFlex model. This can be clearly observed in the steady-state where, even though the maximum blade root moment (10 m/s) has a good agreement between models, differences up to 80% on the integrated load are found at high wind speeds.

The thrust force finds better agreement with a maximum difference of 10% found at maximum thrust, around 11 m/s. These trends were observed in previous simulation work carried out within the PivotBuoy project for the V27 Vestas turbine [110, 111], however they become more noticeable for the 15MW turbine, presumably due to its larger slender blades and higher flexibility.

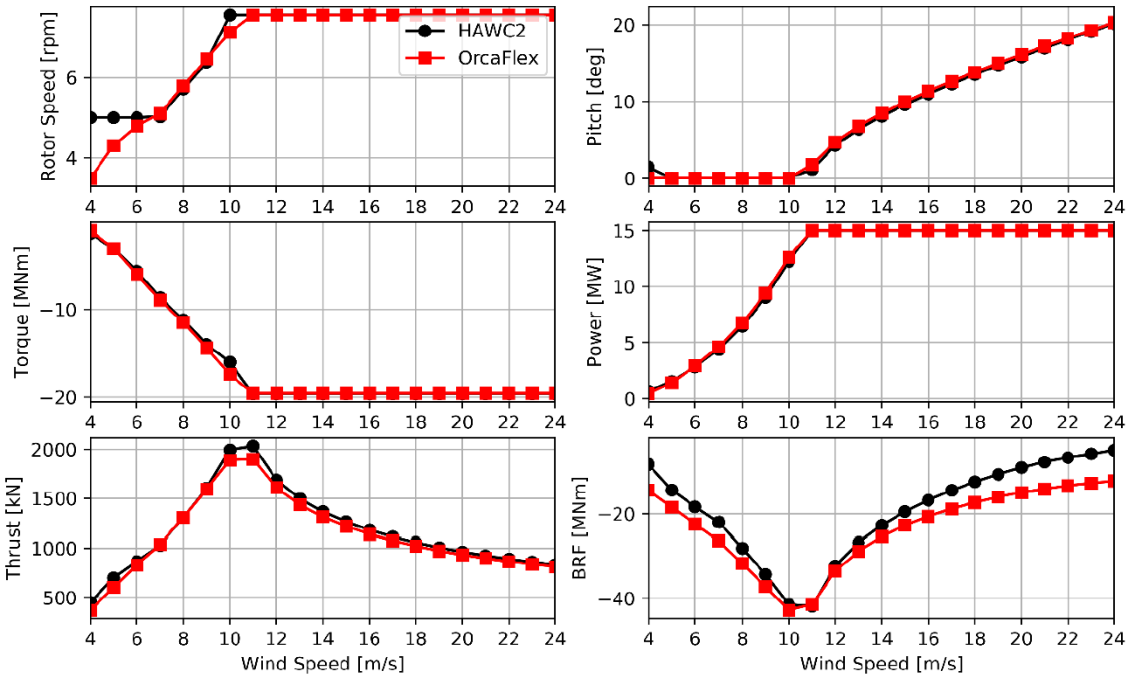

Figure 30 Comparison of steady-state operation of IEA 15MW turbine. From top to bottom, and left to right: rotor speed, generator torque, thrust, pitch, electrical power, and blade root flapwise moment.

This project has received funding from the European Union's Horizon H2020 research and innovation programme under grant agreement No 815159

Some limitations of the current OrcaFlex aeroelastic modelling capabilities have been identified, such as the inability to model blade prebend. Future work is necessary to better understand the differences in hub/tip loss corrections between HAWC2 and OrcaFlex, or cross-sectional effects such as bend-twist coupling, and their impact in the overestimation of the normal loading on the outer sections of the blade.

3.2.3.3 Hydrodynamic Modelling

The HAWC2 first order Morison strip theory hydrodynamic model is compared with the hydrodynamic capabilities of OrcaFlex, which allows for potential flow theory, including higher order effects. A series of simple verification tests were carried out to better understand the hydrodynamic performance of both codes, in order to improve the overall modelling understanding of the X140 system.

A static comparison was first carried out between the OrcaFlex model and the HAWC2 model as a verification step. The difference between the mass properties and tendon pretension between both models, both for TLP only and floater configurations, was under 0.2% which is considered negligible. When adding the turbine, the complete assembly shows under 0.5% difference in pretension and 2% in the final positions between both models. A good agreement between the mass properties and hydrostatic force is found, which is in line with the findings of previous simulation work carried out within the PivotBuoy project for the X30 platform [110, 111].

The dynamic response was then evaluated in terms of natural frequencies, and response amplitude operators (RAOs) for the TLP and complete assembly, followed by regular wave tests. Both codes show good agreement (within 9%) for the natural periods of the complete system, as seen in Table 10. After the submission of deliverable D5.3 [73], the models have since been improved, and a better match is expected with the current version of the models. These results are in agreement with the findings of previous simulation work carried out within the PivotBuoy project for the X30 design [110, 111].

Table 10 Relative difference of the natural periods of the X140 platform estimated with OrcaFlex and HAWC2

	Relative difference [%]
Surge	2.4
Heave	-8.7
Pitch	1.7
Roll	-7.0

This project has received funding from the European Union's Horizon H2020 research and innovation programme under grant agreement No 815159

The response amplitude operators (RAOs) were calculated for the complete assembly, with the aeroelastic modelling disabled. A good agreement was found between HAWC2 and OrcaFlex, with HAWC2 showing slightly larger response in pitch, and slightly lower response in surge for longer wave periods, as shown in Figure 31. However, these differences never exceed 0.2 units/m, which is considered a minor difference.

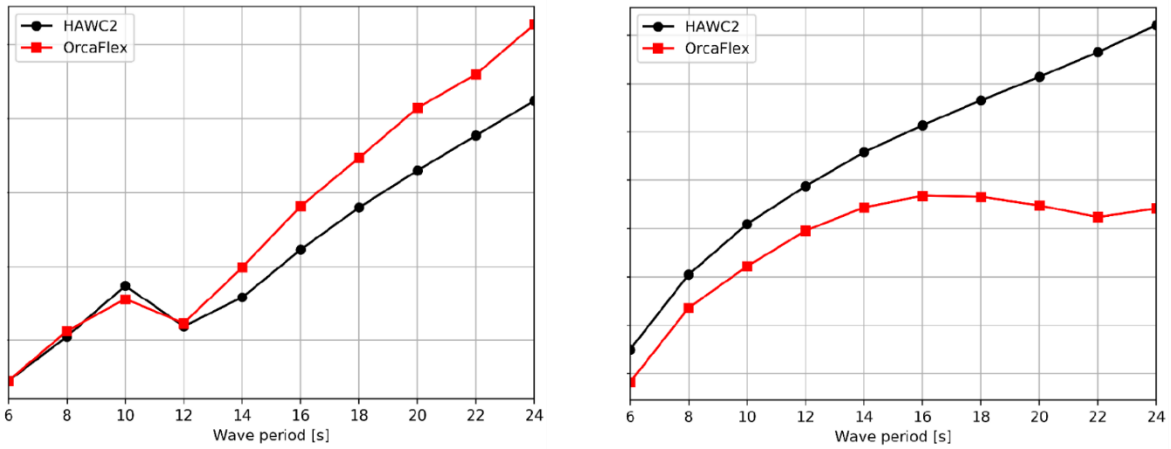

Figure 31 Comparison of the Response Amplitude Operators (RAO) of the surge (left) and pitch (right) mode for the complete PivotBuoy X140 platform (turbine incl.), obtained with HAWC2 (black circles) and OrcaFlex (red squares).

3.2.3.4 Control System Modelling

A floating offshore wind turbine poses new challenges for the controller of the typical fixed wind turbine, as discussed in section 3.1. This mainly stems from the floater natural response and wave excitation range at much lower frequencies than those found at typical fixed wind turbines. The traditional blade pitch controller is slow compared to the change in wind speed induced by tower structural response in bottom-fixed turbines. However, for a floating wind turbine, that same controller is fast enough to respond to the relative wind changes due to low frequency platform motions. A proper control strategy implementation is then necessary to avoid undesirable coupling between the controller and the floater response, which can lead to the negative effects discussed in section 3.1, such as instabilities (negative damping), higher blade loading, and suboptimal turbine performance.

Furthermore, it is also important for all wind turbines to ensure that there are no undesired structural couplings between the tower frequencies and the 1P and 3P. A benefit of the X140 design, which doesn't have a tower in a traditional sense, is that the 1P and 3P frequencies are not close to the structural mast frequencies that support the rotor-nacelle-assembly. However, as shown in Figure 32, the pontoon structural bending frequency lies in the 3P region, which should be considered when analyzing the loads and response of the platform. It should be noted that the structural design has not yet been optimized in the high frequency range, so some structural modes coinciding with blade passing frequencies was to be expected.

This project has received funding from the European Union's Horizon H2020 research and innovation programme under grant agreement No 815159

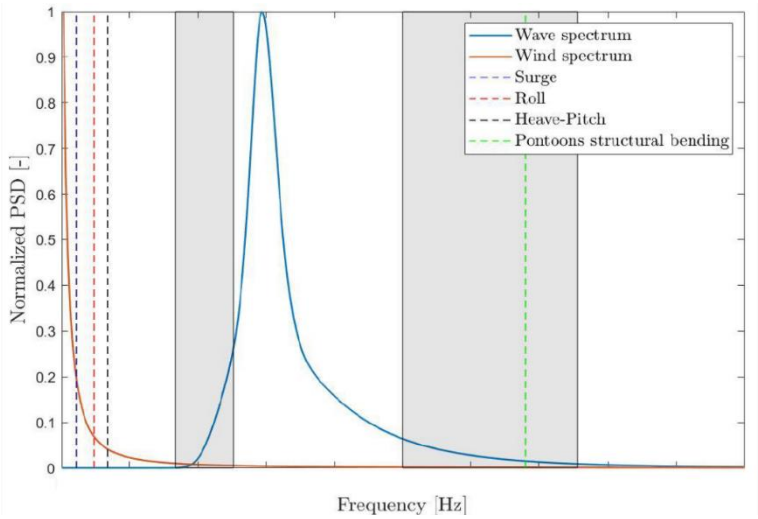

Figure 32 Normalized power spectrum density (PSD) of representative wind and wave spectra, including natural surge, heave, roll and pitch frequencies, and one of the first structural frequencies. Highlighted grey areas represents the 1P and 3P region.

The DTU Wind Energy controller [117, 118] was used for the PivotBuoy X140 analysis. It is based on a PID based regulation of pitch angle and generator torque, consisting in the following three main regions: variable speed at low wind speeds; constant speed region just below rated power, regulated by PID control on the generator torque; constant torque or constant power region for wind speeds above rated, controlled by a PID over the pitch angle.

This controller was tuned to the floating X140 PivotBuoy design through a controller pole placement analysis which has been used for floating concepts with good results [119]. Several combinations of controller frequency and rotor speed filter were tested, and the final combination was selected to provide an acceptable compromise between the turbine performance and turbine loading.

The objective is to achieve a controller frequency below the pitch frequency of the platform, but above the first horizontal translation mode. The focus of the controller tuning is set on the full load region, above rated wind speeds. The selected control strategy is to follow constant torque, as it minimizes the drivetrain loads and reduces the pitch activity of the blades, which is especially important for the offshore and floating wind turbines.

In order to assure a proper alignment of the platform with the wind direction, individual pitch control (IPC) can be used to create a correcting yawing moment. In earlier work, IPC was used within the context of reducing blade and turbine loads [120, 121, 122, 123]. The same IPC approach has been demonstrated to control the yaw moment of a floating wind turbine [124], and further improved by addressing the inherit pitch yaw coupling as response to IPC generated yawing moment [125]. A preliminary assessment of improving the yaw alignment using this strategy is presented in [1]. Figure 33 shows that this strategy can eliminate the yaw misalignment, even for the most demanding operational wind-current misalignment.

This project has received funding from the European Union's Horizon H2020 research and innovation programme under grant agreement No 815159

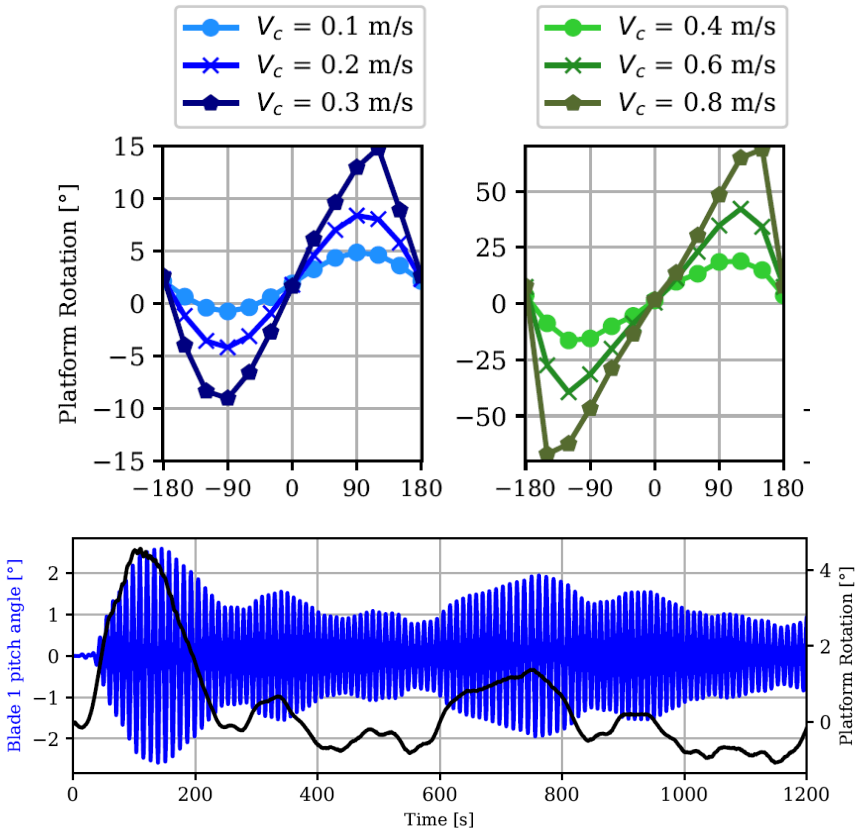

Figure 33 Average platform yaw rotation for moderate (top left) and extreme (top right) current-wind misalignment with an 8m/s unsteady wind and irregular jonswap waves with Hs=2m, Tp=10s. The reduction in yaw misalignment and blade pitch activity due to the IPC is shown in the bottom figure for the worst operational case (90deg current-wind misalignment with 0.4m/s current speed). Reproduced from [1].

The preliminary analysis shown in [1] can be considered as an initial proof-of-concept study for using IPC to control the yaw orientation of the full-scale PivotBuoy X140 platform. Additional research is necessary to evaluate the trade-off between higher energy production and higher blade loading. The suggested path for this assessment is to:

1. Perform a complete gain tuning, scheduling, and coupling matrix study, for a fixed rotor, over the entire operational wind speed range and considering various inflow conditions.
2. Compare the achievable yawing moment with a preliminary estimate of the yawing moment caused under varying external environmental conditions such as current speed and direction.
3. With the obtained gain tuning, scheduling, and coupling matrix parameters, perform a (partial) design load basis and compare the performance of the floating platform with and without the IPC system active. Besides operating yaw error and power output also carefully consider potential blade root bending moment and other potential load increases relative to a reference case without IPC.
4. Define a simplified pitch bearing and actuator damage model to assess the impact the considered IPC strategy might have on them.

This project has received funding from the European Union's Horizon H2020 research and innovation programme under grant agreement No 815159

3.2.3.5 Power Production Analysis

The performance of the IEA15MW during normal operation is as expected. The deviations from the nominal rotor speed are low, however a higher standard deviation is found around rated wind speed (10.6 m/s) due to the transition region from partial to full load. The highest rotor speed values do not exceed 20% of the nominal rotor speed which is a reference value commonly used in the industry.

The total amount of electrical energy produced over a year, or Annual Energy Production (AEP), is used as an indicator to assess the power production for a given site. In order to calculate AEP, the common practice is to distribute over different DLCs the yearly power production. For example, the wind turbine can be operating at normal turbulence and normal sea state 90% of the year (DLC 1.1) while the remaining could be split between extreme power production operations (DLC 1.6) or others DLCs. The AEP calculation presented here only considers DLC 1.1. The values in Table 11 are normalized against the Canary Islands AEP value to facilitate the comparison between sites and preserve confidentiality.

The lower wind resource available at the Begur site, when compared to very similar wind resources available at Silleiro and Canary Islands is the dominating driver in the AEP estimated at these sites.

Table 11 Estimated Annual Energy Production (AEP) for the three considered sites, normalized by the AEP obtained for the Canary Islands.

	Silleiro	Canary Islands	Begur
Annual Energy Production (AEP)	+2.4%	0%	-31.8%

3.2.3.6 Mooring Line Tension

The maximum and minimum mooring line tensions for all the three sites, across all DLCs, are shown in Figure 34. For all sites, the extreme TLP axial force is found on the DLC 7.1- parked with rotor locked, where the turbine is not operating with parked rotor and extreme severe sea state is used. The TLP axial force extreme loading originates by a combination of a high mean water, extreme waves and extreme wind.

For the Canary Islands site, for which the PivotBuoy X140 platform was designed, little variation in the maximum and minimum mooring tensions is observed across all DLCs, with a small range between minimum and maximum loads.

The largest loading is found at the Silleiro site followed by Begur and then the Canary Islands. It is expected that Silleiro, with the highest extreme water level range (EWLR) and the most severe wave and windstorms presents the larger TLP Axial Force. The extreme wave cases and EWLR are not that different from Begur and the Canary Islands, but the windstorm is. Begur, with a 50-year extreme event around 44 m/s, is considerable higher than the 28 m/s of the Canary Islands. This indicates that the extreme is most likely given by the further from the turbine TLP line which is in higher tension due to the increased wind turbine thrust in the Begur Site.

This project has received funding from the European Union's Horizon H2020 research and innovation programme under grant agreement No 815159

The minimum loading is also shown in Figure 34, which is problematic if negative or close to zero values are found, leading to snapping loads on the mooring line. For Silleiro all the cases with extreme sea states (DLC 16, DLC 61 and DLC71) present critically small minimum line tensions. The same occurs at DLC 61 for Begur.

These poorer performances at Silleiro and Begur are a consequence of the assumptions made at the beginning of the deliverable, where the same PivotBuoy X140 designed for the Canary Islands was used for all sites, where in reality there would be design iterations carried out to better suit de design to these new sites.

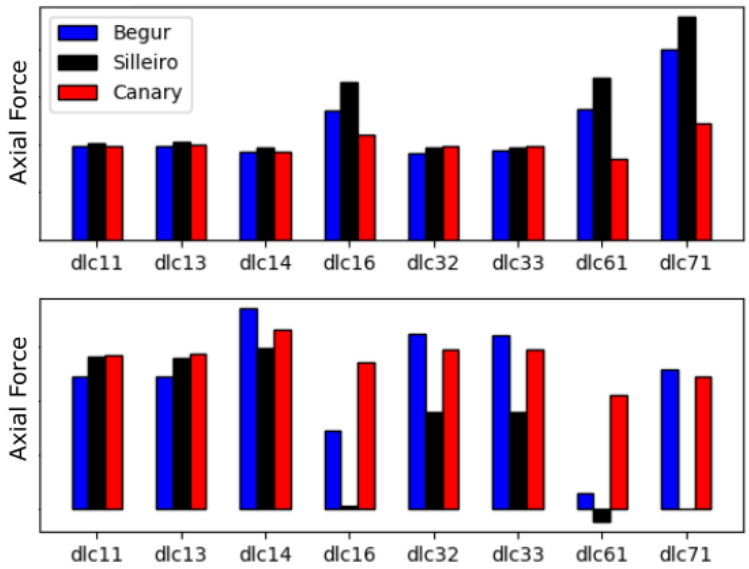

Figure 34 Extreme mooring load comparison for the three sites considered, per DLC. The maximum loads are shown at the top, with the minimum loads shown at the bottom.

3.2.3.7 Yaw Flange Accelerations

The fore-aft and side-side acceleration at the yaw flange, which supports the rotor-nacelle assembly, are presented in Figure 35. The accelerations at the RNA are a key performance indicator of floating foundations, as it impacts directly the turbine performance and loading. Furthermore, if a certain acceleration threshold is exceeded, then the wind turbine will shut down and it can possibly harm the mechanical components on the nacelle. The accelerations are also a good indication of the platform stability during operation and extreme events. The fore-aft and side-side accelerations are lower than 2 m/s^2 for all operational cases, which implies a proper controller tuning and good platform stability.

This project has received funding from the European Union's Horizon H2020 research and innovation programme under grant agreement No 815159

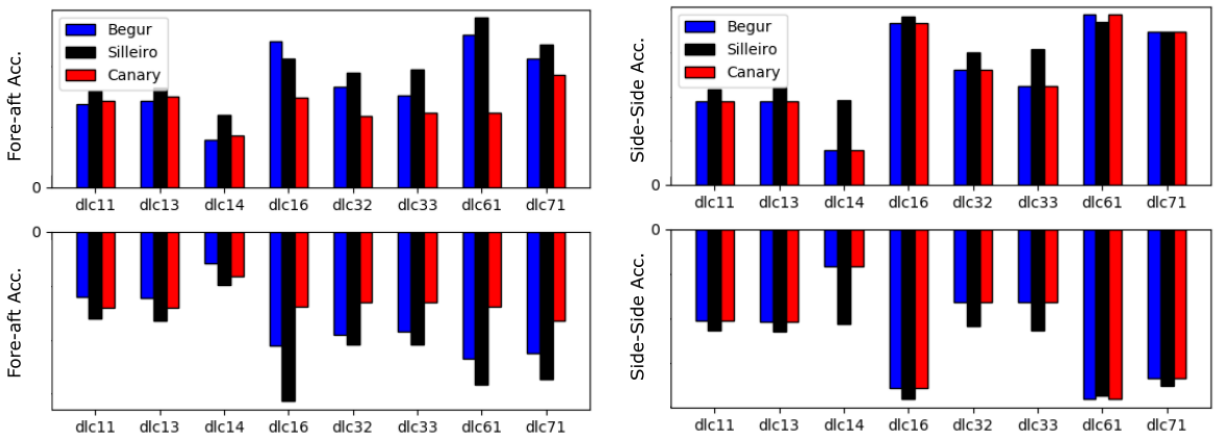

Figure 35 Comparison of the yaw flange fore-aft accelerations (left) and side-side accelerations (right) per DLC and site. The maximum values are presented on the top bar charts, while the minimum values shown in the bottom bar chart.

This project has received funding from the European Union's Horizon H2020 research and innovation programme under grant agreement No 815159

4 BENCHMARK OF PIVOTBUOY FULL-SCALE SYSTEM

In this section the X140 PivotBuoy 15MW system results presented in section 3.2.3 will be compared with other data available in the open literature concerning floating foundations with the same 15MW reference turbine, namely the WindCrete spar and ActiveFloat semi-submersible developed within the EU H2020 COREWIND project [44], and the VolturnUS-S semi-submersible platform developed within the IEA Wind Task 37 [57]. The main system characteristics are discussed in section 4.1, with the main differences in hydrodynamic and aeroelastic modelling discussed in section 0 and 4.3, respectively. Finally, the comparison of the maximum nacelle accelerations and maximum mooring line tension is made in sections 4.4 and 4.5, respectively.

4.1 Comparison of the Main System Properties

The benchmark of the PivotBuoy X140 system is made against other floating offshore wind concepts with the new 15MW reference turbine. Due to the novelty of this turbine, only three other designs were found in the open literature, which are shown in Figure 36 and summarized in Table 12. The ActiveFloat semi-submersible and the WindCrete spar, developed within the EU H2020 COREWIND project, are concrete based designs in order to lower the LCoE (see section 2.2) [114]. The VolturnUS-S is a generic steel version of the original concrete design, which has been developed by the University of Maine (UMaine) and the U.S. Department of Energy [57].

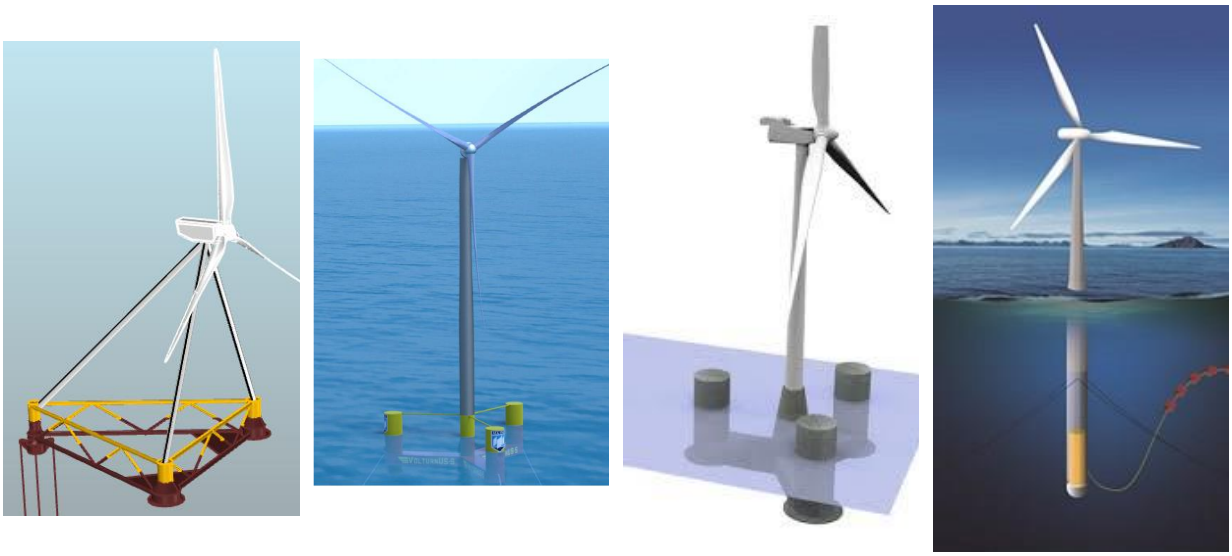

Figure 36 Concepts used to benchmark the full-scale PivotBuoy X140 system, from left to right: PivotBuoy X140 system, VolturnUS-S; ActiveFloat, and WindCrete.

Due to the PivotBuoy system, the X140 platform is able to achieve a 3.5 to 7.5 mass reduction when compared to the other concepts, which results in a favourable power to mass ratio. This also enables a significantly lower operational draft then the other semi-submersible concepts, which facilitates port logistics and assembly. The PivotBuoy X140 system has the highest reported steel consumption,

This project has received funding from the European Union's Horizon H2020 research and innovation programme under grant agreement No 815159

just above the VolturnUS-S design, while the ActiveFloat and WindCrete spar are concrete based structures. Nevertheless, it requires negligible ballast weight when compared with the other designs.

Some differences between the different studies are worth mentioning. For example, all the mentioned studies were carried out for a 200m water depth, while the PivotBuoy X140 analysis considered a 150m water depth. Furthermore, despite all studies using the 15MW offshore reference turbine [59], different hub heights were considered, with the VolturnUS-S being the only one adopting the reference 150m hub height value. Conversely, the VolturnUS-S has assumed a RNA mass of 991 t, which is slightly smaller than the reference value of 1017 t adopted by the other designs.

Another important difference is the site selection for the analysis. The VolturnUS-S has considered a US East Coast reference site [126], while the ActiveFloat and WindCrete considered the same Canary Islands site. The Canary Islands site considered for ActiveFloat and WindCrete is approximately the same as considered for the X140 PivotBuoy system, which makes for a good baseline to benchmark the PivotBuoy X140 full-scale system.

Table 12 Main characteristics of the analysis of 15MW floaters used to benchmark the PivotBuoy full-scale system.

	X140 PivotBuoy	VolturnUS-S	ActiveFloat	WindCrete
Type	Hybrid TLP and semi-submersible system	Steel semi-submersible	Concrete semi-submersible with active ballast system	Concrete spar and tower monostructure
Reference	[112]	[101]	[44]	[44]
Site Selected	Canary Islands, Begur, Silleiro	US East Coast site	Canary Islands	Canary Islands
Water depth	150 m	200 m	200 m	200 m
Main dimension	135 m	102 m	84 m	13.2 m
Operational Draft	9 m	20 m	26.5 m	155 m
Hub Height (wrt mwl)	140 m	150 m	135 m	135 m
Total Mass (turbine incl.)	5429 t	20093 t	36593 t	39805 t
Power to Mass ratio	2.76 W/kg	0.75 W/kg	0.41 W/kg	0.38 W/kg

This project has received funding from the European Union's Horizon H2020 research and innovation programme under grant agreement No 815159

4.2 Comparison of the Hydrodynamic Properties

The hydrodynamic modelling approach is summarized in Table 13. Linear potential flow theory, complemented by the second-order QTFs to account for difference and sum frequencies loading was applied in all projects, except for the PivotBuoy X140 system, where strip theory using Morison formulation was applied. Despite being a magnitude smaller than first order wave excitation, the second order wave forces are known to excite the low frequency response, in particular for the semi-submersibles, as discussed in section 3.1.2. Therefore, the X140 numerical model is expected to underpredict the low frequency response when compared to the other models. All the studies have calibrated the drag elements with previous model test results, with all cases applied Morison formulation, except for the VolturnUS-S, where a quadratic damping model was calibrated with CFD results to complement the potential damping matrix obtained through linear potential theory. Previous comparative analysis on the OC4-DeepCwind semi-submersible has showed better performance for Morison drag elements than for quadratic damping matrices, as discussed in section 3.1.2.

Table 13 Hydrodynamic modelling approach for each selected project.

	X140 PivotBuoy	VolturnUS-S	ActiveFloat	WindCrete
Reference	[112]	[101]	[44]	[44]
Hydrodynamic Solver	HAWC2 internal hydrodynamic solver	OpenFAST (HydroDyn) + WAMIT	OpenFAST (HydroDyn) + ANSYS-AQWA	OpenFAST (HydroDyn) + ANSYS-AQWA
Hydrodynamic Theory	Strip theory with Morison Equation	Potential flow + quadratic drag model + second order QTFs (difference and sum frequencies)	Potential Flow with Drag Morison elements + second order QTFs (difference and sum frequencies)	Potential Flow with Drag Morison elements + second order QTFs (difference and sum frequencies)
Mooring Analysis	HAWC2 internal dynamic mooring solver	MoorDyn Quasi-dynamic model	MoorDyn Quasi-dynamic model	MoorDyn Quasi-dynamic model

The reported natural frequencies obtained from each model is shown in Table 14. The PivotBuoy X140 concept and the WindCrete spar shown natural frequencies well outside the usual wave excitation range, with both semi-submersibles showing heave resonance close the lower limit of the wave excitation range. The semi-submersibles also show low frequency resonance in the surge/sway modes, which is to be expected. The PivotBuoy X140 concept shows natural resonance closer to the semi-submersible range rather than the usual higher frequency natural resonance expected for a conventional TLP.

This project has received funding from the European Union's Horizon H2020 research and innovation programme under grant agreement No 815159

Table 14 Natural periods of the of 15MW floaters considered in the comparison analysis. The PivotBuoy X140 values are omitted for confidentiality reasons, but are within the range defined by the other concepts.

	X140 PivotBuoy	VolturnUS-S	ActiveFloat	WindCrete
Type	Hybrid TLP and semi-submersible system	Steel semi-submersible	Concrete semi-submersible with active ballast system	Concrete spar and tower monostructure
Reference	[112]	[101]	[44]	[44]
Surge	within range	142.9 s	166.7 s	83.3 s
Sway	na[1]	142.9 s	nr[2]	83.3 ([3]) s
Heave	within range	20.4 s	18.2 s	32.3 s
Roll	within range	27.8 s	nr[2]	41.7 ([3]) s
Pitch	within range	27.8 s	32.3 s	41.7 s
Yaw	na[1]	90.9 s	83.3 s	10.9 s

[1]) *PivotBuoy is a weathervanning single point mooring, therefore the sway and yaw response are not reported.*
[2]) *Not reported*
[3]) *Not reported, but assumed due to symmetry.*

While it was not possible to find RAOs for the ActiveFloat or the WindCrete, the VolturnUS-S has published its RAOs, which are compared with the full-scale PivotBuoy X140 in Figure 37. As can be seen, limited first order response is expected for the wave excitation range shown, except for VolturnUS-S close to the natural pitch frequency of 27.8s. Due to second order excitation, it is expected that the low order response is more pronounced than wave frequency response, as discussed in section 3.1.2.

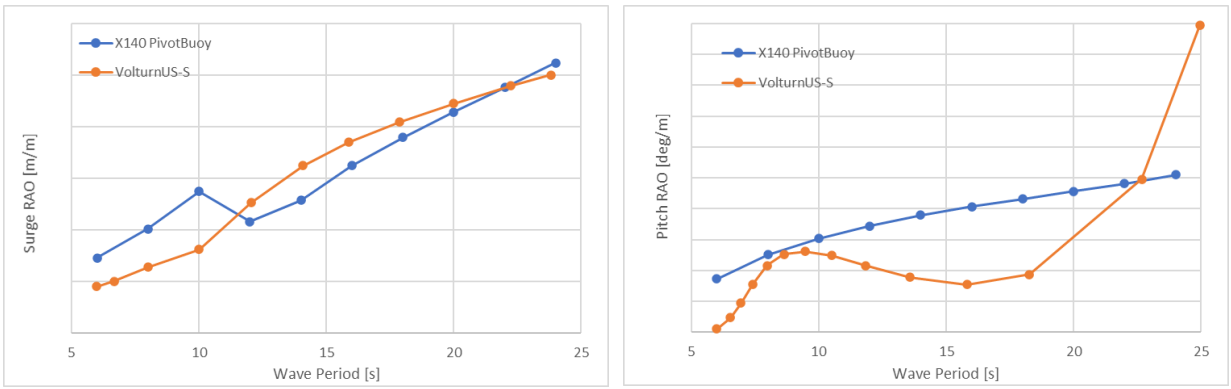

Figure 37 Surge and Pitch RAOs for the full-scale PivotBuoy X140 and VolturnUS-S designs. Values for the VolturnUS-S are obtained with WebPlotDigitizer [127] from the plots shown in [101].

This project has received funding from the European Union's Horizon H2020 research and innovation programme under grant agreement No 815159

4.3 Comparison of the Aeroelastic-Servo Properties

With the exception of the full-scale PivotBuoy X140 which used HAWC2, all other studies have adopted OpenFAST (AeroDyn) for the aeroelastic simulation design, with the ROSCO controller used. All aeroelastic codes used blade momentum theory (BEM) with a 1D beam approximation for the structural model of the blades. All the controllers were tuned to account for the floating foundation dynamics, with the ActiveFloat and WindCrete using exactly the same controller. No significant difference is expected to occur due to the modelling choices here presented.

It is expected that higher differences occur due to the skewed inflow conditions of the X140, which due to the weather vanning nature of the PivotBuoy is expected to experience higher yaw misalignments than the other designs. To mitigate this issue, a preliminary test with and individual pitch controller (IPC) tracking the yaw error was carried out with promising results (see section 3.2.3.4)

Table 15 Aeroelastic-servo modelling approach for each selected project.

	X140 PivotBuoy	VolturnUS-S	ActiveFloat	WindCrete
Reference	[112]	[101]	[44]	[44]
Aeroelastic Solver	HAWC2	OpenFAST (AeroDyn)	OpenFAST (AeroDyn)	OpenFAST (AeroDyn)
Aerodynamic Model	Blade Element Momentum (BEM)	Blade Element Momentum (BEM)	Blade Element Momentum (BEM)	Blade Element Momentum (BEM)
Blades Structural Model	1D beams with a multi-body dynamics method (MBD)	1D beams with a modal approach	1D beams with a modal approach	1D beams with a modal approach
Controller	DTU Wind Energy controller, modified version, collective pitch controller (CPC)	NREL Reference OpenSource Controller (ROSCO), modified version, collective pitch controller (CPC)	NREL Reference OpenSource Controller (ROSCO), modified version, collective pitch controller (CPC)	NREL Reference OpenSource Controller (ROSCO), modified version, collective pitch controller (CPC)

This project has received funding from the European Union's Horizon H2020 research and innovation programme under grant agreement No 815159

4.4 Comparison of the Maximum Nacelle Accelerations

The accelerations at the RNA are a key performance indicator of floating foundations, as it impacts directly the turbine performance and loading. Therefore, keeping the accelerations at the RNA within certain thresholds is an important design criterion, with the COREWIND consortium identifying 3.5 m/s^2 and 2.94 m/s^2 as the survival limit for the WindCrete and ActiveFloat, respectively [44]. For lack of better values, these limits will be used as a reference in the discussion, although they were defined only for the WindCrete and ActiveFloat in the Canary Islands site.

The maximum accelerations reported for DLC6.1 were compiled and are presented in Figure 38. It should be noted that VolturnUS-S results are obtained for a US East Coast reference site, while the other designs are for a Canary Island site, which limits the comparability between VolturnUS-S and the remaining designs. Other DLC are not shown due to either lack of available data or confidentiality reasons.

The maximum fore-aft accelerations are comparable between the different designs, which places the X140 on par with the other designs. Furthermore, all designs are within the operational limits established by the COREWIND project for the WindCrete and the ActiveFloat.

For the side-side accelerations the X140 is providing larger accelerations than for the fore-aft mode, while all other designs show significantly lower accelerations. Nevertheless, the accelerations are within the limits defined by the COREWIND project.

It should be noted that the lighter design of the X140 platform will result in higher accelerations for the same excitation forces, therefore higher accelerations were expected. Furthermore, it should be noted that DLC6.1 includes cross wave-wind conditions, where it is also expected higher accelerations due to the weathervanning nature of the X140 concept. Nevertheless, these conditions have a small probability of occurrence and are therefore expected to have a small impact in the overall lifetime of the turbine.

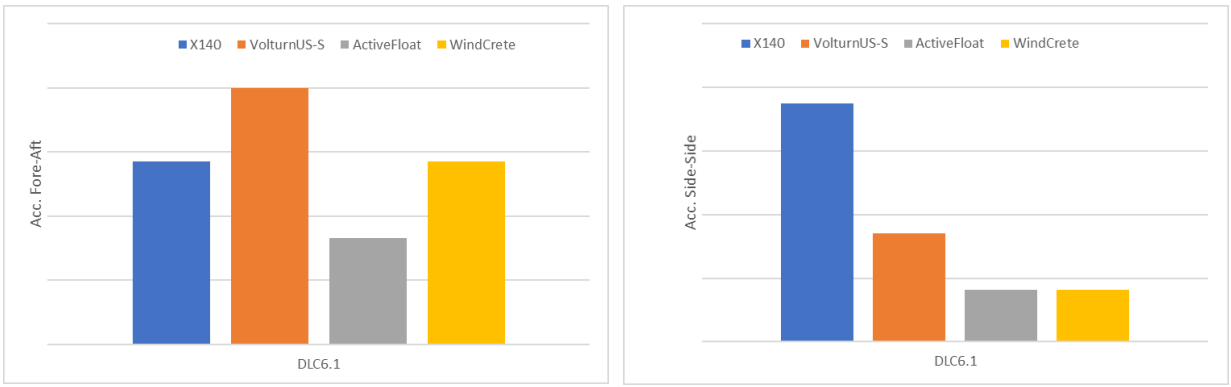

Figure 38 Comparison of the maximum accelerations in DLC1.6 for all the designs considered. Note that VolturnUS-S was evaluated for a typical US East Coast site, while the other concepts were evaluated for a Canary Island site.

This project has received funding from the European Union's Horizon H2020 research and innovation programme under grant agreement No 815159

4.5 Comparison of the Maximum Mooring Line Tension

The maximum mooring line load is an important design criterion to assess the safety of the design. It was only possible to obtain these parameters for the semi-submersible VolturnUS-S, which was analysed for a typical US East Coast site, while the X140 PivotBuoy was analysed for a Canary Island site. Furthermore, the VolturnUS-S mooring system consists of three 850-m-long chain catenary lines in 200m water depth, utilizing the largest chain size currently available, in order to restrict the maximum platform excursions to 25 m. The PivotBuoy mooring system consists of four tensioned vertical tendons in 150m water depth. Another point of difference is the absence of second order wave loads in the analysis of the full-scale X140 PivotBuoy system, which are expected to increase the low frequency response of the floater, increasing the mooring line tensions. Despite the different mooring systems, comparable maximum mooring lines are obtained for both designs.

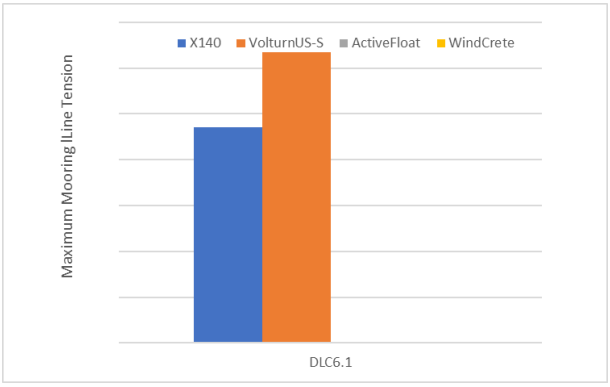

Figure 39 Comparison of the maximum mooring line tension for DLC1.6 for all the designs considered. Note that VolturnUS-S was evaluated for a typical US East Coast site, while the other concepts were evaluated for a Canary Island site. Note that this data is not available for the ActiveFloat or the WindCrete.

This project has received funding from the European Union's Horizon H2020 research and innovation programme under grant agreement No 815159

5 CONCLUSIONS AND FUTURE WORK

A benchmark of the full-scale PivotBuoy X140 system against other large floating offshore wind systems is presented as an outlook for the future commercial floating offshore wind systems in the 15MW range. This benchmark is carried out in two fronts: a design benchmark, positioning the PivotBuoy concept and design approach amongst the current floating offshore wind systems; and a simulation benchmark, by comparison of the simulation approach and estimated response of the full scale PivotBuoy X140 system against other 15MW floating offshore wind designs.

For the design benchmark, the PivotBuoy design is placed in the hybrid category due to its innovative blend of single point TLP mooring, weathervane capacity, downwind turbine, and semi-submersible type floater. This category presents the disruptive and innovative concepts with higher potential benefits, which also carry higher risks due to unproven technology. Therefore, the hybrid category is lagging in TRL when compared to the more established mooring stabilized category (spars) or buoyancy stabilized category (semi-submersibles). Nevertheless, the PivotBuoy concept is well placed within its class in terms of TRL and development plan. A non-exhaustive review of the floating offshore wind concepts was carried out, which as future work can be extended and maintained to reflect the current state of the floating offshore wind industry.

The simulation benchmark of the PivotBuoy design is presented in the context of the current state of the art, presenting different modelling approaches, at different fidelity levels, commonly used for floating offshore wind systems. A floating offshore wind turbine is a complex nonlinear system, involving different physics, and therefore require a multidisciplinary approach to accurately model its behaviour. Typically, this has been accomplished by coupling aeroelastic codes, originally developed for the onshore wind industry, with hydrodynamic and mooring codes, originally developed within the oil and gas industry. However, to address the needs of the nascent offshore wind industry, hydrodynamic codes such as OrcaFlex have been extending their internal capabilities to allow for aeroelastic modelling, and vice-versa (e.g. HAWC2). Nevertheless, this is still a very active research field, with large international collaborative projects such as the OC6 currently ongoing, focusing on improving the numerical modelling capabilities, which so far have been found insufficiently accurate to reduce the safety margins and usher floating offshore wind into competitiveness. Regarding the needs of the PivotBuoy design, a few key points are identified as requiring additional research:

- The best practices for aeroelastic modelling of downwind turbines are currently under research. The three support masts will induce wind shadowing effects and highly unsteady wind conditions, leading to increased non-symmetry on the rotor loading and poorer energy production. Some preliminary research has already been conducted with CFD RANS simulation on the X30 platform, which showed a low velocity deficit due to support shadowing, resulting in almost negligible 3P and 6P excitations. Additional research effort is necessary to properly quantify these effects.

- The current aeroelastic theory is being pushed to the limit with the increasingly large and more flexible rotors. The higher rotor areas capture more unsteady wind inflow effects, and the higher flexibility, coupled with floater response leads to significant blade-wake interaction effects. Particular to the PivotBuoy weathervane capacity is the impact of highly

This project has received funding from the European Union's Horizon H2020 research and innovation programme under grant agreement No 815159

skewed inflow conditions, due to yaw misalignment when compared with other turbines with active yaw systems. There is a demand for better aerodynamic models that can account for these effects in a cost-effective manner.

- The three support masts have the benefit of shifting the tower frequency from the 1P and 3P regions, however these unique structures require specific modelling, and their structural behaviour is important to capture the complete system response.

- The weathervane capacity is an important feature of the PivotBuoy design. To accurately model it, the impacts of the multiple environmental loads need to be accurately assessed. This includes current loading on the underwater structure, wave loading on the wave exposed areas, and wind loading on the above water structure. It should be noted that aerodynamic profiles are envisaged for the masts that support the RNA, and possibly some wings or sails between them, making wind load modelling a critical component to accurately assess the yaw alignment of the turbine.

A noteworthy trend is, while safeguarding the commercial actors' confidentiality concerns, the transition towards open-source codes, open data sharing, and community development, which is expected to accelerate the industry development and reduce the time horizon for full-scale commercial floating offshore wind deployment.

The simulation work carried out so far within WP5 of the PivotBuoy project was summarized, with the relevant results presented, including a comparison of two different numerical codes, one more suited to aeroelastic modelling, HAWC2, and the other to hydrodynamic modelling, OrcaFlex, which were generally found in good agreement. As expected, there is some limitations to the aeroelastic capabilities of the hydrodynamic code OrcaFlex, and some limitations to the hydrodynamic capabilities of the aeroelastic code HAWC2. These limitations have been identified, and future research to better understand the differences have been proposed:

- OrcaFlex currently cannot model blade prebend, although future releases are expected to cover this limitation.

- Future work is necessary to better understand the differences in hub/tip loss corrections between HAWC2 and OrcaFlex, or cross-sectional effects such as bend-twist coupling, and their impact in the overestimation of the normal loading on the outer sections of the blade.

- The limited hydrodynamic capabilities of HAWC2 when compared to Orcaflex. In the present work a first order Morison strip theory was used. This is critical, since second order wave forces have been found to excite the floaters low frequency response, resulting in higher excursions, which leads to higher loadings on the turbine and moorings. Future work using the HAWC2-WAMIT coupling can evaluate the impact of neglecting second order wave loads.

Developing both numerical models in parallel provided valuable insight into the advantages and limitations of each numerical code, and resulted in an overall better numerical model for the PivotBuoy system.

The simulation results for the full-scale PivotBuoy X140 design for three different sites was

This project has received funding from the European Union's Horizon H2020 research and innovation programme under grant agreement No 815159

presented. Yaw misalignment is found in extreme (and unlikely) cross-directional conditions for the PivotBuoy design, which leads to suboptimal turbine performance. Despite having a conservative prediction of the yaw misalignment, this suggests that the weathervane capability can be improved. Strategies for addressing this issue have been investigated, such as individual pitch controller (IPC) which removes the yaw misalignment at the expense of higher blade loading. A preliminary study with promising results has been published in [1].

Finally, open literature results for floating offshore wind foundations equipped with the novel 15MW offshore reference turbine are compiled. The relevant cases found are the WindCrete spar and ActiveFloat semi-submersible, both developed within the EU H2020 COREWIND project, and the VolturnUS-S semi-submersible platform developed within the IEA Wind Task 37. The COREWIND concepts are particularly relevant since their site selection coincides with one of the sites used for the PivotBuoy X140 analysis (Canary Islands). The main system characteristics of these designs were reviewed and compared, and despite having the largest steel consumption, the PivotBuoy design enables a 3.5 to 7.5 weight reduction when compared to the other designs. The hydrodynamic and aeroelastic models used in all studies are discussed, and the lack of second order wave forces on the PivotBuoy is identified as a current limitation of the numerical model, which should be improved for future versions.

The maximum nacelle accelerations, a key performance indicator of floating foundations, are then compared between the different projects for the DLC6.1. The PivotBuoy X140 performs comparably to the reference projects.

The maximum mooring line tension is then compared with the VolturnUS-S design, which is moored with a catenary system. The COREWIND designs were not included due to lack of data. The maximum loads on the tendons of the Pivotbuoy X140 design are comparable to those found in the catenary mooring of the VolturnUS-S.

This review has found the large scale PivotBuoy X140, designed for the 15 MW offshore reference turbine, to be on par with other hybrid concepts in terms of TRL and development plan, and comparable in terms of predicted response when compared to other floating designs for the same turbine.

It should be noted that these simulations are carried out for future preliminary designs, and therefore significant uncertainties are present in the analysis Furthermore, the numerical model is currently being improved and fine tuned as more information becomes available. The value of this benchmarking exercise is not to rank designs, but to establish a common baseline and provide confidence in the simulation results, which can then be used to identify the challenges and potential of these large scale floating offshore wind designs.

This project has received funding from the European Union's Horizon H2020 research and innovation programme under grant agreement No 815159

6 BIBLIOGRAPHY

[1] A. M. Úrban, L. Voltà, W. H. Lio and R. Torres, "Preliminary assessment of yaw alignment on a single point moored downwind (under review)," in *EERA Deepwind 2021*, 2021.

[2] A. Myhr, "Developing Offshore Floating Wind Turbines: The Tension-Leg-Buoy Design," Ås, Norway, 2016.

[3] Quest Floating Wind Energy Q FWE, "Moorings," [Online]. Available: https://questfwe.com/documentation-center/moorings/.

[4] J. Sanz, "The Iberian region as a hub for technology development and industrial leadership in the field of floating offshore wind," EIT InnoEnergy, 2020.

[5] S. Burmester, G. Vaz and O. el Moctar, "Towards credible CFD simulations for floating offshore wind turbines," *Ocean Engineering,* vol. 209, p. 107237, 2020.

[6] M. Hannon, E. Topham, J. Dixon, D. Mcmillan and M. Collu, "Offshore wind, ready to float? Global and UK trends in the floating offshore wind market," University of Strathclyde, Glasgow, 2019.

[7] M. Cruciani, "Offshore Wind Power Floating in its Industrial and Technological Dimension," Études de l'Ifri, Paris, France, 2019.

[8] S. Butterfield, W. Musial, J. Jonkman, P. Sclavounos and L. Wayman, "Engineering Challenges for Floating Offshore Wind Turbines," in *Copenhagen Offshore Wind Conference*, Copenhagen, Denmark, 2005.

[9] M. T. Andersen, "Floating Foundations for Offshore Wind Turbines," Aalborg, Denmark, 2016.

[10] S. Mewes, "Numerical Prediction of Hydrodynamic Damping and Loads on a Floating Offshore Wind Turbine," Duisburg, Germany, 2021.

[11] J. Amate, G. Sánchez and G. González, "Development of a Semi-submersible Barge for the installation of a TLP floating substructure: TLPWIND case study," *Journal of Physics: Conference Series,* vol. 749, p. 012016, 2016.

[12] CarbonTrust, "Floating Wind Joint Industry Project: Phase I Summary Report," 2018.

[13] J. M. Jonkman and D. Matha, "Dynamics of offshore floating wind turbines - analysis of three concepts," *Wind Energ.,* vol. 14, pp. 557-569, 2011.

This project has received funding from the European Union's Horizon H2020 research and innovation programme under grant agreement No 815159

[14] Y.-H. Lin, S.-H. Kao and C.-H. Yang, "Investigation of Hydrodynamic Forces for Floating Offshore Wind Turbines on Spar Buoys and Tension Leg Platforms with the Mooring Systems in Waves," *Applied Sciences,* vol. 9, p. 608, 2019.

[15] Glosten, "PelaStar Cost of Energy: A cost study of the PelaStar floating foundation system in UK waters," PELASTAR, Washington, 2014.

[16] Pelastar, [Online]. Available: https://pelastar.com/.

[17] offshorewind.biz, "GE, Glosten Present 12 MW Floating Wind Turbine Concept," 5 May 2021. [Online]. Available: https://www.offshorewind.biz/2021/05/25/ge-glosten-present-12-mw-floating-wind-turbine-concept/.

[18] GICON-SOF, "MEDIA," [Online]. Available: http://www.gicon-sof.de/en/media.html.

[19] F. Adam, T. Myland, F. Dahlhaus and J. Grossmann, "GICON®-TLP for wind turbines – the path of development," in *1st International Conference on Renewable Energies Offshore (RENEW)*, Lisbon, Portugal, 2014.

[20] GICON-SOF, "Technical Solution," [Online]. Available: http://www.gicon-sof.de/en/technical-solution.html. [Accessed February 2021].

[21] M. Kausche, F. Adam, F. Dahlhaus and J. Grossmann, "Floating offshore wind - Economic and ecological challenges of a TLP solution," *Renewable Energy,* vol. 126, 2018.

[22] J. V. Taboada, "Comparative Analysis Review on Floating Offshore Wind Foundations (FOWF)," in *54º Congreso de Ingeniería Naval e Industrial Marítima*, Ferrol, Spain, 2015.

[23] M. Leimeister, A. Kolios and M. Collu, "Critical review of floating support structures for offshore wind farm deployment," *Journal of Physics: Conference Series,* 2018.

[24] J. Jonkman and W. Musial, "Offshore Code Comparison Collaboration (OC3) for IEA Task 23 Offshore Wind Technology and Deployment," 2010.

[25] Fukushima Offshore Wind consortium, "Photo," [Online]. Available: http://www.fukushima-forward.jp/english/photo/index.html.

[26] Equinor, "Hywind Tampen: the world's first renewable power for offshore oil and gas," [Online]. Available: https://www.equinor.com/en/what-we-do/hywind-tampen.html. [Accessed February 2021].

[27] S. I. S. T. Utsunomiya T., "Floating Offshore Wind Turbines in Goto Islands, Nagasaki, Japan," in *WCFS2019*, Springer Singapore, 2020, pp. 359-372.

This project has received funding from the European Union's Horizon H2020 research and innovation programme under grant agreement No 815159

[28] T. Utsunomiya, I. Sato, O. Kobayashi, T. Shiraishi and T. Harada, "Design and Installation of a Hybrid-Spar Floating Wind Turbine Platform," in *ASME 2015 34th International Conference on Ocean, Offshore and Arctic Engineering*, St. John's, 2015.

[29] T. Utsunomiya, I. Sato, S. Yoshida, H. Ookubo and S. Ishida, "Dynamic Response Analysis of a Floating Offshore Wind Turbine During Severe Typhoon Event," in *ASME 2013 32nd International Conference on Ocean, Offshore and Arctic Engineering*, Nantes, 2013.

[30] S. Ishida, K. Kokubun, T. Nimura, T. Utsunomiya, I. Sato and S. Yoshida, "At-Sea Experiment of a Hybrid SPAR Type Offshore Wind Turbine," in *ASME 2013 32nd International Conference on Ocean, Offshore and Arctic Engineering*, Nante, 2013.

[31] T. Utsunomiya, S. Yoshida, S. Kiyoki, I. Sato and S. Ishida, "Dynamic Response of a Spar-Type Floating Wind Turbine at Power Generation," in *ASME 2014 33rd International Conference on Ocean, Offshore and Arctic Engineering*, San Francisco, 2014.

[32] H. Yoshimoto, T. Natsume, J. Sugino, H. Kakuya, R. Harries, A. Alexandre and D. McCowen, "Validating Numerical Predictions of Floating Offshore Wind Turbine Structural Frequencies in Bladed using Measured Data from Fukushima Hamakaze," 2019.

[33] R. Ebenhoch, D. Matha, S. Marathe, P. C. Muñoz and C. Molins, "Comparative Levelized Cost of Energy Analysis," *Energy Procedia,* vol. 80, pp. 108-122, 2015.

[34] M. Lerch, M. De-Prada-Gil, C. Molins and G. Benveniste, "Sensitivity analysis on the levelized cost of energy for floating offshore wind farms," *Sustainable Energy Technologies and Assessments,* vol. 30, pp. 77-90, 2018.

[35] M. Mahfouz, M. Salarai, S. Hernández, F. Vigara, C. Molins, P. Trubat, H. Bredmose and A. Pegalajar-Jurado, "D1.3 Public design and FAST models of the two 15MW floater-turbine concepts," 2020.

[36] A. Courbois, E. Tcheuko, B. Bouscasse, O. Kimmoun and R. Mariani, "Study of Viscous Effects on Wave Drift Forces on a Rectangular Pontoon With a Damping Plate by Using CFD Code OpenFOAM," in *ASME 2018 37th International Conference on Ocean, Offshore and Arctic Engineering*, Madrid, Spain, 2018.

[37] L. Guignier, A. Courbois, R. Mariani and C. Thomas, "Multibody Modelling of Floating Offshore Wind Turbine Foundation for Global Loads Analysis," in *26th International Ocean and Polar Engineering Conference*, Rhodes, Greece, 2016.

[38] T. Choisnet, "Ideol's french and japanese demonstrators, a necessary stepping stone on the way to commercial-scale projects," in *Floating Offshore Wind Turbines 2019*, Montpellier, France, 2019.

This project has received funding from the European Union's Horizon H2020 research and innovation programme under grant agreement No 815159

[39] Ideol, "Projects," [Online]. Available: https://www.ideol-offshore.com/en/our-projects. [Accessed February 2021].

[40] A. Robertson, J. Jonkman, M. Masciola, H. Song, A. Goupee, A. Coulling and C. Luan, "Definition of the Semisubmersible Floating System for Phase II of OC4," National Renewable Energy Laboratory, Golden, CO, 2014.

[41] A. Yamaguchi and T. Ishihara, "PO.ID 332 Current Status of Research Activity on Floating Offshore Wind Turbine In Japan," in *EWEA OFFSHORE*, Frankfurt, 2013.

[42] EDP, [Online]. Available: https://www.edp.com/pt-pt/inovacao/windfloat.

[43] W. Musial, P. Beiter and J. Nunemaker, "Cost of Floating Offshore Wind Energy Using New England Aqua Ventus Concrete Semisubmersible Technology," NREL/TP-5000-75618, Golden, CO, United States of America, 2020.

[44] M. Y. Mahfouz, M. Salari, S. Hernández, F. Vigara, C. Molins, P. Trubat, H. Bredmose and A. Pegalajar-Jurado, "D1.3 Public design and FAST models of the two 15MW floater-turbine concepts," 2020.

[45] D. Roddier, C. Cermelli, A. Aubault and A. Weinstein, "WindFloat: A floating foundation for offshore wind turbines," *Journal of Renewable and Sustainable Energy,* vol. 2, no. 3, p. 033104, 2010.

[46] Principle Power, "Key Market Projects," [Online]. Available: https://www.principlepowerinc.com/en/windfloat/key-markets-projects.

[47] M. Komatsu, H. Mori, H. Tanaka, M. Ohta, K. Karikomi and H. Ishii, "Comparison between measured value and simulated value of motion and mooring force in mitsubishi 7MW floating offshore wind turbine," in *Grand Renewable Energy*, Yokohama, 2018.

[48] J. Jonkman, S. Butterfield, W. Musial and G. Scott, "Definition of a 5-MW Reference Wind Turbine for Offshore System Development," National Renewable Energy Laboratory, Golden, CO, 2009.

[49] A. Robertson, J. Jonkman, F. Vorpahl, W. Popko, J. Qvist, L. Frøyd, X. Chen, J. Azcona, E. Uzunoglu, C. Guedes Soares, C. Luan, H. Yutong, F. Pengcheng, A. Yde, T. Larsen, J. Nichols, R. Buils, L. Lei, T. Nygard and M. Guerinel, "Offshore Code Comparison Collaboration Continuation Within IEA Wind Task 30: Phase II Results Regarding a Floating Semisubmersible Wind System," 2014.

This project has received funding from the European Union's Horizon H2020 research and innovation programme under grant agreement No 815159

[50] A. Robertson, F. Wendt, J. Jonkman, W. Popko, H. Dagher, S. Gueydon, J. Qvist, F. Vittori, J. Azcona, E. Uzunoglu, C. Guedes Soares, R. Harries, A. Yde, C. Galinos, K. Hermans, J. Vaal, P. Bozonnet, L. Bouy, I. Bayati and Y. Debruyne, "OC5 Project Phase II: Validation of Global Loads of the DeepCwind Floating Semisubmersible Wind Turbine," *Energy Procedia,* vol. 137, pp. 38-57, 2017.

[51] U.S Department of Energy, "Projects," [Online]. Available: https://a2e.energy.gov/projects/oc6.

[52] L. Wang, A. Robertson, J. Jonkman and Y.-H. Yu, "Uncertainty Assessment of CFD Investigation of the Nonlinear Difference-Frequency Wave Loads on a Semisubmersible FOWT Platform," *Sustainability,* vol. 13, p. 64, 2020.

[53] Y. Wang, H.-C. Chen, G. Vaz and S. Mewes, "CFD Simulation of Semi-Submersible Floating Offshore Wind Turbine Under Pitch Decay Motion," in *2nd International Offshore Wind Technical Conference IOWTC2019*, St. Julian's, Malta, 2019.

[54] S. Mewes, G. Vaz, S. Gueydon and O. Moctar, "Investigation of a semi-submersible floating wind turbine in surge decay using CFD," *Ship Technology Research,* vol. 67, pp. 2-14, 2020.

[55] Y. Wang, H.-C. Chen, G. Vaz and S. Mewes, "CFD Simulation of Semi-Submersible Floating Offshore Wind Turbine under Regular Waves," in *30th International Ocean and Polar Engineering Conference*, Virtual, 2020.

[56] The University of Maine (UMaine), "DeepCwind Consortium," [Online]. Available: https://composites.umaine.edu/research/deepcwind-consortium/. [Accessed February 2021].

[57] C. Allen, A. Viselli, H. Dagher, A. Goupee, E. Gaertner, N. Abbas, M. Hall and G. Barter, "Definition of the UMaine VolturnUS-S Reference Platform Developed for the IEA Wind 15-Megawatt Offshore Reference Wind Turbine," National Renewable Energy Laboratory, NREL/TP-5000-76773, Golden, CO, USA, 2020.

[58] D. Matha, J. Cruz, M. Masciola, E. E. Bachynski, M. Atcheson, A. J. Goupee, S. M. H. Gueydon and A. N. Robertson, "Modelling of Floating Offshore Wind Technologies," in *Floating Offhsore Wind Energy*, Springer, Cham, 2016.

[59] A. Myhr, C. Bjerkseter, A. Ågotnes and T. A. Nygaard, "Levelised cost of energy for offshore floating wind turbines in a life cycle perspective," *Renewable Energy,* vol. 66, pp. 714-728, 2014.

[60] E. Baita-Saavedra, D. Cordal-Iglesias, A. Filgueira-Vizoso, À. Morató, I. Lamas-Galdo, C. Álvarez-Feal, L. Carral and L. Castro-Santos, "An Economic Analysis of An Innovative Floating Offshore Wind Platform Built with Concrete: The SATH® Platform," *Applied Sciences,* vol. 10, no. 11, p. 3678, 26 05 2020.

This project has received funding from the European Union's Horizon H2020 research and innovation programme under grant agreement No 815159

[61] A. Durakovic, “BlueSATH Floating Wind Prototype Capsizes During Hurricane Epsilon,” OffshoreWind.biz, [Online]. Available: https://www.offshorewind.biz/2020/11/04/bluesath-floating-wind-prototype-capsizes-during-hurricane-epsilon/.

[62] EOLINK, “Projects,” [Online]. Available: http://eolink.fr/en/. [Accessed February 2021].

[63] PLOCAN , [Online]. Available: https://www.plocan.eu/en/the-w2power-prototype-test-is-successfully-completed-in-the-plocan-test-site/. [Accessed February 2021].

[64] Hexicon, “About,” [Online]. Available: https://www.hexicon.eu/hexicon/. [Accessed February 2021].

[65] A. Connolly, M. Guyot, M. Le Boulluec, L. Héry and A. O’Connor, “Fully Coupled Aero-Hydro-Structural Simulation of New Floating Wind Turbine Concept,” in *ASME 2018 1st International Offshore Wind Technical Conference*, San Francisco, California, USA, 2018.

[66] G. Doisenbant, M. Le Boulluec, Y.-M. Scolan and M. Guyot, “Numerical and experimental modeling of offshore wind energy capture: Application to reduced scale model testing,” *Wind Engineering,* vol. 42, no. 2, pp. 108-114, 2018.

[67] Eolink; EC-Nantes, “EOLINK's latest-generation floating wind turbine tobe tested on Centrale Nantes’ SEM-REV offshore test site,” Press Release, Nantes, France, 2020.

[68] Hexicon, “Hexicon Presentation at Pareto Power and Renewables Energy Conference,” 2021. [Online]. Available: https://www.hexicon.eu/news/.

[69] K. L. McTiernan and K. T. Sharman, “Review of Hybrid Offshore Wind and Wave Energy Systems,” *Journal of Physics: Conference Series,* vol. 1452, p. 012016, 2020.

[70] K. L. McTiernan and K. T. Sharman, “Review of Hybrid Offshore Wind and Wave Energy Systems,” *Journal of Physics: Conference Series,* vol. 1452, 2020.

[71] E. Gaertner, J. Rinker, L. Sethuraman, F. Zahle, B. Anderson, G. E. Barter, N. J. Abbas, F. Meng, P. Bortolotti, W. Skrzypinski, G. N. Scott, R. Feil, H. Bredmose and K. Dykes, “IEA Wind TCP Task 37: Definition of the IEA 15-Megawatt Offshore Reference Wind Turbine,” NREL/TP-5000-75698, Golden, CO, 2020.

[72] Enzen Spain, “The Iberian region as a hub for technology development and industrial leadership in the field of floating offshore wind - Summary Report,” Madrid, Spain, 2020.

[73] PivotBuoy Project, “D5.3 Full Scale PivotBuoy System Simulation,” 2020.

This project has received funding from the European Union’s Horizon H2020 research and innovation programme under grant agreement No 815159

[74] P. Veers, K. Dykes, E. Lantz, S. Barth, C. L. Bottasso, O. Carlson, A. Clifton, J. G. P. Green, H. Holttinen, D. Laird, V. Lehtomäki, J. K. Lundquist, J. Manwell, M. Marquis, C. Meneveau, P. Moriarty, X. Munduate, M. Muskulus, J. Naughton, L. Pao, J. Paquette, J. Peinke, A. Robertson, J. S. Rodrigo, A. M. Sempreviva, C. J. Smith, A. Tuohy and R. Wiser, "Grand challenges in the science of wind energy," *Science,* vol. 366, no. 6464, 2019.

[75] T. Larsen and T. Hanson, "A method to avoid negative damped low frequent tower vibrations for a floating, pitch controlled wind turbine," *Journal of Physics: Conference Series,* vol. 75, p. 012073, 2007.

[76] G. E. Barter, A. Robertson and W. Musial, "A systems engineering vision for floating offshore wind cost optimization," *Renewable Energy Focus,* vol. 34, pp. 1-16, 2020.

[77] T. Salic, J. F. Charpentier, M. Benbouzid and M. Le Boulluec, "Control Strategies for Floating Offshore Wind Turbine: Challenges and Trends," *Electronics,* vol. 8, no. 10, 2019.

[78] L. Pustina, C. Lugni, G. Bernardini, J. Serafini and M. Gennaretti, "Control of power generated by a floating offshore wind turbine perturbed by sea waves," *Renewable and Sustainable Energy Reviews,* vol. 132, p. 109984, 2020.

[79] G. E. Barter, A. Robertson and W. Musial, "A systems engineering vision for floating offshore wind cost optimization," *Renewable Energy Focus,* vol. 34, pp. 1-16, 2020.

[80] W. Musial, P. Beiter, P. Spitsen, J. Nunemaker and V. Gevorgian, "2018 Offshore Wind Technologies Market Report," NREL/TP-5000-74278, Golden, CO, USA, 2018.

[81] L. Wang, X. Liu and A. Kolios, "State of the art in the aeroelasticity of wind turbine blades: Aeroelastic modelling," *Renewable and Sustainable Energy Reviews,* vol. 64, pp. 195-210, 2016.

[82] P. Bortolotti, A. Kapila and C. L. Bottasso, "Comparison between upwind and downwind designs of a 10\,MW wind turbine rotor," *Wind Energy Science,* vol. 4, pp. 115-125, 2019.

[83] A. Ning and D. Petch, "Integrated design of downwind land-based wind turbines using analytic gradients," *Wind Energy,* vol. 19, no. 12, pp. 2137-2152, 2016.

[84] N. Johnson, P. Bortolotti, S. Carron, C. Ivanov, N. Abbas and E. Loth, "IEA Task 40. U.S. progress in downwind turbine R&D," IEA Wind, 2020.

[85] A. Lamei and M. Hayatdavoodi, "On motion analysis and elastic response of floating offshore wind turbines," *Journal of Ocean Engineering and Marine Energy,* vol. 6, no. 1, pp. 71-90, 2020.

[86] D. Matha, M. Schlipf, A. Cordle, R. Pereira and J. Jonkman, "Challenges in Simulation of Aerodynamics, Hydrodynamics, and Mooring-Line Dynamics of Floating Offshore Wind Turbines," in *Twenty-first International Offshore and Polar Engineering Conference*, Maui, Hawaii, USA, 2011.

This project has received funding from the European Union's Horizon H2020 research and innovation programme under grant agreement No 815159

[87] P. Moriarty and A. Hansen, "AeroDyn Theory Manual," NREL/TP-500-36881, Golden, CO, USA, 2005.

[88] A. Shourangiz-Haghighi, M. A. Haghnegahdar, L. Wang, M. Mussetta, A. Kolios and M. Lander, "State of the Art in the Optimisation of Wind Turbine Performance Using CFD," *Archives of Computational Methods in Engineering,* vol. 27, no. 2, pp. 413-431, 2020.

[89] B. Sanderse, S. van der Pijl and B. Koren, "Review of computational fluid dynamics for wind turbine wake aerodynamics," *Wind Energy,* vol. 14, no. 7, pp. 799-819, 2011.

[90] M. Make and G. Vaz, "Analyzing scaling effects on offshore wind turbines using CFD," *Renewable Energy,* vol. 83, pp. 1326-1340, 2015.

[91] M. Make, G. Vaz, G. Fernandes, S. Mewes and S. Gueydon, "Analysis of Aerodynamic Performance of Floating Wind Turbines Using CFD and BEMT Methods," in *ASME 2015 34th International Conference on Ocean, Offshore and Arctic Engineering* , St. Johns, Newfoudland, Canada, 2015.

[92] Y. Liu, Q. Xiao, A. Incecik and C. Peyrard, "Aeroelastic analysis of a floating offshore wind turbine in platform-induced surge motion using a fully coupled CFD-MBD method," *Wind Energy,* vol. 22, no. 1, pp. 1-20, 2019.

[93] N. Khlaifat, A. Altaee, J. Zhou and Y. Huang, " A review of the key sensitive parameters on the aerodynamic performance of a horizontal wind turbine using Computational Fluid Dynamics modelling," *AIMS Energy,* vol. 8, no. 3, pp. 493-524, 2020.

[94] A. N. Robertson, S. Gueydon, E. Bachynski, L. Wang, J. Jonkman, D. Alarcón, E. Amet, A. Beardsell, P. Bonnet, B. Boudet, C. Brun, Z. Chen, M. Féron, D. Forbush, C. Galinos, J. Galvan, P. Gilbert, J. Gómez, V. Harnois, F. Haudin, Z. Hu, J. L. Dreff, M. Leimeister, F. Lemmer, H. Li, G. Mckinnon, I. Mendikoa, A. Moghtadaei, S. Netzband, S. Oh, A. Pegalajar-Jurado, M. Q. Nguyen, K. Ruehl, P. Schünemann, W. Shi, H. Shin, Y. Si, F. Surmont, P. Trubat, J. Qwist and S. Wohlfahrt-Laymann, "OC6 Phase I: Investigating the underprediction of low-frequency hydrodynamic loads and responses of a floating wind turbine," *Journal of Physics: Conference Series,* vol. 1618, p. 032033, 2020.

[95] O. Faltinsen, Sea Loads on Ships and Offshore Structures, Cambridge University Press, 1993.

[96] J. M. J. Journée and W. Massie, Offshore hydromechanics, Delft University of Technology, 2001.

[97] M. Borg and M. Collu, "Offshore floating vertical axis wind turbines, dynamics modelling state of the art. Part III: Hydrodynamics and coupled modelling approaches," *Renewable and Sustainable Energy Reviews,* vol. 46, pp. 296-310, 2015.

This project has received funding from the European Union's Horizon H2020 research and innovation programme under grant agreement No 815159

[98] F. Lemmer, W. Yu, B. Luhmann, D. Schlipf and P. W. Cheng, "Multibody modeling for concept-level floating offshore wind turbine design," *Multibody System Dynamics,* vol. 49, no. 2, pp. 203-236, 2020.

[99] L. Roald, J. Jonkman, A. Robertson and N. Chokani, "The Effect of Second-order Hydrodynamics on Floating Offshore Wind Turbines," *Energy Procedia,* vol. 35, pp. 253-264, 2013.

[100] M. Philippe, A. Babarit and P. Ferrant, "Aero-Hydro-Elastic Simulation of a Semi-Submersible Floating Wind Turbine," *Journal of Offshore Mechanics and Arctic Engineering,* vol. 136, no. 2, 2014.

[101] C. Allen, A. Viselli, H. Dagher, A. Goupee, E. Gaertner, N. Abbas, M. Hall and G. Barter, "Definition of the UMaine VolturnUS-S Reference Platform Developed for the IEA Wind 15-Megawatt Offshore Reference Wind Turbine," NREL/TP-5000-76773, Golden, CO, (United States of America), 2020.

[102] a. Li and E. E. Bachynski, "Experimental and numerical investigation of nonlinear diffraction wave loads on a semi-submersible wind turbine," *Renewable Energy,* vol. 171, pp. 709-727, 2021.

[103] Y. Liu, Q. Xiao, A. Incecik, C. Peyrard and D. Wan, "Establishing a fully coupled CFD analysis tool for floating offshore wind turbines," *Renewable Energy,* vol. 112, pp. 280-301, 2017.

[104] T. T. Tran and D.-H. Kim, "A CFD study of coupled aerodynamic-hydrodynamic loads on a semisubmersible floating offshore wind turbine," *Wind Energy,* vol. 21, no. 1, pp. 70-85, 2018.

[105] M. Masciola, J. Jonkman and A. Robertson, "Implementation of a Multisegmented, Quasi-Static Cable Model," in *International Offshore and Polar Engineering Conference*, Anchorage, Alaska (United States of America), 2013.

[106] M. Hall, "MoorDyn V2: New Capabilities in Mooring System Components and Load Cases: Preprint," NREL/CP-5000-76555, Golden, CO (United States), 2020.

[107] Y.-H. Lin and C.-H. Yang, "Hydrodynamic Simulation of the Semi-Submersible Wind Float by Investigating Mooring Systems in Irregular Waves," *Applied Sciences,* vol. 10, p. 4267, 2020.

[108] M. Masciola, A. Robertson, J. Jonkman, A. Coulling and A. Goupee, "Assessment of the Importance of Mooring Dynamics on the Global Response of the DeepCwind Floating Semisubmersible Offshore Wind Turbine," in *International Offshore and Polar Engineering Conference*, Anchorage, Alaska, (United States of America), 2013.

[109] A. J. Coulling, A. J. Goupee, A. N. Robertson, J. M. Jonkman and H. J. Dagher, "Validation of a FAST semi-submersible floating wind turbine numerical model with DeepCwind test data," *Journal of Renewable and Sustainable Energy,* vol. 5, no. 2, 2013.

This project has received funding from the European Union's Horizon H2020 research and innovation programme under grant agreement No 815159

[110] PivotBuoy Project, “D5.1: Set-up and calibration of numerical models,” (Confidential), 2019.

[111] PivotBuoy, “D5.2: Simulation results for PLOCAN 1:3 part-scale prototype,” (Confidential), 2020.

[112] PivotBuoy, “D5.3: Full-scale PivotBuoy System Simulation,” (Confidential), 2020.

[113] DTU Wind Energy, “HAWC2,” [Online]. Available: https://www.hawc2.dk.

[114] L. Vita, “Offshore Vertical Axis Wind Turbine with Floating and Rotating Foundation,” Technical University of Denmark, Kgs. Lyngby, Denmark, 2011.

[115] Orcina, “Documentation,” [Online]. Available: https://www.orcina.com/resources/documentation/.

[116] IEC, “International Standard - IEC 61400-3 Part 3: Design requirements for offshore wind turbines”.

[117] M. H. Hansen and L. C. Henriksen, “Basic DTU Wind Energy controller,” DTU Wind Energy, 2013.

[118] F. Meng, W. H. Lio and T. Barlas, “DTUWEC: an open-source DTU Wind Energy Controller with advanced industrial features,” *Journal of Physics: Conference Series,* vol. 1618, p. 022009, 2020.

[119] T. J. Larsen and T. D. Hanson, “A method to avoid negative damped low frequent tower vibrations for a floating, pitch controlled wind turbine,” *Journal of Physics: Conference Series,* vol. 75, p. 012073, 2007.

[120] E. A. Bossanyi, “Individual Blade Pitch Control for Load Reduction,” *Wind Energy,* vol. 6, no. 2, pp. 119-128, 2003.

[121] E. A. Bossanyi, “Further load reductions with individual pitch control,” *Wind Energy,* vol. 8, no. 4, pp. 481-485, 2005.

[122] Q. Lu, R. Bowyer and B. Jones, “Analysis and design of Coleman transform-based individual pitch controllers for wind-turbine load reduction,” *Wind Energy,* vol. 18, no. 8, pp. 1451-1468, 2015.

[123] S. Cacciola and C. Riboldi, “Equalizing Aerodynamic Blade Loads Through Individual Pitch Control Via Multiblade Multilag Transformation,” *Journal of Solar Energy Engineering-transactions of The Asme,* vol. 139, p. 061008, 2017.

[124] S. T. Navalkar, J. W. v. Wingerden and G. A. M. v. Kuik, “Individual blade pitch for yaw control,” *Journal of Physics: Conference Series,* vol. 524, p. 012057, 2014.

This project has received funding from the European Union’s Horizon H2020 research and innovation programme under grant agreement No 815159

[125] S. P. Mulders, A. K. Pamososuryo, G. E. Disario and J.-W. v. Wingerden, "Analysis and optimal individual pitch control decoupling by inclusion of an azimuth offset in the multiblade coordinate transformation," *Wind Energy,* vol. 22, no. 3, pp. 341-359, 2019.

[126] G. M. Stewart, A. Robertson, J. Jonkman and M. A. Lackner, "The creation of a comprehensive metocean data set for offshore wind turbine simulations," *Wind Energy,* vol. 19, no. 6, pp. 1151-1159, 2016.

[127] A. Rohatgi, *Webplotdigitizer: Version 4.4,* https://automeris.io/WebPlotDigitizer, 2020.

[128] F. Adam, T. Myland, F. Dahlhaus and J. Grossmann, "GICON®-TLP for wind turbines – the path of development," in *RENEW*, Lisbon, 2014.

[129] Y. Ohya, T. Krasudani, T. Nagai and K. Watanabe, "Wind lens technology and its application to wind and water turbine and beyond," *Renewable Energy and Environmental Sustainability,* vol. 2, p. 2, 2017.

[130] GICON-SOF, "Economics," [Online]. Available: http://www.gicon-sof.de/en/economics.html. [Accessed February 2021].

This project has received funding from the European Union's Horizon H2020 research and innovation programme under grant agreement No 815159